The design, construction and validation of a radon chamber for the calibration of radon monitors at the North-West University, South Africa

MM Radebe

orcid.org/0000-0002-0017-4145

Thesis accepted in fulfilment of the requirements for the degree of *Doctor of Philosophy in Science with Radiation Science* at the North-West University

Promoter: Prof M Mathuthu

Co-Promoter: Prof VM Tshivhase

Graduation ceremony: May 2024

Acknowledgement

I would like to acknowledge and thank people who made the study complete. The completion of this study would have been impossible without the involvement of the following people:

- Professor Victor Tshivhase, my supervisor, for his patience and mentorship throughout the study. In addition, his help in identifying the suitable design of radon chamber and suggestion of proper equipment to be used in the study, for calibration of radon monitors.
- Professor Manny Mathuthu, for patience and understanding and opportunities.
- Dr Thulani Dlamini, for support and ideas throughout the study.
- Ms Monde Kakula and Tsholofelo Mokgele, for administrative assistance and moral support.
- Mr Joseph Mathuthu, for the provision and application of the silicon adhesive that made the radon generation system tight.

My family and friends, for comforting words and encouragement.

I would like to thank God Almighty, for continual strength.

Abstract

Radon is a radioactive gas that emits alpha particles, hence it has high radiological risk if inhaled. The concentration of radon in air, particularly indoor, must be monitored using well calibrated devices to ensure it does not exceed reference levels. The aim of this study was to design and construct a radon chamber for the calibration of radon monitors at the Centre for Applied Radiation Science and Technology (CARST). It is made of perspex sheet material of thickness 6 x 10^{-3} m and of volume 0.5 m^3. The radon chamber housed Alphapump, two Alphaguards, an Airthing Wave Plus monitor, an EB85 liquid radium standard solution and electrical wires. The two Alphaguards and Airthing Wave Plus monitors were exposed to a radon atmosphere and found not to be in proximity to the calibration curve computed using EB85 liquid radium standard solution values over a period of 40 days. To align to the calibration curve, calibration factors were obtained for AG2260 and AG2261 as 1.55 kBq/m^3 and 1.42 kBq/m^3, respectively. The temperature observed during the experiment ranged from 19.8 °C to 27.68 °C and relative humidity ranged from 49.63% to 84.75%. The designed chamber was operated without an Alphapump mechanism, the results were found to be in agreement with the US National Radon Safety Board criteria.

Keywords: Radon chamber, radon monitors, calibration, environmental parameters

List of abbreviations

AARST	American Association of Radon Scientists and Technologists
CARST	Centre of Applied Radiation Science and Technology
CMI	Czech Metrology Institute
CRM	Continuous Radon Monitor
E-PERM	Electret Passive Environmental Radon Monitor
FWHM	Full Width at Half Maximum
HPA	Health Protection Agency
HPGe	High Purity Germanium
IAEA	International Atomic Energy Agency
ICRP	International Commission on Radiological Protection
KRISS	Korea Research Institute of Standards and Science
NIRS	National Institute of Radiological Science
NIST	National Institute of Science and Technology
NPL	National Physical Laboratory
NRPI	National Radiation Protection Institute
NRSB	National Radon Safety Board
PTB	Physikalisch Technische Bundesanstalt
SRM	Standard Reference Material
USA	United States of America
ZnS	Zinc sulphide

Table of contents

List of figures

List of tables

CHAPTER 1: INTRODUCTION AND PROBLEM STATEMENT

1.1 Introduction

Radon is the most contributing source of ionizing radiation in the atmosphere. It is soluble in water, colorless, odorless gas that causes lung cancer due to greater levels of absorbed radiation dose (Sanjon et al., 2019). Organizations such as the International Commission on Radiological Protection (ICRP) have stipulated that the radon concentration in dwellings should not exceed 300 Bq/m^3 (Fuente et al., 2018). However, many residents, without this knowledge, build their dwellings on or near gold/uranium mine dump where radon concentration can exceed the ICRP limit.

There are many radon detectors for determining radon concentration. However, not all radon detectors are well calibrated, some radon detectors need to be frequently calibrated in radon chambers to produce accurate and reliable radon concentration measurement (Azimi-Garakani, 1992). The most common method of calibrating the radon detectors is exposing them to a steady radon concentration from a standard radon source in an airtight radon chamber, under controlled environmental parameters. One of such facilities for calibrating radon detectors has now been constructed at the Centre of Applied Radiation Science and Technology (CARST).

1.1.1 Radon properties

^{222}Rn is a noble radioactive isotope of atomic number 86, which originates from the decay chain of ^{238} U as one of its decay products, ^{226}Ra transforms into ^{222}Rn by alpha particle emission as seen in Figure 1.1. The other isotopes of radon are ^{220}Rn and ^{219}Rn which are from the decay chains of ^{232}Th and ^{235}U, respectively. The isotope of interest is ^{222}Rn for radon studies because of its half-live of 3.8 days which is longer-lived than other radon isotopes: radon-220 and radon-219 have half-lives less than a minute i.e., 56 seconds and 4 seconds, respectively, meaning that after being produced they quickly disappear in the atmosphere in less than a minute (Jacobi and Andre, 1963). Radon as an alpha emitter (5.5 MeV), decays to other alpha emitting nuclei such as polonium (^{214} Po,^{218}Po). Polonium (^{218}Po) with half-life of 3.1 minutes has energy of 6.0 MeV, while polonium (^{214}Po) emits alpha particle which has energy of 7.7 MeV. Therefore, radon decay products are more damaging to the lungs if inhaled or swallowed.

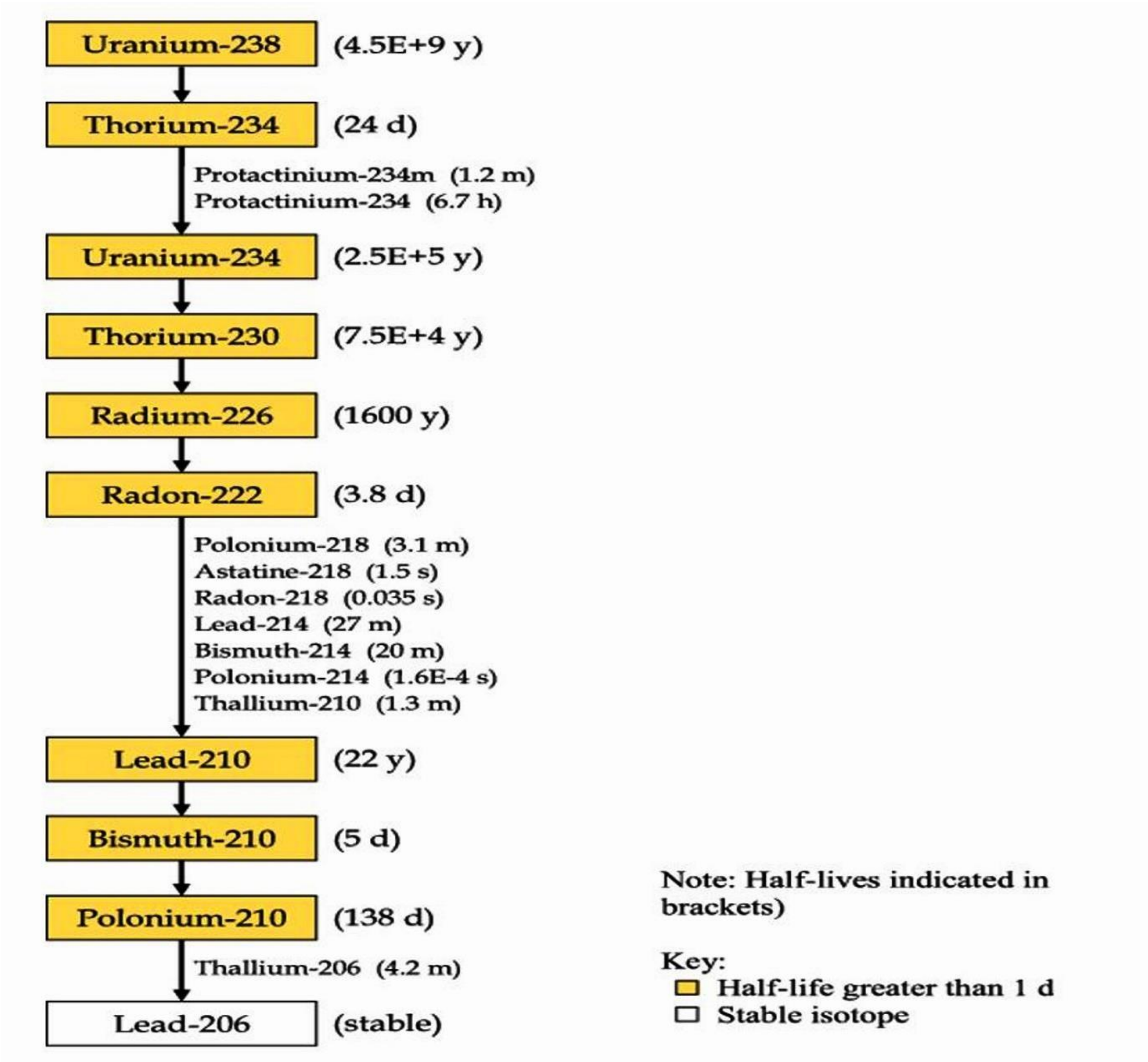

Figure 1.1**:** Radon and its decay products in the U-238 decay series (Hararah, 2007; Shivakumara et al., 2014).

The other properties of radon are thermal and chemical properties, whereby thermal properties include the boiling point of radon, which is at 208 °K and melting point 202 °K. Chemical properties include the ionization enthalpies, the higher the ionization enthalpy the more stable the radon atom is. Baskaran (2016) states that “The first ionization energy (energy needed to remove one electron from the outer most filled shell) of radon is 1,037 kJ mol^{-1} and it increases with decreasing atomic number for the noble gases” as seen in Table 1.1 and Figure 1.2. Radon is a group 18 element on the periodic table with properties [noble gas, p-block period 6; [Xe]^{4}f1^{4} 5d^{10} 6s^{2} 6p^{2}] and it is less soluble in water than organic liquids (Baskaran, 2016). The chemical, thermal and physical properties are listed in Table 1.1 and Table1. 2, respectively.

Table 1.1: The chemical and thermal properties of radon (Baskaran, 2016).

PROPERTY	**VALUE**
Atomic Number	86
Atomic Mass [amu]	222
Density [kg m^{-3} (at 0°C, 1.013 * 10^5 Pa)]	9.73
Chemical properties	
Outer Shell Electron Configuration	$6s^2 6p^6$
Possible Oxidation States	0,2,6
Electronegativity [Pauling scale]	2.2
1st Ionization Energy [kJ mol^{-1}]	1037
Thermal properties	
Melting Point [°K]	202
Boiling Point [°K]	208.2
Thermal Conductivity [W/m K]	0.00361
Specific Heat [J /g K]	0.09
Heat of Fusion [kJ mol^{-1}]	3.247
Heat of Vaporization [kJ mol^{-1}]	18

Table 1.2: The physical and nuclear properties of radon (Keith, 2012).

Parameter	**Symbol**	**^{222}Rn**
Half life	$T_{1/2}$	3.823 days
Decay constant	λ	2.098 x 10^{-6} s^{-1}
Average recoil energy on formation	E_r	86 keV
Diffusion coefficient in air	D_a	1 x 10^{-5} m^2 s^{-1}
Diffusion coefficient in water	D_w	1 x 10^{-9} m^2 s^{-1}

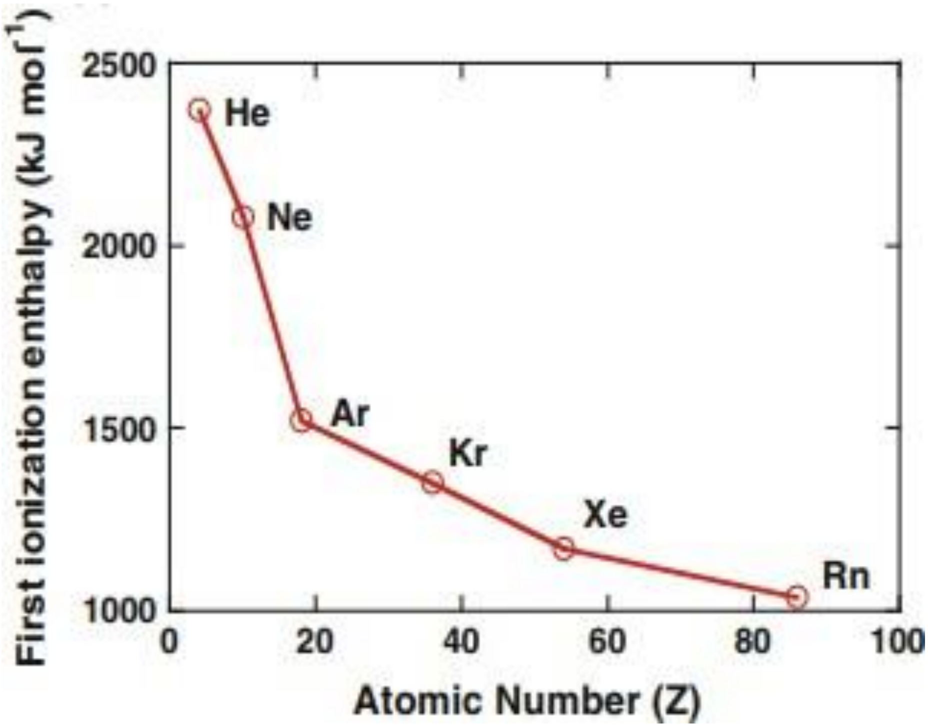

Figure 1.2: First ionization enthalpy from helium to radon. Ionization enthalpy decreases with increasing atomic number of noble gases (Macrae and Kemp, 2018; Baskaran, 2016).

1.1.2 Radon in the environment

Radon is found in rocks and soils, its abundance in the environment depends on moisture, porosity and the activity of uranium and radium. Since radon is a gas, its mobility in rocks and soils is more than that of radium and uranium. It moves easily from rocks and soils by alpha recoil into pores of soil and rock fractures (Sukanya et al., 2022). When a radium nuclide decays in a soil grain, an alpha particle is released and a newly formed radon nucleus recoils in the opposite direction to the alpha particle. If the radium nuclide is located near the surface of the soil grain, the newly formed radon nuclide escapes the soil into soil pores. If the location of the radium nucleus is at the centre of the rock or soil, the daughter product will be embedded in the rock or soil during decay (Sukanya et al., 2022).

Factors which affect the mobility of radon in the soil include porosity, moisture content and permeability. Moisture content is the amount of water in the soil, a slight increase of the soil moisture content increases the radon emanation. Hosoda (2007) and Sahu et al. (2016) found that the moisture content of soil in the range of 0 to 8 % in a rectangular volume of 2840 cm^3, increases radon emanation but a moisture content that is above 8 % decreases radon emanation.

Permeability of soil such as gravel and sand allow the transportation of radon gas from several depths in the ground, as seen in Figure 1.3. Impermeable soil such as clay and silt have low porosity and therefore the transport of radon is small. Decreased levels of radon in clays is due to the amount of water content in them, but in the dry clays with cracks, radon migration is more (Othman et al., 2021).

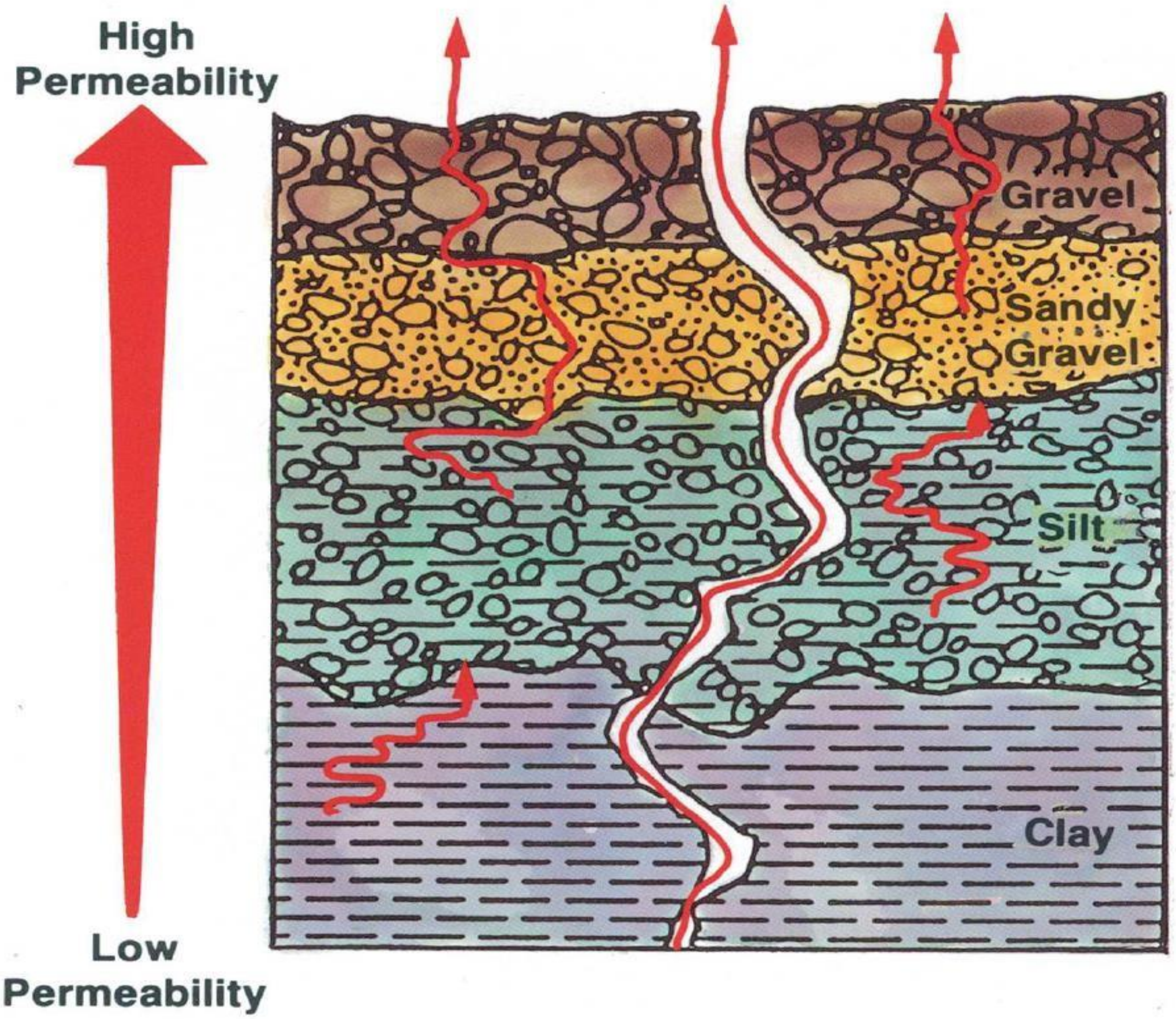

Figure 1.3: Permeability of soil from underground to surface soil (Othman et al., 2021; Gundersen et al., 1992).

Rock fracture caused by roots, ice, water or any physical weathering emanate radon at higher levels such as granite rock which has high permeability and dark shale, volcanic rocks and phosphates as seen in Table 1.3 (Hararah, 2007; Khan et al., 2022).

Table 1.3: Radium from different types of rocks and soil (Awhida, 2017).

Rock type	^{226}Ra activity concentration (Bq kg^{-1})	Soil type	^{226}Ra activity concentration (Bq kg^{-1})
Granite, normal	25 - 80	Till, with normal Ra content	15 - 65
Granite, uranium rich	100 - 500	Till, with fragments of granite	130 - 125
Sandstone	1 - 60	Till, with fragments of U-rich granite	125 - 360
Limestone	5 - 40	Gravel	30 - 75
Shale	10 - 125	Sand	5 - 35
Black shale	10 -2000	Silt	10 - 50
Alum shale	125 - 4300	Clay	10 - 100
Uranium ore	12000 2.5-10^5	Soils with fragments of alum shale	175 - 2500

In Table 1.3, different types of rocks and soil are listed with corresponding radium concentrations. The groundwater contains radon due to the movement of water through radon producing rocks consisting of varying levels of uranium and radium content underground. ^{222}Rn is in abundant concentration in underground water as it is trapped (Novikov et al., 2021). The methods of extraction of groundwater for the survival of mankind, including boreholes and wells disperse the abundantly resting radon to the surface. In addition, intake of radon in amounts greater than the public should be exposed to, leads to gradual health risk, including lung cancer (Lopes et al., 2017). Figure 1.4 shows the movement of radon in water and rocks.

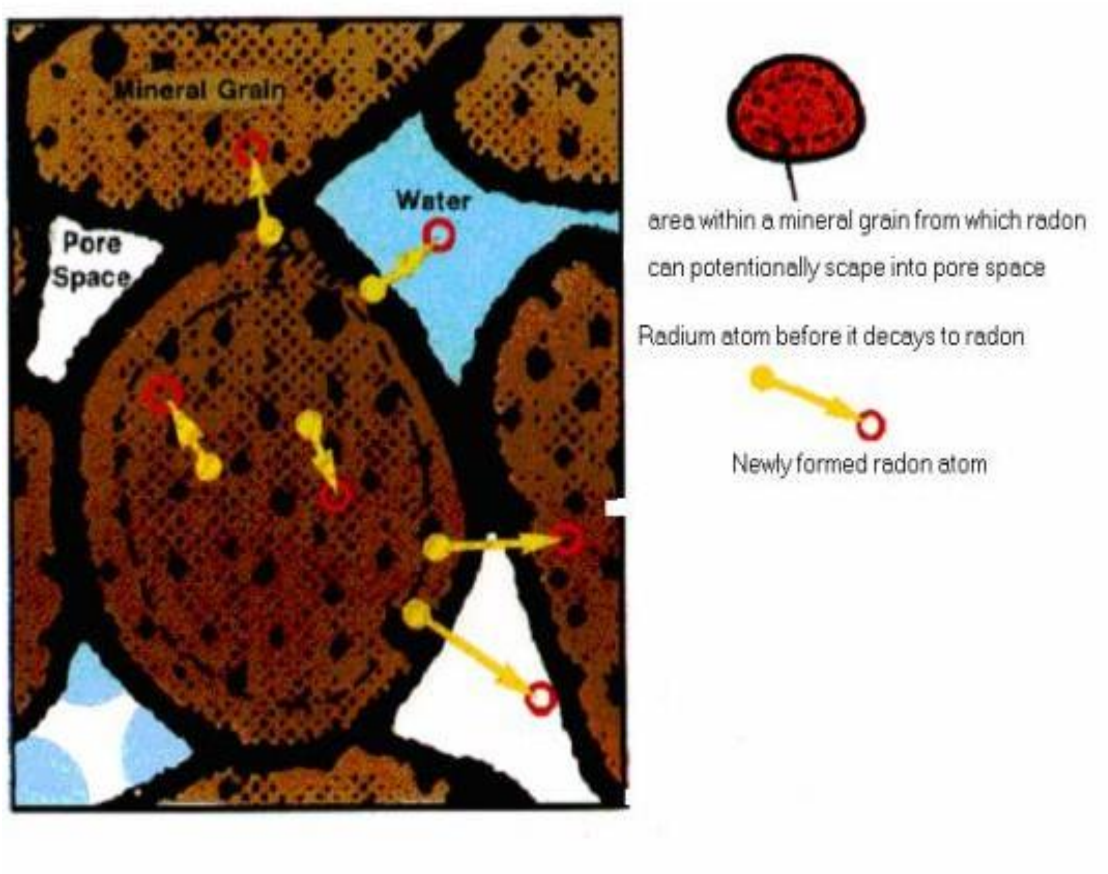

Figure 1.4: The emission of radon from radium in underground rocks to water (Hararah, 2007; Ezzulddin and Mansour, 2020).

1.2 Radon detector calibration

A radon chamber is a housing or container constructed to perform radon detector calibration for research purposes. Centomani et al. (2019) stated that radon calibration can focus on different parameters and aspects of radon measurements such as radon concentration, range control, volume, material, radon source, reference radon detector, humidity, temperature control and aerosol concentration. Small size radon chambers, are used for testing limited numbers of radon monitors, while the big ones are used to test many radon detectors simultaneously, according to National Radon Safety Board (NRSB, 2012). There is a flow-through, walk-in and accumulation type of radon chamber (Kotrappa and Stieff, 2012). The walk-in type allows the placing of materials to be used and monitored by personnel through their entry with protective clothing. The flow-through type is used for a performance test of radon detectors by certified radon professionals. Accumulation type of radon chambers are small and cost less to build than the flow-through type.

The purpose of a radon chamber is to perform calibration by exposing radon detectors to a steady flow of radon concentration in a chamber under parameters such as relative humidity and temperature (Tin, 2014). Calibration is the alignment of the well-known tested detector to known reference values.

1.3 Problem statement

It is reported that large amounts of uranium tailings are produced from mining activities in South Africa (Hnizdo et al., 1997; Nwaila et al., 2021; Farjana et al., 2018). It is of outmost importance that human dwellings nearby radon prone areas such as near the mine tailings are frequently checked to ensure acceptable levels of radon by utilising radon monitors (Kamunda et al., 2017). Accurate measurement of radon levels among communities nearby high-level radon areas is possible with radon monitors that must be calibrated annually. There are radon monitors in many facilities around South Africa (RGM, 2008), but there are no known calibration facilities within the country. Therefore, there is a need to design radon chambers, to meet the needs of the country in calibrating radon detectors.

1.4 Research aim and objectives

Aim

The aim of this study was to design and construct a radon chamber for the calibration of radon monitors at the Centre for Applied Radiation Science and Technology (CARST)

Objectives

The objectives of the study were to:

- design a prototype radon chamber for CARST,
- measure the radon activity, relative humidity, air pressure and temperature in the chamber,
- use a radon standard to calibrate radon detectors,
- device a method to measure radon leakage and
- apply a mitigation strategy to reduce radon if there is leakage.

CHAPTER 2: LITERATURE REVIEW

2.1 Radioactivity

Radioactivity is a phenomenon characterized by spontaneous disintegration of an unstable nucleus to form a stable nucleus. Radioactivity was discovered in the 18th century by a French scientist named Henri Becquerel when he observed that rays released from uranium salt passed through a paper and formed an image on a photographic plate (Malley, 2011). The unstable atom that decays by emitting energy is called a radionuclide and can undergo radioactive decay by alpha or beta decay then followed by gamma emission. Radioactive decay is the spontaneous disintegration of an unstable parent radionuclide with the release of particles or photons transforming into a daughter nuclide. In addition, when the daughter nuclide is unstable, the decay process occurs until a stable nuclide is reached. It is a random process that one cannot tell when a particular parent nucleus will disintegrate (Sóti et al., 2019). The probability of decay in a substance containing N number of nuclei is given by the decay law:

$$\mathrm{dN} = -\lambda \mathrm{Ndt} \quad (2.1)$$

where dN is the number of nuclei decaying at time interval dt. The decay constant λ, is the probability for a nuclide to decay per unit of time. The negative sign in the equation means that the number of radionuclides given by N decreases during the decay process (Kanivets et al., 2020). If at time t = 0, the number of radionuclides is N_0 then the number of nuclides that remain after radioactive decay at time t is:

$$N(t) = N_{(0)}\, e^{-\lambda t} \quad (2.2)$$

2.1.1 Half-life

The half-life is the time taken by a nuclide to reduce to half of its initial amount. In equation form the half-life is expressed as:

$$t_{\frac{1}{2}} = \frac{In2}{\lambda} = \frac{0.693}{\lambda} \quad (2.3)$$

If the decay constant of a nuclide is known, then half-life can be determined. The radioactive decay process can be described in terms of time scale by mean life or half-life of a nuclide or sample. The mean time, τ of a radionuclide until the decay of a radionuclide is the inverse of the decay constant given as:

$$\tau = \frac{1}{\lambda} \quad (2.4)$$

2.1.2 Activity

Activity A is defined as the number of disintegrations per unit time. When a source is highly radioactive, it means that the number of disintegrations per unit time is very high. The rate at which a radioactive material disintegrates in equation form is:

$$A = \frac{dN}{dt} = \lambda N \qquad (2.5)$$

where, dN is the number of disintegrations that take place with respect to time dt. In terms of mass of radioactive material m (kg), activity can be described as:

$$A = \lambda N_A \frac{m}{M} \qquad (2.6)$$

where, N_A stands for the Avogrado's number and the molar mass of the radioactive material is represented by M in kg/mol (Magill and Galy, 2005).

Activity of radionuclides is measured in SI unit; Becquerel (Bq) and in non-SI unit, Curie (Ci). The relationship between Becquerel (Bq) and Curie (Cu) is that 1 Ci=$3.7\text{x}10^{10}$ Bq, which is the activity of one gram of ^{226}Ra. Most used multiples of Becquerel for activity measurement are MegaBecquerel (1MBq = 10^6 sec^{-1}), KiloBecquerel (1 kBq =$10^3 sec^{-1}$) and GigaBecquerel (1GBq = 10^9 sec^{-1}). Commonly used multiples in activity measurements involving Curie (Ci) are microCurie (1 µCi =10^{-3}mCi), nanoCurie (1nCi =10^{-9} Ci) and kiloCurie (1kCi=1000Ci).

2.1.2.1 Bateman equation

The Bateman equation is used to obtain the activity concentration of the daughter from the parent nuclide. The Bateman equation is expressed as:

$$A_d = \frac{\lambda_d}{\lambda_d - \lambda_P} * (A_P) * (e^{-\lambda_P t} - e^{-\lambda_d t}) \qquad (2.7)$$

where the activity of the daughter nuclide is represented as A_d and the activity of the parent nuclide is A_p. The decay constants of the daughter nuclide and parent nuclide are represented by λ_d and λ_p, respectively (Bateman, 1910).

2.1.3 Types of decay

2.1.3.1 Alpha decay

Alpha decay is a nuclear disintegration process that occurs in radionuclides with atomic number that is greater than 81 but less than 92 (L'Annunziata, 2016). It occurs in heavy nuclei due to the many protons in the nucleus with a charge of +Z repelling each other and releasing an alpha particle. A heavy radionuclide, for instance uranium-238, transforms into a daughter nucleus by emission of alpha particles and some rare earth material decay by alpha emission. Alpha decay is symbolized by the following equation:

$$^{A}_{Z}X = ^{A-4}_{Z-2}Y + ^{4}_{2}He \qquad (2.8)$$

where $^{A}_{Z}X$ is the parent nuclide, $^{A-4}_{Z-2}Y$ is the daughter nuclide and $^{4}_{2}He$ is the emitted alpha particle, also known as helium. A and Z are the number of nucleons and protons, respectively. Alpha particles are high energy particles with kinetic energy from 4 – 10 Mev, that can travel in the air a distance of 5 – 11 cm and are stopped by a sheet of paper (Danforth et al., 2023).

An alpha particle consists of two protons and neutrons that are tightly bound together in a stable atomic configuration. In quantum mechanics, alpha particles with energy of 4.8 MeV escape the potential barrier with a height of 25 MeV by a process called quantum tunneling (Reinders, 2021). However, in classical mechanics this is impossible since the height is 25 MeV and the alpha particle energy is 4.8 MeV as seen in the Figure 2.1. This means that the alpha particles energy is insufficient to escape the potential barrier of height 25 MeV.

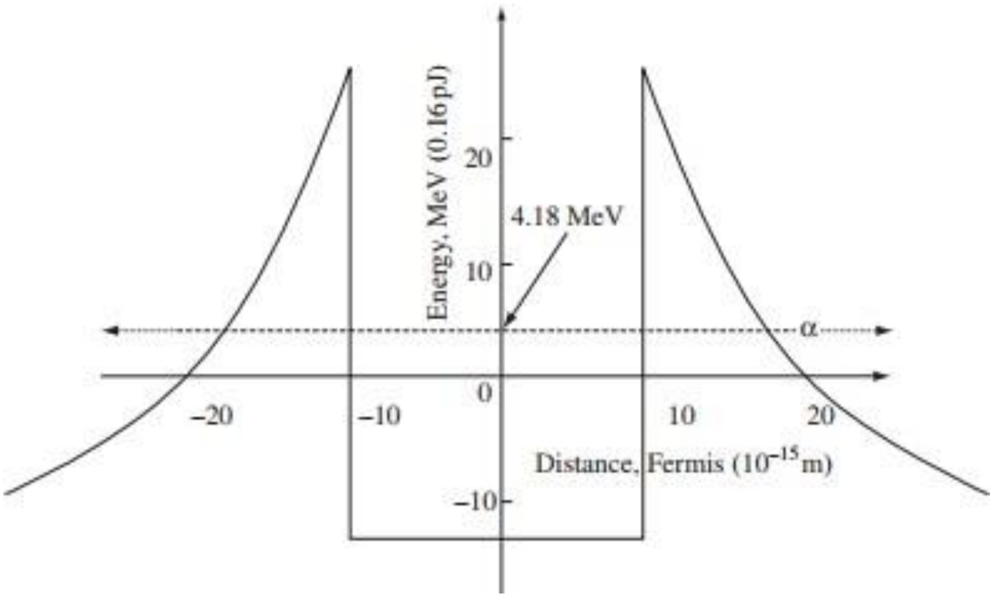

Figure 2.1: Schematic of an alpha decay(Magill and Galy, 2005; Reinders, 2021).

2.2.3.2 Beta decay

Beta-decay is a process whereby an unstable atomic nucleus emits a beta particle (energetic electron or protons), to transform the nucleus into an isobar. Isobars are nuclides with same mass number but different atomic number. A beta particle created during the beta decay process, whereby there is an emission of high energy, high-speed electron or positron due to disintegration of excess protons or neutrons in the nucleus. In addition, due to instability of atoms, orbital electron are captured by the nucleus in a phenomenon known as electron capture. Modes of beta decay are beta-plus and beta-minus, whereby in beta-minus, a neutron in the nucleus transforms into a proton, an electron and an antineutrino are emitted as described by the following equation:

$$_{0}n^{1} \rightarrow {}_{1}P^{1} + {}_{-1}e^{0} + \bar{\nu}_{e} \qquad (2.9)$$

where, $_{0}n^{1}$ is the neutron, $_{-1}e^{0}$ is the electron and $\bar{\nu}_{e}$ is the antineutrino and P^{1} is the proton.

The difference between beta emission and alpha emission is that beta particles have continuous spectrum of energies from zero to a maximum energy. Neutrino is emitted during positive beta-decay and anti-neutrino is emitted during a negative beta-decay. Beta particles can be stopped by thin layers of glass, water, metal and have energy ranging from 10 KeV to 4 MeV (Jenkins, 2020).

In beta-plus decay, from a proton level: a proton turns into a neutron and emits a positron and neutrino, as seen in equation 11.

$$p^{+} \rightarrow n + e^{+} + v_{e} \qquad (2.10)$$

Beta-minus decay occurs when the number of neutrons in relation to protons is excessive, whereas beta-plus decay occurs when there is excess protons compared to neutron (Kónya and Nagy, 2018).

2.1.3.3 Gamma emission

In gamma emission, a pure energy is emitted in a form of a photon by an unstable nucleus. It occurs following a beta or alpha decay when the progeny is formed in an excited state, which returns to the ground state by releasing a photon (Ojovan and Lee, 2014). Gamma radiation is emitted during the de-excitation of an excited nucleus.
Gamma decay process can be described as:

$$^{A}_{Z}X \rightarrow {}^{A}_{Z}X + \gamma \qquad (2.11)$$

Gamma rays from emitters such as cobalt-60, have a high penetrating power and are attenuated by materials such as steel, concrete and lead (Collum, 2017). According to the electromagnetic spectrum, they are from the same family as visible light and radio waves, as seen on Figure 2.2.

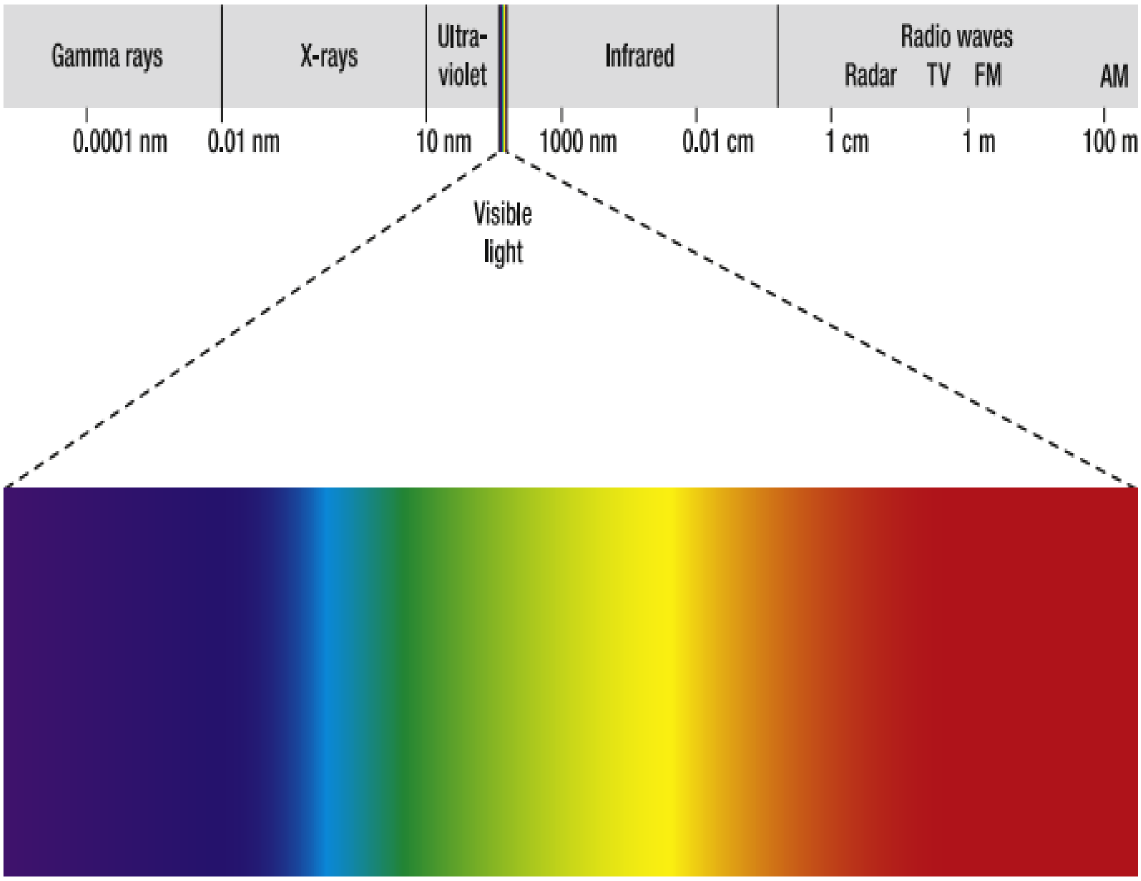

Figure 2.2: Electromagnetic spectrum showing relative position gamma ray (Collum, 2017)**.**

2.2 Radioactive equilibrium

Radioactive equilibrium is the relationship between the decay rates of parent and daughter radionuclides. The radioactive equilibrium in equation form is described as:

$$\lambda_1 N_1 = \lambda_2 N_2 \qquad (2.12)$$

where, λ_1 is the decay rate and N is the number of atoms.

The types of radioactive equilibrium are namely, secular equilibrium and transient equilibrium (Magill and Galy, 2005).

2.2.1 Secular equilibrium

Secular equilibrium is a state where the parent radionuclide activity is equal to the daughter radionuclide activity. The half-life of the parent nuclide is longer than daughter nuclide, therefore the activity of the parent nuclide decreases slowly compared to the activity of the daughter nuclide (L'Annunziata, 2020). Secular equilibrium can be described by equation:

$$\frac{N_2}{N_1} = \frac{\lambda_1}{\lambda_2} = \frac{\tau_2}{\tau_1}, then\ A_1 = A_2 \quad (2.13)$$

where, A is the activity described as λN of the parent that is in equilibrium with the activity of the daughter as seen in Figure 2.3 (L'Annunziata, 2020). N_1 is the parent nuclide, N_2 is the daughter nuclide, λ_1 is the decay constant of the parent nuclide, λ_2 is the decay constant of the daughter nuclide. τ_2 and τ_1 are half-lives for the parent and daughter nuclide, respectively. A_2 and $A_1$are the activity of the parent and daughter nuclide.

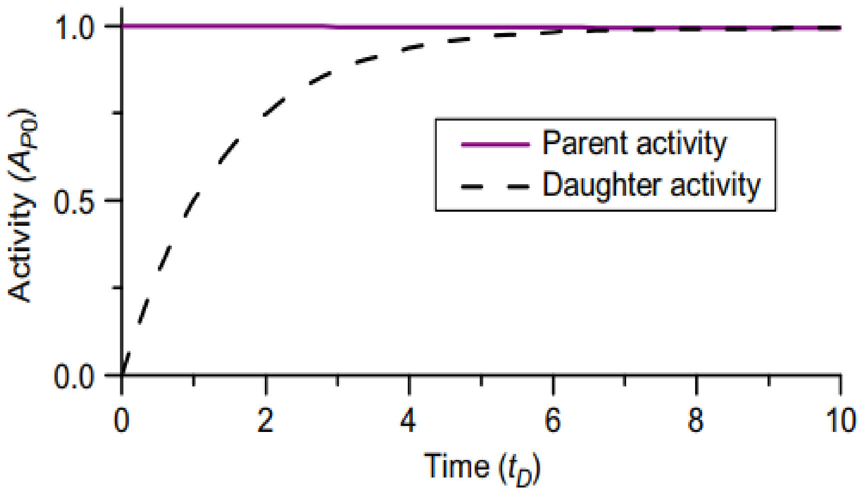

Figure 2.3: The build-up of the daughter activity to equal parent activity (L'Annunziata, 2020).

2.2.2 Transient equilibrium

Transient equilibrium exists when the half-live of the parent is greater than that of the daughter, but not infinitely. During the period of radioactive decay, the parent nuclide decays, while the daughter nuclide builds up until equilibrium is reached. After a state of equilibrium is reached, the activity of the daughter becomes greater than that of the parent nuclide. The daughter and the parent nuclide decay at the same rate. An example of transient equilibrium is between the parent nuclide ^{140}Ba and daughter nuclide ^{140}La as seen in Figure 2.4. The parent and daughter activities in transient equilibrium are given by:

$$A_D = \frac{A_p \lambda_D}{(\lambda_D - \lambda_P)} \quad (2.14)$$

Where A_D is the activity of the daughter, A_p is the activity of the parent. λ_D, λ_P are the half life of the daughter and parent nuclide.

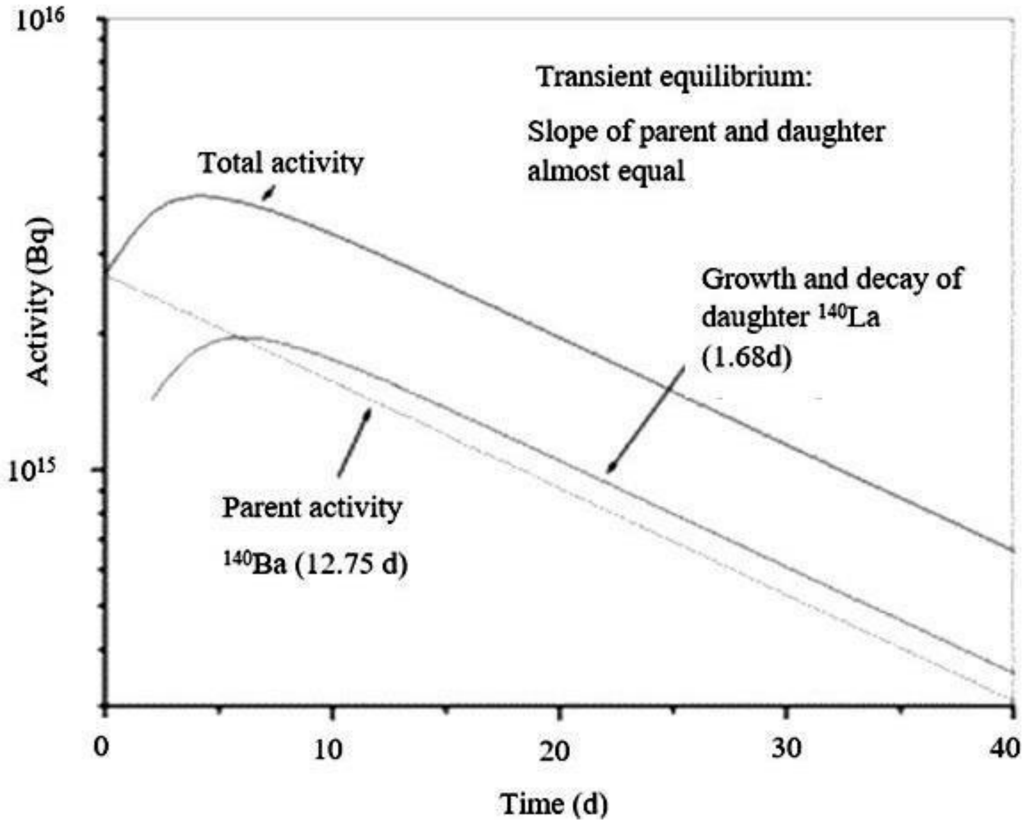

Figure 2.4: Illustration of an example of transient equilibrium between ^{140}Ba and progeny ^{140}La (Lehto et al., 2017; Magill and Galy, 2005).

2.2.3 Non equilibrium

A non-equilibrium condition is a condition when the half-life of the daughter nuclide is greater than that of the parent nuclide. In this condition, the parent nuclide has a short half-life than that of the daughter. Then the daughter nuclide grows to the maximum activity and decays.

.

2.3 Design and components of radon chamber

Successful operation of a radon chamber for calibration and radon study purposes is made possible by the equipment for temperature, humidity, homogeneity and radon measurement.

2.3.1 Radon chamber

A radon chamber can be likened to a container, housing or room designed whereby a reference radon atmosphere is produced by a radium source under certain environmental conditions. There are three categories of radon chamber laboratory for the radon calibration and radon studies namely the primary, secondary and tertiary radon chambers of which their operation varies. A primary radon chamber can perform radon and radon progeny testing and calibration, is sophisticated in design and it is traceable to National Institute of Science and Technology.

Secondary radon chamber are radon reference chambers at facilities that are traceable to a national standard or international reference standard (AARST, 2015). A secondary radon chamber in laboratories is used to perform quality assurance exposures such as proficiency tests, spikes, calibration test and performance evaluations.

Tertiary radon chambers compares with a secondary radon chamber and is used for spiking, calibration and evaluation of devices by manufacturers (Bredhoff, 2014). In primary and secondary chambers, detailed device evaluation and proficiency testing are performed. However, that is not the case for tertiary chambers as stringent standard and capabilities are required for device approval (George, 2021).

2.3.2 Radon measurement

Radon is measured by a wide range of techniques developed over years and improved in sensitivity, portability and performance (El-Taher, 2018). The radon measurement technique mostly depends on the concentration of radon-222 and the characteristics used to classify them, as follows:

- whether the technique measures radon-222 and radon progeny
- detection of radioactive decay whether alpha, beta or gamma
- time resolution

An alpha particle detected can be used to measure radon-222 decay products by using scintillation counters. Conversely, in the measurement of radon-222, gamma rays emitted from radon-222 daughters can be used to determine or measure radon-222, for example bismuth-214 and lead-214 (Elzain, 2017).

Time resolution sampling analysis and measurement are classified into three techniques, namely; grab sampling, continuous technique and integrating technique. Integrating technique utilizes passive detectors to measure the integrated radon-222 concentration annually or monthly, mostly in buildings. Continuous technique provides the simultaneous act of sampling and determination of radon-222 in samples of soil or water in minutes, hours and days with a device such as scintillation radon monitors and smart-radon duo. Grab sampling technique includes the collection of samples of groundwater, in a short time whereby devices such as RAD7 are used to measure radon-222 in samples collected. Awhida (2017) states that radon measurement techniques differ to the point that one technique cannot meet the requirements such as radon survey type, environmental parameter measurement and cost of the apparatus (Awhida, 2017).

2.4 Radon measurement devices

2.4.1 Solid state nuclear track detector

Solid state nuclear track detector is a detector which is insensitive to beta and gamma particle, but sensitive to alpha particles in the range of the energy produced by radon. To determine the alpha particles on the detector, a chemical etching process is conducted whereby tracks caused by alpha particles can be seen by an optical microscope and can be counted manually or by an automated counting device. Solid state nuclear tract detectors are not affected by environmental parameters such as temperature, humidity, and they function without a power supply. Furthermore, such detectors are suitable for long-term measurement and radon progenies, can be filtered out of the detector to measure radon only by use of diffusion membranes.

2.4.2 Alpha card

Alpha card is one of the passive radon-detecting technique for radon in soil, with dimensions of 4.5 cm x 5 cm card and 2.5 cm diameter hole, covered in a membrane located in the center of the alpha card. For usage, the alpha card is placed in the ground, in such a way that it is suspended in an inverted cup for over twelve hours to a couple of days. After being collected from the ground, two silicon detectors facing each other are used to read the alpha particles (Ayman et al., 2017).

2.4.3 Electret detector

Electret radon monitor is a device that measures the average radon concentration over a period of time in the field. The electret is a dielectric material that functions as a source of electric field that exhibit a permanent electric charge. The charge generates a strong electrostatic field that attracts ions of opposite signs, which result in decreasing the total charge of electret (Kotrappa, 2015). An electret radon monitor is made up of a steel canister and electret dosimeter, which is inside the top of the steel canister. A small inlet located at the bottom of the steel canister allows radon to enter the volume through a filter. When radon decays, it produces ionizing particles that produce ions in the volume of the device. Moreover, the produced ions change the total charge of the electret and the electric surface potential charge is measured by the shutter method, which is a non-destructive method. The electrets can be measured more than once, with assurance that their charge value is not altering. Electret dosimeter has several advantages, such as the ability to store information over a long period of time and the information is easily readable. Furthermore, the electret dosimeter is independent of humidity (Welch et al., 2016). The electret dosimeter, in comparison to other detectors, has a response curve whereby the very low or high doses are not efficiently covered, and it is sensitive to normal gamma background radiation (Welch et al., 2016).

2.4.4 Thermoluminescent detectors

Thermoluminescent detectors are utilised for measuring ionizing radiation exposure by measuring light photons emitted from thermoluminescent crystal or chip embedded in the detector. The thermoluminescent detector chip is in contact with the beta or alpha particles, the gamma particles in a form of light are emitted by radon and its progeny. Then, it is collected and "read" in a detector's apparatus and radon concentration is measured.

2.4.5 Activated charcoal detector

Activated charcoal detector are passive devices that can be deployed for several days for detection of radon (Riggio and Santulin, 2015). The activated charcoal detector consists of a metal canister with a removable lid and has a metal mesh which firmly holds the granulated activated charcoal (Nastro et al., 2018). Prior to the detector being used, there is a removal of any absorbed water vapor and absorbed gas carried out by heating the open canister. Then, the lid is closed, and the canister is sent to the place, where the canister lid is opened to expose the charcoal for radon measurement. After the exposure period, the canister is closed and sent to the gamma-ray spectrometric laboratory for measurement.

The activated charcoal detector uses an absorption technique whereby the detector's activated charcoal absorbs the radon gas in air. The other method of measuring the radon absorbed by the activated charcoal detector sample is by liquid scintillation, whereby the activated charcoal is mixed with a liquid scintillation cocktail for radon to dissolve and the solution is monitored in a liquid scintillation counter.

2.4.6 Alpha scintillation cells

Alpha scintillation cells consist of silver activated zinc sulfide phosphorus to measure radon concentration in air, workplaces and field measurement (Abdalla et al., 2019). Alpha scintillation cells work with a monitor that includes a pulse counter and a photon detector, which may be a solid state detector or photomultiplier tube (Division, 2018). Scintillation cells have an interior wall that is coated with an alpha scintillation material, ZnS (AG), that produces a photon as a result of being struck by an alpha particle. Photomultiplier tubes amplify or multiply electric pulses generated by detecting photons which generate electrons: dynodes in the photomultiplier, amplify electrons and results in electric pulses (Cho, 2003). The function of a photon detector in the monitor is to change the photon to an electrical pulse, secondly it amplifies the pulse and sends it to the monitor's amplifier and counter circuit. The radon concentration in a gas sample can be measured based on the number of counts over time.

2.4.7 Ionization chambers

Ionization chambers are measurement instruments that are accurate and are traceable to reference standards (Ayman et al., 2017). They consist of electrodes with a gas filled space, whereby an electric field is established between electrodes. Air enters the chamber through the flow-through method or diffusion, then, ionization in the chamber occurs, a current is generated and is detected. The measurement technique by the instrument can be by ionization current measurement or alpha pulse counting.

2.5 Determination of radon-222 by its progeny

2.5.1 ^{222}Rn determination by solid – surface barrier detector

One of the ways of determining ^{222}Rn activity is through alpha spectrometry by counting alpha emitting progenies of ^{222}Rn.

A known quantity of radon air is drawn by two filters in a cylindrical system, whereby one filter keeps the radon progeny and particulate matter, the other filter receives radon. On the second filter, ingrowth of radon takes place, the second filter faces the surface barrier detector and therefore alpha spectra is produced. In a simple method, positively charged progenies are collected onto a metal surface that is placed inside the chamber's negative potential. For example, the positively charged ^{218}Po particles gathered on a metal surface are counted by a surface barrier detector. The advantage of using a surface-barrier detector is high resolution, low background, ability to distinguish the signals of ^{222}Rn progenies and ^{222}Rn due to the fact that they have varying alpha energies (Baskaran, 2016).

2.5.2 ^{222}Rn determination using beta counter

Assuming that there is secular equilibrium between ^{222}Rn and its progeny, the beta particles of ^{214}Pb and ^{124}Bi on a filter can be used for determining the radon concentration by measuring their beta activity. Beta counter such as Geiger Muller counter are used to count the radon progeny on filter paper. Also, plastic scintillators installed in photomultipliers tubes can be used to determine activity.

2.5.3 Direct progeny monitoring technique

One way of measuring a time integrated radon progeny for determination of radon is with a direct radon progeny sensor, which is made up of a solid-state nuclear track detector fitted with an absorber of sufficient thickness. The direct radon progeny absorber comprises of aluminized Mylar and cellulose nitrate of appropriate thickness of 37 µm, whereby 7.67 MeV alpha particles emitted from ^{214}Po are detected (Singh et al., 2015).

2.6 Temperature and humidity

2.6.1 Temperature

In physics, temperature is the measure of the average kinetic energy in a material caused by heat absorbed by a material. The greater the heat applied to the object, the more the vibration of the particles in the object, resulting in the object being warmer. Temperature is measured in three different scales, namely Kelvin, Fahrenheit and Celsius.

The Celsius scale is named after Anders Celsius, who was a Swedish astronomer in the 17th century. It is also called the centigrade scale and reading on the Celsius scale are identified as degree Celsius. The Kelvin scale is the mostly used temperature scale in physical sciences (Materese, 2018). It is named after the renowned British Physicist Lord Kelvin (1824-1907), it describes temperature as it starts at absolute zero and a change in one Kelvin unit is equal to the change of one degree Celsius. Temperature on the Kelvin scale is measured as Kelvins K and it is also the SI unit of the thermodynamic temperature (Materese, 2018).

The Fahrenheit scale, devised by Gabriel Daniel Fahrenheit in 1724, has a difference of 180-degree interval between boiling point and melting point of water. Daniel Fahrenheit is the inventor of the high mercury thermometer that is still used today, he calibrated a thermometer using salt sea water because of its low freezing point when compared to water. He established that the boiling point of water is 212 °F and the freezing point at 32°F.

2.6.2 Humidity

The term humidity refers to the amount of moisture in the air (Tiefenbacher, 2019). According to Fontes (2005), absolute humidity and relative humidity are the commonly used terms to express humidity. The term absolute humidity refers to the quantity of water vapour in the unit volume of air expressed as grams of water vapor per cubic meter of air (g/m^3) (Peci et al., 2019). Shaoxian and Shizhu (2019) state that absolute humidity p_v is the density of water vapour in wet air, given by the equation (15):

$$p_v = \frac{m_v}{v} \qquad (2.15)$$

where, m_v stands for mass of water vapour and the volume of the water vapour is v.

Absolute humidity is reliant on the actual temperature, for instance at low temperature at 0 ºC absolute humidity is usually 4.9 g/m^3 and at higher temperature at 30 ºC the absolute humidity is 30.1g/m^3 (Tiefenbacher, 2019). The relationship between temperature and absolute humidity in relation to air is that at high temperature, the air contains a lot of moisture and at low temperature, the absolute humidity is low.

Relative humidity (RH) is a percentage of the quantity of moisture that can be kept by the atmosphere at a particular temperature and pressure without condensation (Yahia, 2019). In simplicity, relative humidity is how much water vapour is in the air, expressed in terms of percentage of the amount required to reach saturation. Relative humidity at 0 % means absolute dry air or no water vapour content, while at 100 % it implies that air contains water vapour that it holds at a given temperature and water vapour content in air greater than 100% means that there will be formation of water droplets. Materials that absorbs or desorbs moisture at a particular relative humidity of ambient air reaches equilibrium relative humidity, which is a state of where a material, for example hydroscopic materials, never lose or gain moisture at certain temperature (Tiefenbacher, 2019).

2.6.3 Relationship between humidity and temperature

According to Akbari and co-workers (2013), increase in temperature or decrease in temperature or humidity, has an effect on the level of radon indoors. Temperature increase cause radon levels to decrease, while an increase in humidity causes an increase in indoor radon level (Akbari et al., 2013).

Chung (2020) developed a temperature and humidity sensor module, as seen in Figure 2.5, for determining the relationship of indoor radon, temperature and humidity. The temperature and humidity sensor module is a combination of Arduino Mega 2560 and DHT22 (Asong Eletronics Co, China) with measurement errors for temperature range of -40ºC to 80 ºC at ± 0.5 ºC, and relative humidity range at 0 % to 100 % at a measurement error of ± 2 %.

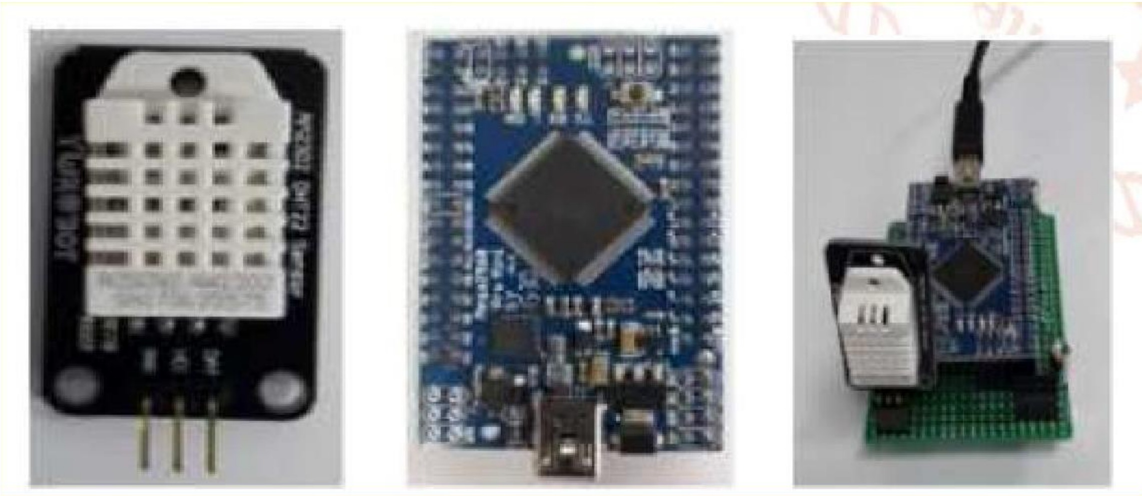

Figure 2.5: Tool for measuring temperature and humidity (Jai-Won Chung, 2020).

Moreover, other materials used to regulate temperature in chambers are the air conditioner, heater and freezer. In the National Institute of Radiological Science radon chamber temperature and humidity are controlled by air conditioner which provides heating, cooling and maintenance of humidity. The exposure chamber designed by Leung et al. (1992), uses a heater and freezer for regulating temperature and humidity, moreover, cooling in the chamber is implemented by passing a gas through the freezer to the chamber. The chamber is heated through an electric coil that converts electrical energy to a heat.

Chung (2020) states that an increasing humidity can increase the amount of radon emission from building materials such as bricks and cement. Therefore, what causes an increase in indoor radon levels is the increase in humidity. Decreasing temperature, regardless of relative humidity, increases the radon levels indoors.

Furthermore, in a study by Mahat (2001) and Arnold and co-workers (2020), it was shown that humidity has an effect on radon emanation and radon activity. Mahat (2001) used a small radon chamber of volume 200 ml to expose electret detector and sun nuclear monitor to a radon atmosphere generated by a monazite sand. The response of the electret dosimeter showed increasing levels of relative humidity correlated to increasing levels of radon activity concentration in the chamber as seen in Figure 2.6. However, for the sun nuclear detector, the increasing humidity levels kept the radon activity concentration at constant ranges of 20 Bq/m^3 to less than 40 Bq/m^3.

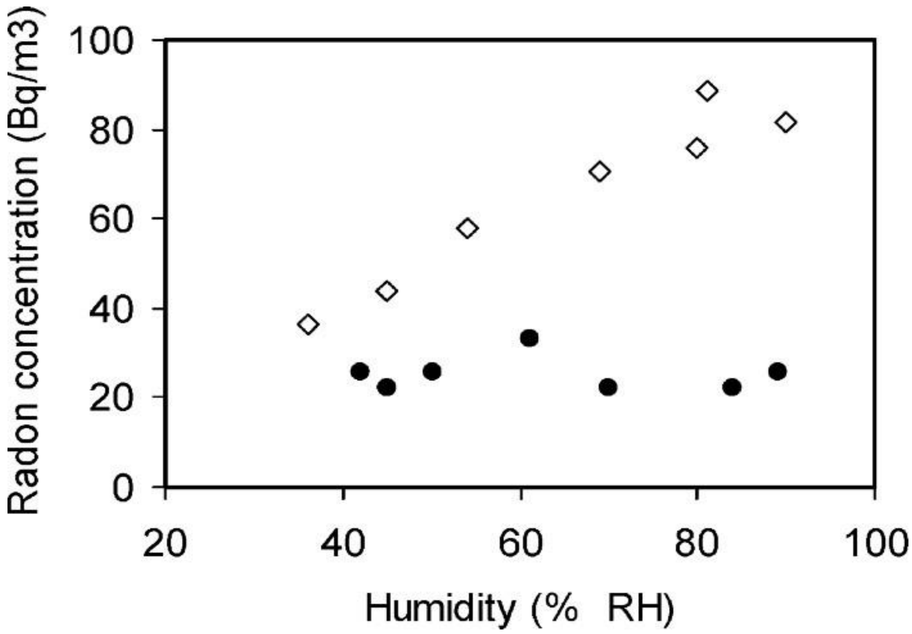

Figure 2.6: Radon concentration and humidity (Electret dosimeter response represented by a transparent dice spot and Sun nuclear monitor response represented by a black dot) (Mahat et al., 2001).

A study by Arnold and co-workers (2020) with the aim of evaluating the influence of environmental parameters on the emanation power of a designed radon source discovered that the decrease of humidity, lowers the emanation power of the radon source. As seen in Figure 2.7, a drop of humidity from 100 % to 60 % has an effect on the gradual decrease of the emanation power of the source from 0.85 to 0.75 with respect to time (Arnold et al., 2020).

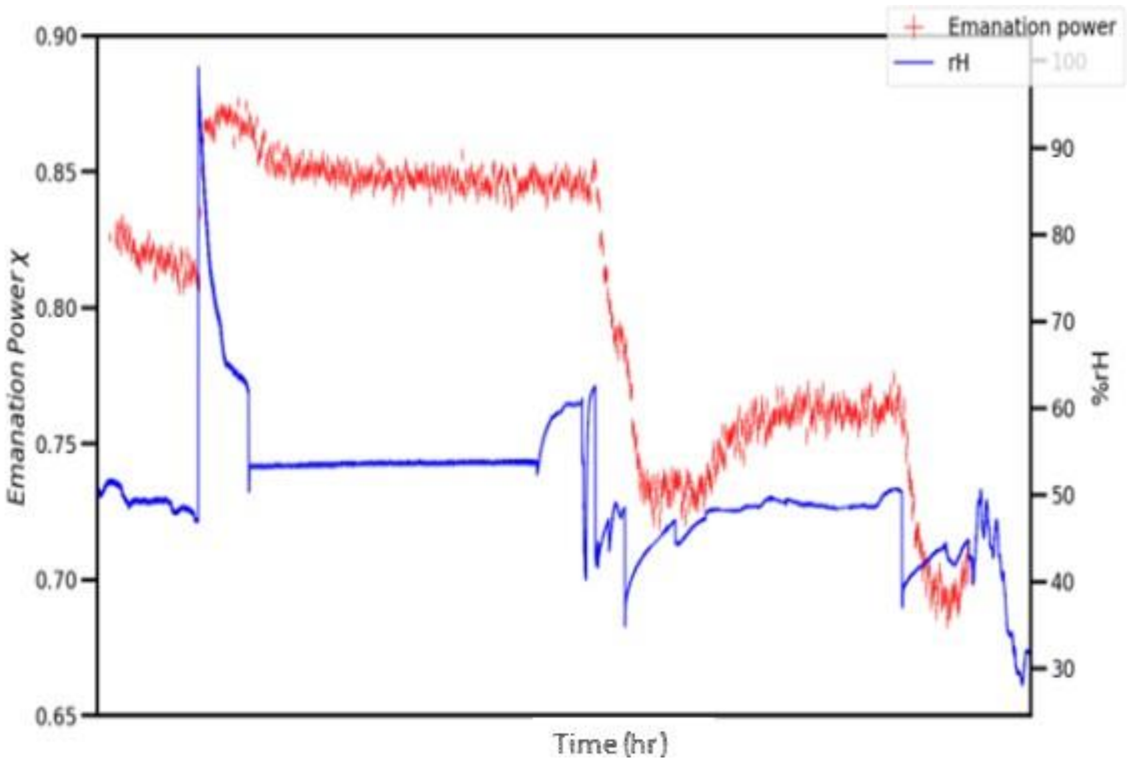

Figure 2.7: The relationship between relative humidity and emanation power of a radon source over a period of time (hours) (Arnold et al., 2020).

2.7 Radon sources and measurement

Radon is produced from the natural radioactive decay of uranium in soil and uranium rich rocks. It is present as a gas in groundwater, ground cracks and produced air. For radon studies, radon is extracted from radium and is measured with various instruments. The purpose of radon sources is to generate a standard and well-known radon activity concentration inside chambers. Shweikani et al. (1995), in their newly designed chamber for calibrating solid state nuclear detectors, used 1.5 kg of uranium ore (pitchblende) as a source of radon. To measure the accumulation of radon in this chamber, a silicon surface barrier detector was used to get the counts of the decay of radon and daughters (^{218}Po, ^{214}Po) for a period (Shweikani and Raja, 2005). As chambers are designed differently, radon is emanated differently, some emanate radon outside their main chamber and inject it in their main chamber. One such chamber is an exposure chamber made by Radioisotope Unit at the university of Hong Kong (Leung et al., 1992). This exposure chamber has the conditioning chamber and the main chamber. Radon gas, water vapour and aerosol are mixed in the conditioning chamber, after being mixed they are injected into the main chamber where exposure takes place. While the National Institute of

Radiological Science (NIRS) walk-in radon chamber radon gas emanates from ceramic sources of ^{226}Ra located outside of the chamber.

In some chambers, especially of small size, dry radium (^{226} Ra) is used without being mixed with other solutions. At the University of Kebangsaan in Malaysia, an airtight chamber was constructed to determine the emanation and activity of radon. The radon source used was a mineral called xenotime in quantities of 0.15 kg, 0.25 kg and 0.50 kg. Xenotime has a high concentration of the radioactive radium, which decays to radon. In these airtight chambers, radon was generated by exposing the xenotime to air in the chamber that is the same as air outside the chamber. The radon in the chamber was measured by a continuous radon monitor (Khalid et al., 2014).

2.8 Homogeneity and radon leakage

Homogeneity in the chamber is a state of constancy of radon concentration achievable by air-tightness of the chamber that minimises the loss of radon gas. In other words, all the positions in the chamber must be of the same radon concentration. The methodology of testing the homogeneity of radon concentration in the chamber was proposed by Heidary et al. (2011), whereby CR-39 detectors were put in different locations of the chamber to determine the uniformity of radon concentration in the chamber in different locations. Afterwards, CR-39 detectors underwent a chemical etching process with 6.2 NaOH at 70 ºC for six hours to get the track counts by an optical microscope. The track density obtained is proportional to the radon concentration in the chamber. It was found that the CR-39 track counts were the same and that the radon concentration in the chamber is the same in all locations.

2.8.1 Radon leak test

Radon leakage is the gradual or sudden loss of radon gas due to the faulty conditions encountered in a designed chamber. Besides the conditions of the chamber in terms of design, factors that lead to radon leakage may arise from a personnel entry during examination of devices under calibration test and monitoring of environmental parameters.

Strategies to hinder radon leakage include the use of tightening material namely glycerine, silicon rubber and O-ring for joints connected to the chamber (Janik et al., 2009). The use of silicon rubber for tightening of joints for connection was put in practice by Janik and co-workers (2009) and Hosoda and co-workers (2007) with National Institute of Radiological Sciences (NIRS) radon chamber system consisting of a connection of a stainless-steel tank and radon measuring system. Also, silicon glue was used by Heidary et al. (2011) to attach plexiglas windows to the chamber's structure as seen in Figure 2.8 where a double door lock system plays an important role in restricting radon leakage. The radon chamber used by Heidary et al. (2011) consists of a solenoid valve connected to the vacuum compressor pump that moves radon back and forth. The vacuum compressor pump that pumps lost radon to the chamber and sustains the radon in the chamber.

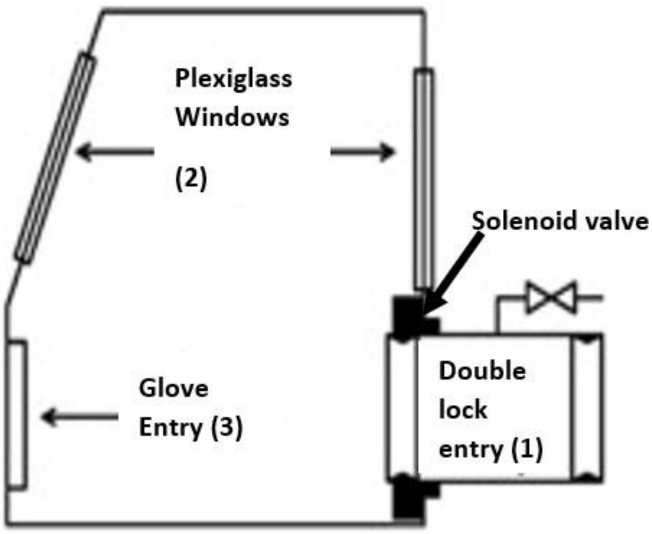

Figure 2.8: A design of an airtight chamber, that maintains the radon atmosphere (1) Double door lock system.(2) Plexiglas windows (3) Glove Entry (Heidary et al., 2011).

Furthermore, with regard to radon leakage, some materials used in the design of the radon chamber can cause a decrease in the radon concentration. Such materials include tubes used for tightening joints or connections; chambers where such tubes were had a leakage rate as shown in Table 2.1, which is determined by radon concentration with respect to time (Radebe, 2019).

Table 2.1: Variation of leakage rate and various tubes with diameter and thickness (Radebe, 2019).

Type of tube	**Tube diameter and thickness (mm x mm)**	**Leakage rate *L* (Bq m^{-3} h^{-1})**
Open emanation source	8 x 2	79.2 (8)
Silicon rubber	8 x 3	72.6 (12)
Silicon rubber	9.6 x 1.6	73.4 (10)
Norprene	10 x 2	30.6 (8)
Tygon	5.3 x 1.5	16.4 (6)
Polyethylene	8 x 2	11.8 (4)
PVC	9 x 4	6.36 (12)
High pressure	10 x 2	6.13 (12)
Gas burner	8 x 3	4.13 (16)
PVC	10 x 1	2.18 (10)
Teflon		0.55 (8)

2.8.2 Radon leakage determination

Prediction or mathematical modelling of equations of radon build-up activity radon leakage must be developed for evaluating radon activity and the expected output. Moore and Kearfott (2005) stated that in an airtight chamber, the activity of radon is calculated by:

$$A(t)_{Rn} = A_{Ra}(1 - e^{-\lambda_{Rn}\,t}) \qquad (2.16)$$

where, the radon activity is $A(t)_{Rn}$ and A_{Ra} is the radium source activity and λ_{Rn} is the decay constant of radon.

Moore and Kearfott (2005) further stated that when the chamber is not airtight, radon leaks from the chamber, the activity of radon is calculated as:

$$A(t)_{Rn} = \frac{A_{Ra}}{\lambda_{Rn}+\lambda_{leak}}\left[1 - e^{-(\lambda_{Rn}+\lambda_{leak})t}\right] \qquad (2.17)$$

where, λ_{leak} is the leak constant. In an airtight chamber, if the radon emanation source is removed, the radon concentration inside the chamber decreases. The decrease in radon concentration is calculated by:

$$A(t)_{Rn} = A(t_0)_{Rn}e^{-(\lambda_{Rn})t} \qquad (2.18)$$

Where, $A(t)_{Rn}$ is the radon activity at time t, $A(t_0)_{Rn}$ is the initial radon activity. A radon leaking chamber's radon activity can be calculated using equation (19), when the radon emanation source is removed:

$$A(t) = A(t_0)_{Rn}e^{-(\lambda_{Rn}+\lambda_{leak})t} \qquad (2.19)$$

A small airtight chamber designed by Khalid et al. (2014) was tested for radon leakage by sticking a tissue on the outer edges of the chamber to check the wetness of the tissue when blue dye water filled the chamber.

A plastic chamber designed by Lucas and Markun (1992) was tested for radon leakage by enclosing it in a tank. The determination of the leakage in their designed chamber was by evaluation of the difference of radon concentration in the tank and plastic, assuming that the radon in the plastic bag is of a known concentration. Therefore, an increase in the ^{222}Rn activity of the tank indicates a leakage of ^{222}Rn from the plastic bag.

The studies carried out by Abo-Elmagd (2014) and Syam co-workers (2020), showed that the radon leakage from the radon chamber can be determined by ventilation. In both studies, a radon source was used to generate radon in the chamber and then the radon source was removed from the chamber for determination of decay curves. Syam and co-workers (2020) used ^{226}Ra soil as a radon source and measured the decay curve using the RAD7 monitor as seen in Figure 2.9. Then, ^{222}Rn activity concentration in a chamber is calculated as:

$$\frac{dC_L}{dt} = -(\lambda + \lambda_v)C + \lambda_v C_0$$

$$C_L = \left[C_b - \frac{\lambda_v c_0}{\lambda+\lambda_v}\right] e^{-(\lambda+\lambda_v+\lambda_b)t} + \frac{\lambda_v c_0}{V(\lambda+\lambda_v)} \qquad (2.20)$$

C_b stands for initial ^{222}Rn concentration, C_L is the ^{222}Rn concentration in Bqm^{-3} with leakage, C_0 is the background ^{222}Rn concentration in the laboratory, C is the radon concentration inside the chamber at time *t*, the leakage rate is λ_v and the ^{222}Rn decay constant is symbolised as λ (Syam et al., 2020).

The theoretical initial slope for the decay curve with leakage is expressed as M_L depicted in Figure 14 (Abo-Elmagd, 2014, Syam et al., 2020).

$$M_L = \frac{dC_L}{dt_{t\to 0}} = -(\lambda + \lambda_v)\left[C_b - \frac{\lambda_v C_0}{\lambda + \lambda_v}\right]$$

$$M_L = -C_b\lambda - \lambda_v(C_b - C_0) \qquad (2.21)$$

The experimental initial decay curve M_I is given by:

$$C_1 = C_b e^{-\lambda t}$$

$$M_I = \frac{dC_I}{dt_{t\to 0}} = -C_b \lambda \qquad (2.22)$$

Finally, the leakage rate λ_v by both theoretical decay curve and measured experimental decay curve as seen in Figure 2.10 given by (Abo-Elmagd, 2014; Syam et al., 2020).

$$\lambda_v = \frac{M_I - M_L}{C_b - C_0} \qquad (2.23)$$

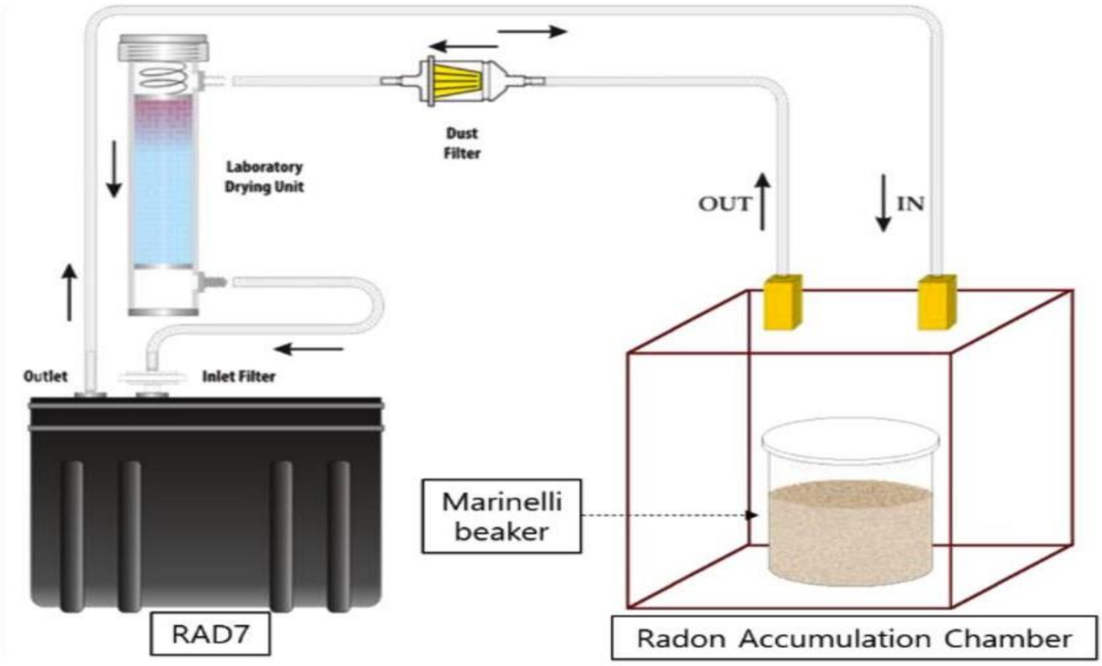

Figure 2.9: ^{222}Rn leakage determination in an accumulation chamber (Syam et al., 2020).

Figure 2.10 depicts the graphical representation of the leakage rate of the chamber by comparing the theoretical decay curve with the measured decay curve. The ^{226}Ra soil sample was placed in the accumulation chamber and the ^{222}Rn concentration was measured with RAD7. The soil sample was removed and ^{222}Rn was measured to determine the leakage rate of the accumulation chamber.

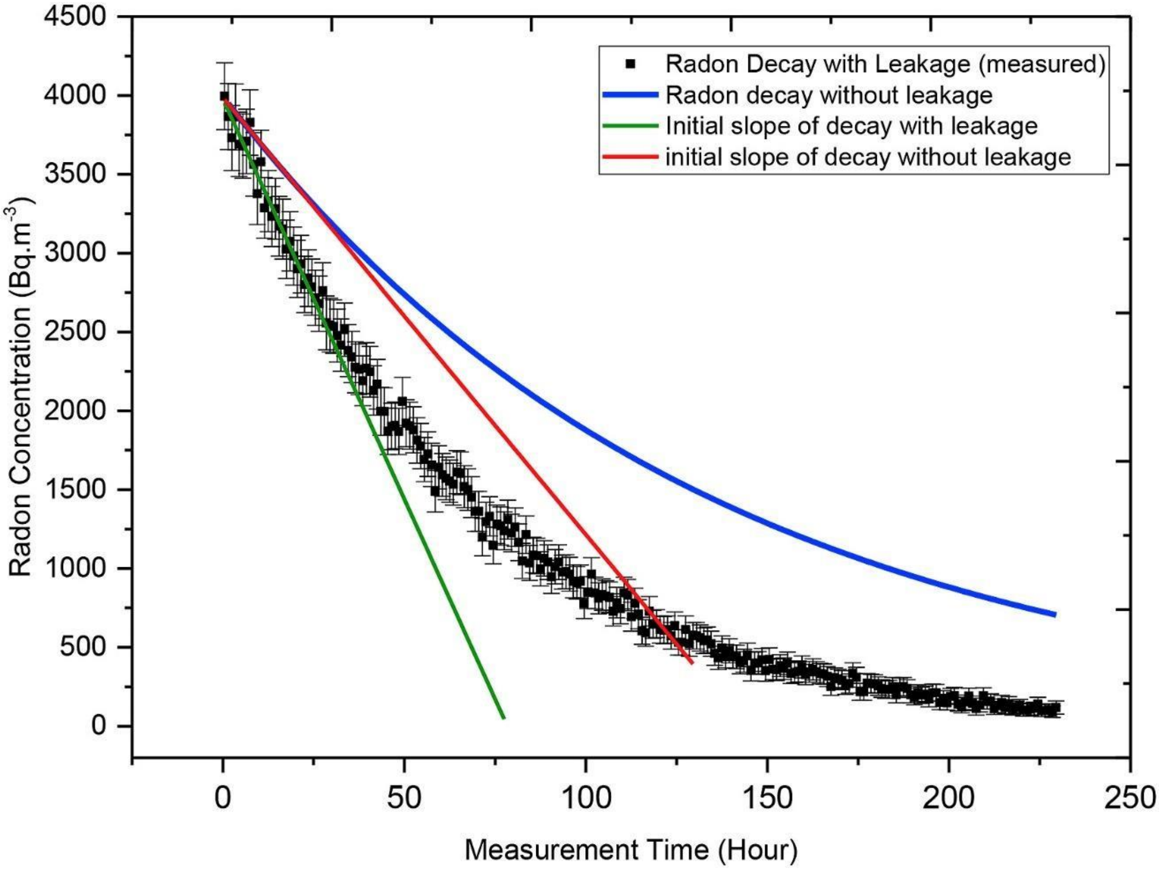

Figure 2.10: Radon chamber leakage rate determination (Syam et al., 2020).

2.9 Calibration and intercomparison

Calibration of a radon detector is an activity of necessity that must be conducted over time to minimise errors of inaccurate radon measurement in any field. For attainment of quality results during the calibration activities, it is necessary that a steady flow of radon concentration is kept together with constant environmental parameters (Kim et al., 2013). During calibration activity, various detectors that are active and passive, are exposed to a radon concentration, active detectors give results quickly while passive detectors take time to give results based on the duration of the measurement activity.

2.9.1 Calibration by a steady flow of radon

During calibration with a steady flow method of radon, different flow rates are used and the time for calibration of radon monitors is less than that of radon accumulation in the chambers. Radon accumulation chamber are chambers that allow the increase of radon within the chamber and the continuous measurement of radon at any time (Kotrappa and Stieff, 2012). Steady flow method provides fast calibration for instance, the chamber volume of 50 L by Taheri (2013) reaches a constant radon level within 150 min, ready for calibration with different flow rates ranging from 0.8l / min to 2.2l / min as seen in Figure 2.11.

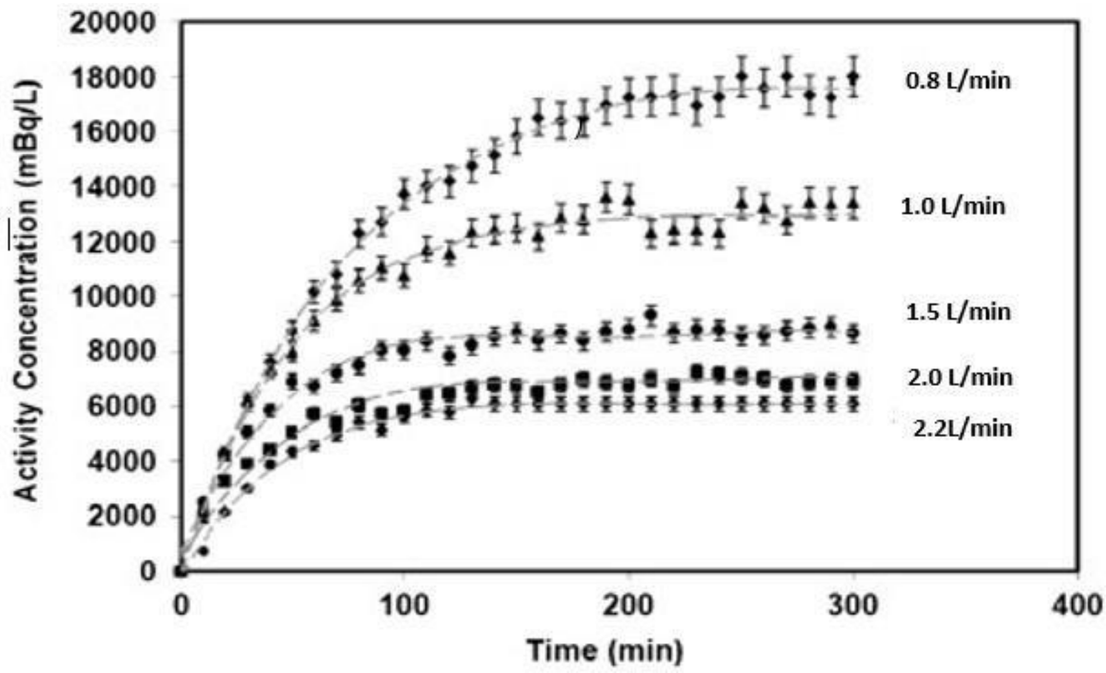

Figure 2.11: Calibration with steady flow of radon (Taheri, 2013).

According to the Figure 2.11, it is clear that with a 50 L chamber, the high radon concentration activity is obtained with less flow rate and a lower radon concentration activity is obtained with a high flow rate. Higher flow rates from 1.5 L / min to 2.2 L / min results in the radon activity concentration becoming steady after 100 minutes in the chamber. Lower flow rates of 0.8 L / min and 1.0 L / min results in the radon activity concentration becoming steady as from 200 minutes.

The calibration procedure begins with the introduction of one or more radon monitors into the radon chamber for exposure to a constant flow of radon activity emanating from a NIST standard source. The radon activity concentration is measured and recorded according to flow rates during the radon exposure period. Table 2.2 shows an example of radon calibration with a constant flow of radon at varying flow rates, where two radon monitors are compared to a

NIST radon standard source by calculating their ratios to the standard radon source (Kotrappa and Stieff, 2012).

Table 2.2: Different flow rates for calibration. NIST DC is the emanated radon activity. AG is the Aphalguard measured radon concentration. BG is the background and FT is the Femto Tech detector measured radon concentration (Kotrappa and Stieff, 2007).

Flow rate (l min^{-1})	**NIST (Bq m^{-3})**	**NIST DC (Bq m^{-3})**	**AG-BG (Bq m^{-3})**	**AG-BG / NIST DC (Bq m^{-3})**	**FT-BG (Bq m^{-3})**	**(FT-BG) / (NIST DC) (Bq m^{-3})**
0.104	1097	1046	1013	0.969	985	0.942
0.203	562	549	576	1.050	606	1.104
0.392	291	287	280	0.977	289	1.007
0.607	188	186	190	1.023	191	1.027
0.796	143	142	144	1.009	141	0.993
0.961	119	119	118	0.993	126	1.059

2.9.2 Reference devices

Reference devices play a role in calibration activities by being a point of references when calibrating non-calibrated radon devices. Reference devices from a primary radon chamber or secondary radon chamber are of use in calibrating other radon devices, this is seen in the work of Irlinger (2015). The steel pot chamber by Irlinger (2015) consisted of two radon devices and a radon source namely pitchblende. The calibration plan was that two reference devices exposed to a radon concentration in an airtight chamber must have similar measurement or a difference that is less compared to the known radon source, in order for them to be used as reference devices to calibrate other detectors in various chambers.

2.9.3 Intercomparison

Intercomparison is an activity test of comparison of radon monitors by laboratories to check, maintain or adjust the radon monitors under test to a known radon activity concentration by a trusted national or international radon laboratory. Intercomparison begins by the selection of a calibrated radon monitor that is calibrated from a primary national reference standard laboratory, and then the calibrated radon monitor is used as a transfer standard whereby it is sent to other laboratories, that are designed in such a way that they have System for Test Atmospheres with Radon (STAR) (Zeeb et al., 2009). Zeeb and group (2009) defines STAR as an "acronym used to designate the equipment needed for the creation and use of an atmosphere containing a reference concentration of radon". The transfer standard with other radon monitors is exposed to the radon atmosphere and measurements are done in order to check the measurement error of devices under test subject to the transfer standard. The role of a transfer standard is to check traceability of devices under test to a national reference standard. Errors identified by the reference laboratory of radon monitors under test, are used to rectify discovered errors of radon monitors under test (Miller, 2020).

During intercomparison exercise, the host entity receives radon monitors from participating laboratories. The host entity exposes radon monitors to certain levels of radon atmosphere, then it returns the radon monitors to the participating radon laboratories without giving them the results. The participating laboratories, after exposing their radon monitors to certain levels of radon activity, return their results to the host laboratory. The host laboratory sends a report of their results in comparison to the participating laboratory results.

In radon intercomparison exercises, data analysis between the reference laboratory and participating laboratory is done by indexes such as zeta-score, z-score and percentage difference. Rabago et al. (2020) states that the zeta score is "the statistical index used to compare intercomparison results where the uncertainty in the measurement results is included." It is determined by the following equation:

$$\xi = \frac{E_i - E_{ref}}{\sqrt{u^2(E_i) + u^2(E_{ref})}} \tag{2.24}$$

where, E_i is the laboratory results arithmetic mean, in terms of radon exposure. E_{ref} stands for reference values and $u(E_i)$ is the participating laboratories radon uncertainty measurement. While $u(E_{ref})$ is the radon measurement uncertainty by the reference device (Rabago et al., 2020). If $\xi \leq 1$, the results are satisfactory and if $\xi > 1$, the results are not satisfactory. Cardellini et al. (2016) defines ξ as the number performance level.

The z-score is the standardized measure of the performance determined by using participating laboratory results, expressed as follows:

$$z_i = \frac{(E_i - E_{ref})}{\sigma_\rho} \qquad (2.25)$$

where, σ_ρ is the "standard deviation proficiency assessment chosen as a target for the intercomparison exercise" (Cardellini et al., 2016).

The difference between a participant's test data and the reference value, divided by the reference value, and multiplied by 100 is the percent difference (PD) performance statistic (Janik, 2017). It is given by:

$$PD[\%] = \frac{(C_{lab} - C_{ref})}{C_{ref}} X100\% \qquad (2.26)$$

where, C_{lab} is each laboratory's average radon concentration and C_{ref} is the average radon concentration by a reference measured in the radon chamber (Janik, 2017).

Furthermore, data analysis for intercomparison by Miller (2020) is based on the performance classification scheme or ranking scheme, which is described by parameters such as :

- percentage biased error, which is basically for measuring the bias of the measurement
- percentage precision error, which is defined as the precision of the measurement measured as a percentage precision error
- percentage measurement error, which combines the percentage bias error and percentage precision error.

$$percentage\ biased\ error = \frac{Measured\ mean - Reference\ value}{Reference\ value} X\ 100 \qquad (2.27)$$

$$percentage\ precision\ error = \frac{Standard\ deviation}{Measured\ mean} X\ 100 \qquad (2.28)$$

$$percentage\ measurement\ error = \sqrt{percentage\ biased\ error^2 + percentage\ precision\ error^2} \qquad (2.29)$$

Moreover, Miller (2020) ranked or classified the performance of participating laboratories measurement error exposures individually from; A which is classification for best performance and F which is for worst performance as seen in Table 2.3. For each exposure, each participating laboratory was assigned a classification ranging from A to F as seen in Table 2.3. The following are the criteria for each of the classification groups.

Table 2.3: Performance classification (Miller, 2020).

Range of measurement error (%)	**Performance classification**
less than 10%	A
greater than or equal to 10% and less than 20%	B
greater than or equal to 20% and less than 30%	C
greater than or equal to 30% and less than 40%	D
greater than or equal to 40% and less than 50%	E
greater than or equal to 50%	F

2.9.3.1 Preparation of the radon monitors for measurement

The radon monitors calibration validity is evaluated, whereby host institution for calibration have databases with radon monitor's names that help with checking whether the instrument is within calibration range. For active radon monitors, all accessories needed for using the radon monitor or that will be needed for sampling in the field are checked (Iovine et al., 2022). Also, memory for storing data especially for active radon monitors is checked. Furthermore, internal intercomparison measurements, intercomparison of procedures and techniques, background checks of devices before going to the field are conducted.

For passive radon monitors, it is important to check whether the monitor is well packaged to avoid any measurement errors that may be caused by contamination, during transport or in transit. For field work it is necessary to choose a suitable radon detector instrument that has a barcode or labelling for example SSNTD LR-115, CR39 or charcoal detectors. For the charcoal detectors, the mass of the detector before and after the field trip/work are measured.

2.9.3.2 Use of intercomparison results in laboratories

The use of intercomparison results received from a host institution that conducted calibration exercises to the participating laboratory is important as accuracy assessment can be validated. Other benefits that the participating laboratory include detection of systematic errors, identification of the need for equipment maintenance or verification. Systematic errors are errors that occur repeatedly during calibration, and they cause a high or low bias in the measurement results. Other important points include the ability to monitor human errors that may occur during sample preparation or handling. Furthermore, the performance of the laboratory can be evaluated and, if the laboratory performance of radon monitors received from intercomparison test is unsatisfying, recalibration can be done.

2.9.3.4 The use of calibration results

Calibration results can be used to get the calibration factor, which is necessary for tuning the calibrated device using the correction factor to test if the instrument is measuring accurately. Calibration results help when using the background value and sensitivity of the instrument at different activity levels of exposure. The software used for radon monitors to retrieve data can be updated with new calibration data and the old calibration data can be compared with the new calibration data.

2.10 Quality assurance of ^{222}Rn of measurements

To ensure quality, reliability, traceability of data, certain control measures have to be evaluated namely:

- background measurements,
- duplicate or collocated measurement,
- calibration measurement,
- inter-laboratory comparisons,
- routine instrument performance checks.

2.10.1 Background measurements

Continuous use of both active and passive detectors increases the background activity of the detector. Therefore, detectors must be assessed annually to detect the background of activity that accumulated. Radon progenies, in the detectors reach equilibrium namely, ^{210}Bi and ^{210}Po, as ^{210}Po increase, resulting in the increase of the background activity concentration of the detectors (Röttger et al., 2021, Sukanya et al., 2022). Therefore, the sensitivity of the detector is limited and it affects the results (Pelczar et al., 2021).

2.10.2 Calibration measurements

Calibration of both active and passive detectors must be conducted annually and periodically by authorized personnel in manufacturer's laboratory. Critical steps to be followed in the process comprise of:

- comparison check of voltage at critical points in the circuit,
- inspection of the condition of the batteries, whether they need to be recharged or replaced,
- evaluation of discriminator settings for correction or adjustment,
- running background measurement in a radon free air and exposing the detector to known activity concentration of radon atmosphere.

2.11 Radon chamber design in different continents

Europe

The Government Office of the Capital City Budapest (BFKH) in Hungary is equipped with a radon calibration chamber of volume 840 L. The chamber is made of a stainless steel and has a radon source, nitrogen gas, pump, computer for controls and data processing as seen in Figure 2.12 (Pierre et al., 2021). Prior to use, after being sealed, the radon measurement system was flushed with nitrogen gas. Two-position electronic valves are utilized to link the chamber and a buffer tank to a flow-through ^{226}Ra source, which is employed as a radon source to generate radon at a desired activity concentration. In addition, in order to prevent the concentration from falling below a certain concentration, the radon gas is automatically fed into the chamber by opening the valves using a computer-based controller unit (Tamakuma et al., 2023). The homogeneity of the radon gas in the chamber is through two internal fans, the calibrated Alphaguard radon monitor measures the ^{222}Rn activity. The chamber can maintain relative humidity at 20 - 80 %, ^{222}Rn activity concentration at 100-5,000 Bq m^{-3} and temperature at 15 – 60 ºC.

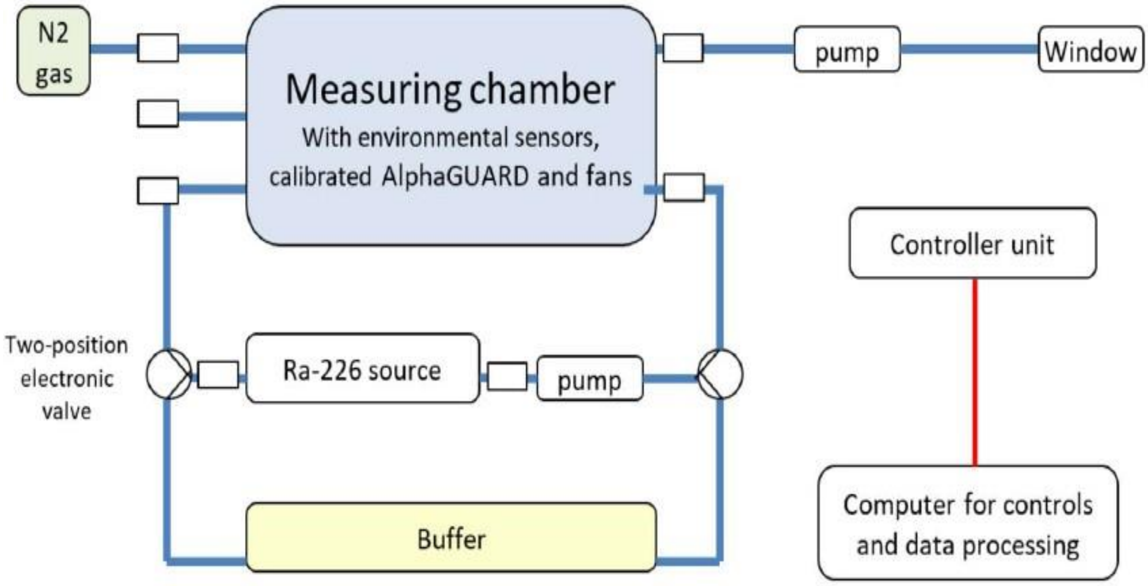

Figure 2.12: Budapest, government office radon chamber scheme (Pierre et al., 2021).

In Poland, at the Central Laboratory for Radiobiological Protection, a walk-in radon chamber was constructed. The chamber has an internal volume of 12.38 m^3, and consist of a viewing window, manipulating gloves, input ports for radon injection as seen in Figure 2.13. The chamber has two flow-through ^{226}Ra sources of activity 137 kBq connected externally on the opposite sides of the chamber. ^{222}Rn atmosphere transferred to the chamber is maintained by continuous pumping of radon ^{226}Ra (Mamont-Cieśla et al., 2010). The temperature in the chamber is controlled at the range of 10 °C to 60 °C and relative humidity at 10 % to 95 %. The maximum radon activity reached by the two ^{226}Ra is 50 000 Bq.

Figure 2.13: Walk-in radon chamber (Mamont-Cieśla et al., 2010).

In Slovak Republic, a radon calibration chamber was established at the Slovak Institute of Metrology (SMU) with the aim of using the Alphaguard as a secondary standard, to offer traceability to other laboratories (Blahušiak et al., 2020). The chamber is a horizontal stainless-steel cylinder with a diameter of 0.8 m, length of 2.0 mm and internal volume of 1.0 m^3. The source used to generate radon is a dry flow through source which contains radium salt, and is manufactured by Czech Metrological Institute (Blahušiak et al., 2020). As shown in Figure 2.14, the radon chamber is connected to the personal computer (PC), continual monitor of radon (CMR) and Lucas cell (LC) for point sampling. The chamber is equipped with a pTHf monitor for processing and storing thermodynamic parameters such as pressure, temperature and relative humidity. In order to ensure the tightness of the chamber during operation, its standard working pressure is set between 980 to 990 hPA. Homogenous radon atmosphere is achieved by fans installed (Tamakuma et al., 2023).

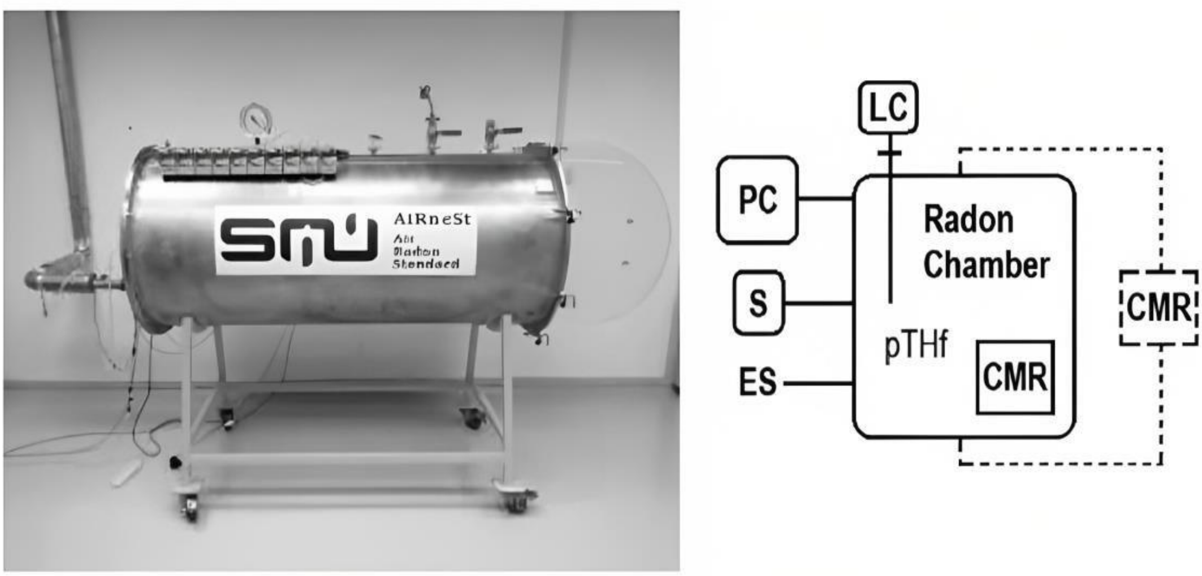

Figure 2.14: Slovak Institute of Metrology, radon chamber (Blahušiak et al., 2020).

Asia

In Kuwait, at the College of Technological Studies, a radon chamber from Genitron was used for calibration. The radon chamber has a volume of 101 L, height and diameter of 67 cm and 45 cm, respectively. The upper lid of the radon chamber is removable for introduction and removal of radon monitor and other peripherals such as fan and electrical cables for power supply to radon monitors and data transfer (Al-Azmi, 2009). The upper lid has ports and inlet and outlet valves for the flow of radon in and out of the chamber. The steel belt as shown in Figure 2.15 assist in sealing the lid during measurements. The Alphapump is used to draw radon from the ground at a ground-depth of 0.5 m using soil probe. The drawn radon is transferred to the radon reservoir tanks of differing volume of up to 20 L. An hour is taken before filling the chamber, to allow the short-lived thoron gas to completely decay. Radon reservoir tank have two plastic tubes which have Quick-Lock coupling connector on its opening. The lock connectors are made up of tube nipple and tube coupling, as well as internal valves that instantly close when the clutch disengages. The lock connectors play a role of preventing radon leakage during the filling of the radon reservoir and the transfer of radon to the chamber (Al-Azmi, 2009). The Alphaguard radon monitor is used in flow mode during the filling of the radon reservoir and in diffusion mode, when placed in the chamber.

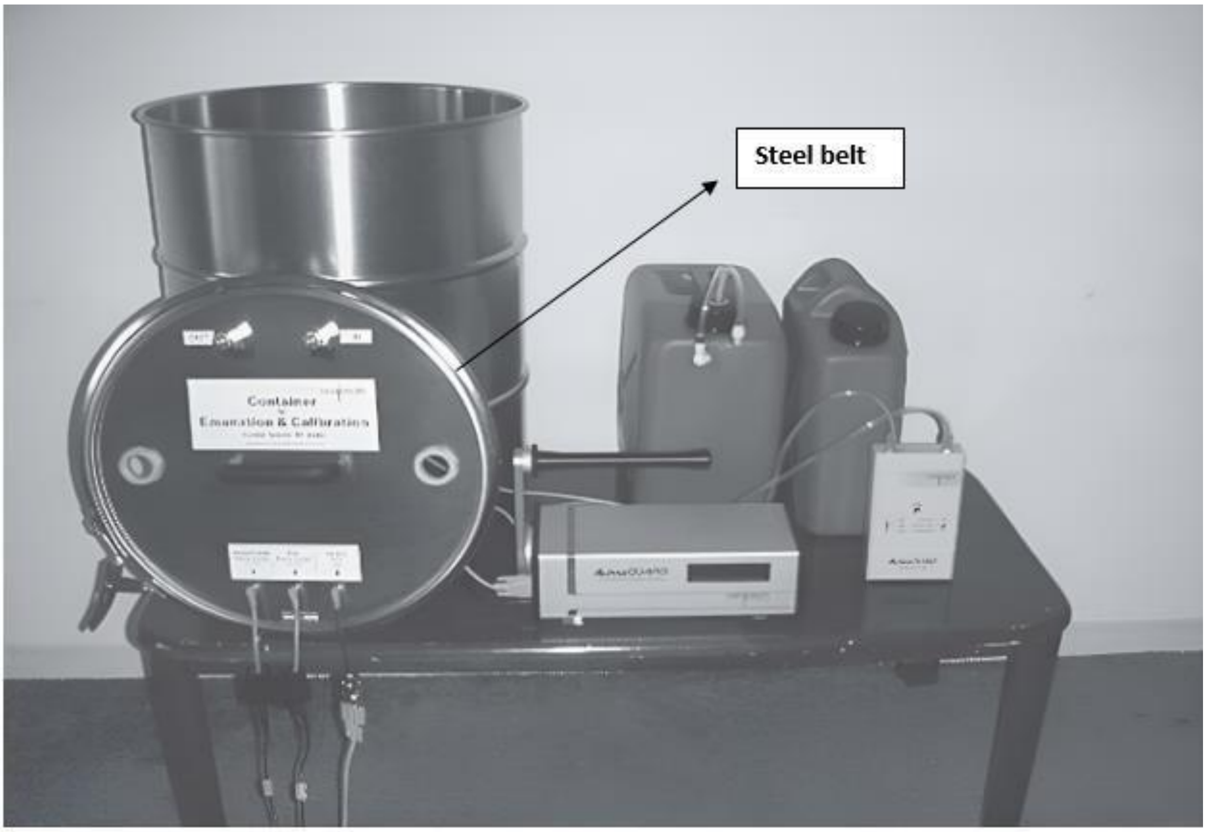

Figure 2.15: Radon chamber with radon reservoir tank (Al-Azmi, 2009).

In Malaysia, at the University of Kebangsaan, a radon chamber was constructed for the determination of radon activity using a continuous radon monitor (Sun Nuclear model 1029). The chamber is made of Perspex material of 0.006 m thickness and has an internal volume of 0.07 m^3. To ensure airtightness of the chamber, silicon glue was utilized to affix the pieces of the Perspex material together (Khalid et al., 2014). The chamber has a door with a handle and two-key mechanism; for insertion and removal of samples and devices, as seen in Figure 2.16. At the edges of the door, plasticine was applied to enhance the airtightness of the chamber. The radon atmosphere is generated by the xenotime mineral and is measured at hourly intervals for 96 hours.

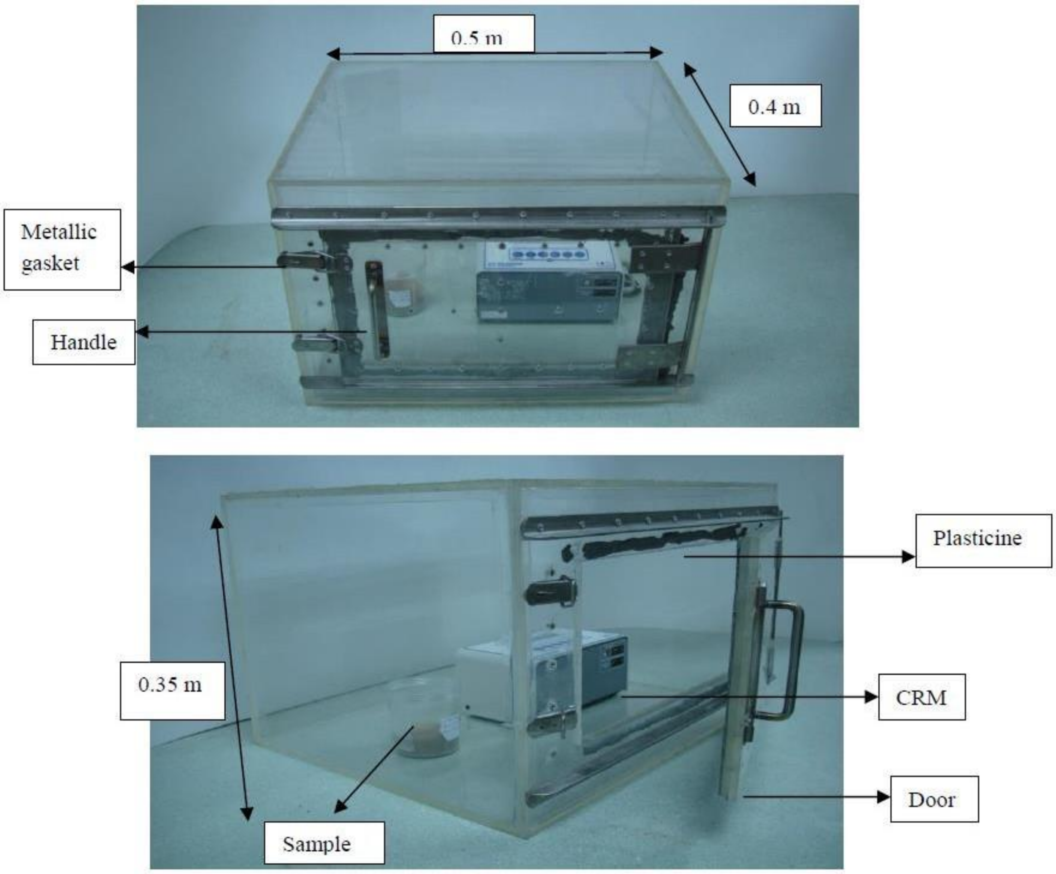

Figure 2.16: Radon chamber with xenotime sample and continuous radon monitor (Khalid et al., 2014).

Africa

In Egypt, at the National Institute for Standards, a radon chamber was designed for accurate measurements of radon. The chamber is made of a firm corrosion resistant 1 mm stainless steel and is parallelepiped shaped with a volume of 0,05 m^3. During the experiment, the hygrometer, barometer and thermometer are employed to measure relative humidity, pressure and temperature, respectively within the chamber (Abo-Elmagd, 2014). The exposure shutter, situated at the top side of the chamber in Figure 2.17 is used for insertion of animals to be exposed to a radon atmosphere. Uranium ore is used as a radon source and the Alphapump is used to monitor the radon activity inside the chamber. The two electric fans are used for homogenizing the radon atmosphere.

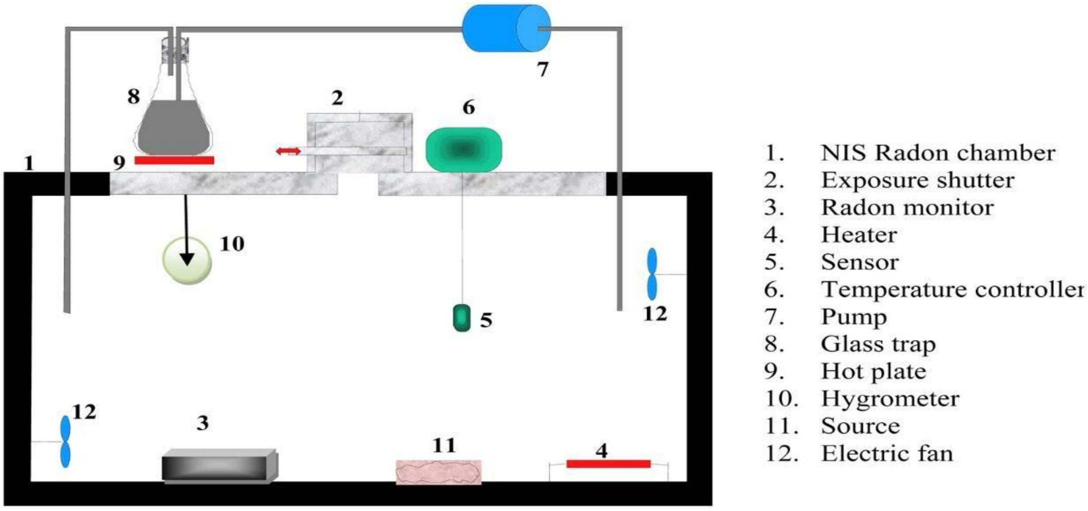

Figure 2.17: Radon chamber at Egypt, National Institute for Standards (Abo-Elmagd, 2014).

CHAPTER 3: METHODOLOGY

The construction of the radon chamber and its use for calibration of radon detector are presented in this chapter. Also presented are brief descriptions of the features of the major devices and materials used, including the radon detectors, Alphapump, power supply, radon source, etc.

3.1 Radon chamber

The radon chamber wall is made of 6x10^{-3}m thick sheets of perspex materials. Six perspex sheets were joined together to form a rectangular box of volume 0.5 m^3 with dimensions of 0.8 m (length) x 1 m (breadth) x 0.6 m (height) as is seen in Figure 3.1. On the frontal side of the chamber there is a door of length 0.46 m and width 0.32 m, which was used for the insertion of the radon source, radon monitors, electrical wires and the Alphapump. The door has two hinges and four locks; plasticine was applied on the edges on the door for airtightness of the chamber (Khalid et al., 2014). Figure 3.1 depicts the materials that were added to the radon chamber in the grey shade after it was airtight. The Mecer inverter acted as a power supply to electrical equipment during power-cuts.

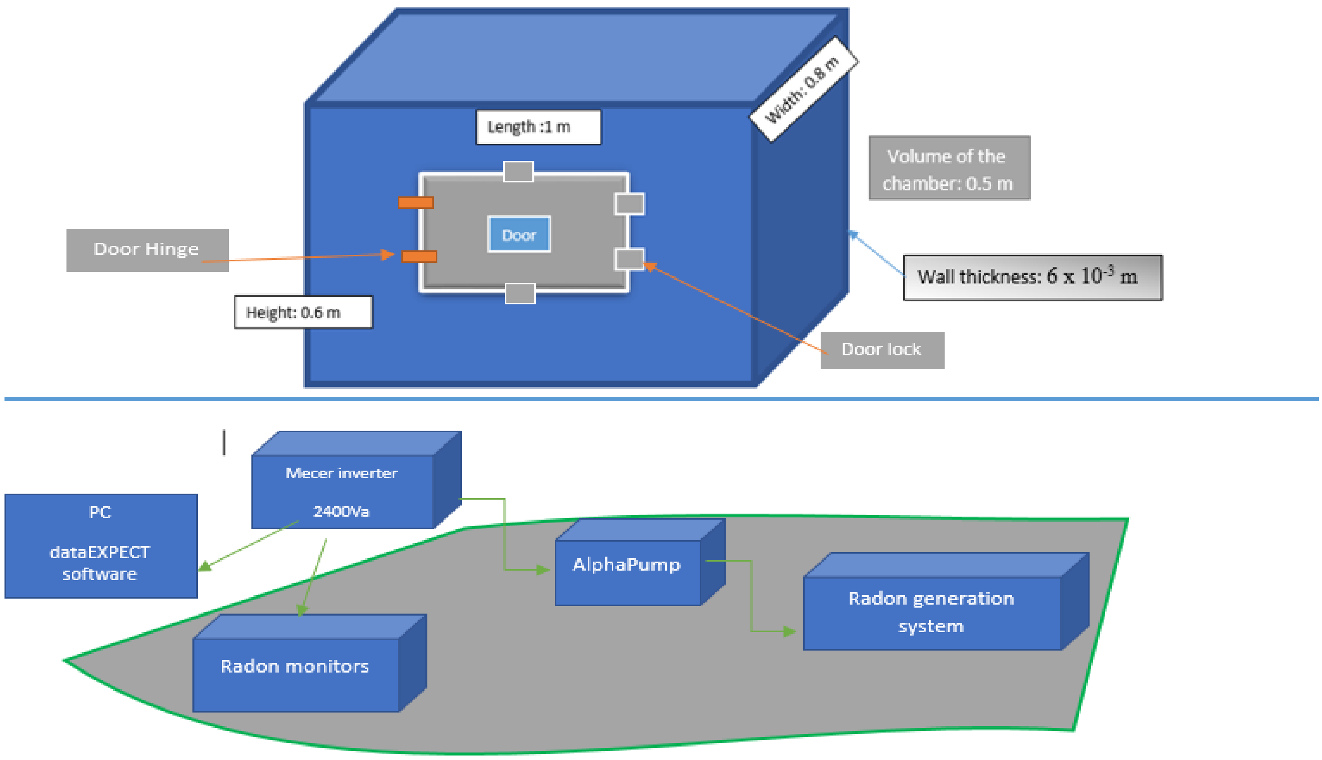

Figure 3.1: Radon chamber design at the CARST.

The decision to use the Perspex sheet material was influenced by the chamber constructed by Khalid and co-workers (2014), in Chapter 2 section 2.11. The Perspex sheet material has high impact resistance, good chemical resistance and good weatherability. Depending on its use, the Perspex sheet material could be employed at temperatures ranging between -30 °C to 90 °C (Plastic, 2023). Depending on the measure of its thickness, ionizing radiation such as alpha particle, beta particles, X-ray and gamma radiation can be blocked (Altuglas, 2006). Therefore, the Perspex sheet is suitable for study.

3.1.1 State of the previous radon chamber

In the earlier study (Radebe, 2019), soil was used as the radon source and brown tape was used as sealant as seen in Figure 3.2. The Perspex sheet, also known as acrylic sheet, tends to expand when there is an increase in humidity or temperature (Acme, 2022) while, it tends to contract in dry or cold conditions. It was observed that the door of the chamber was not linear but curved, and there were gaps as a sheet of paper passed by the door in Figure 3.2. Necessary steps were taken to minimise the radon leakage.

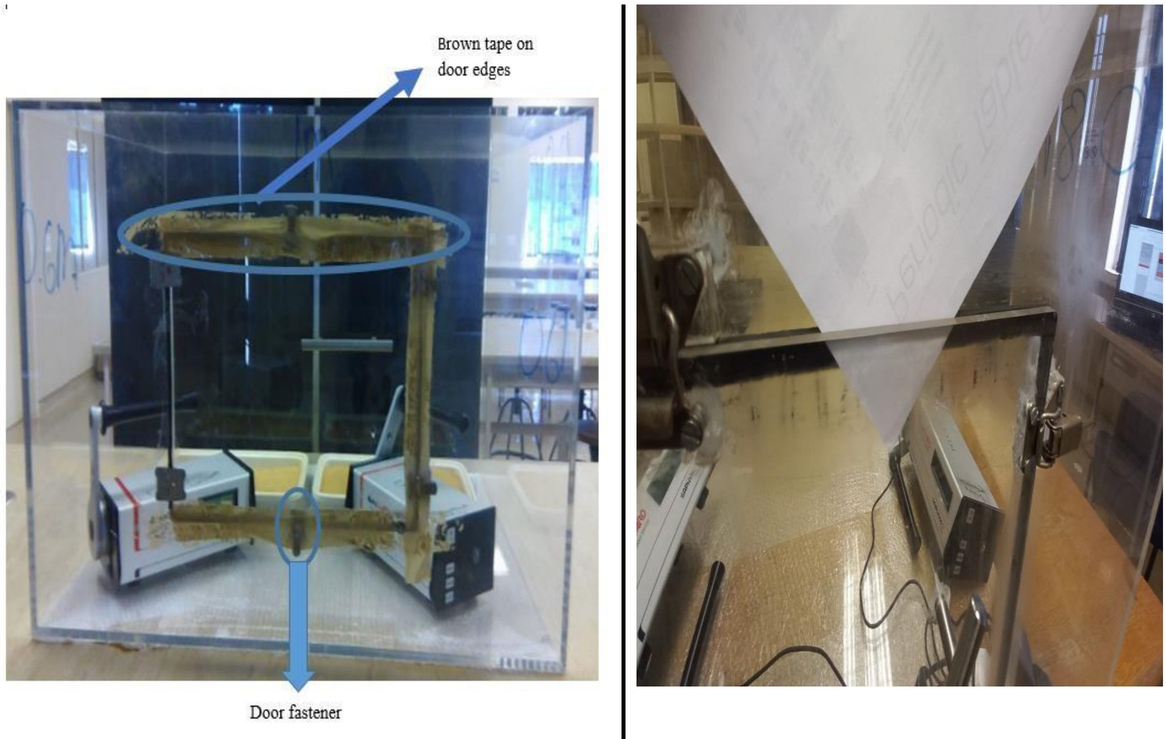

(a) Radon chamber with two Alphaguards for measuring radon activity from the soil	(b) ^{222}Rn escaping points due to gaps on the door

Figure 3.2: State of the previous radon chamber: (a) brown tape as sealant around the door; (b) gaps along joints.

3.2 Sealing of the chamber

The foam-sealing strip was a manufactured closed-cell sponge strip self-adhesive on one side for use as a sealing strip which is resistant to dust, moisture, light, air, and water. It is suitable for all types of doors, boots, bonnets, canopies, boats, caravans, trailers, motorcycles, vents, windows and roofing. It stops vibrations and serves as an excellent sound dampener and draught sealer. The foam sealing strip and a silicone sealant were used to make the radon chamber airtight.

Figure 3.3: Application of silicon sealant.

The surface where the clear silicon sealant and sealing foam strip were applied was thoroughly cleaned in such a way that the surface was dry and free of grit. Silicone sealant was applied even on the screws that fasten the door and left to dry as shown in Figure 3.3. Then the foam sealing strip was applied slowly on the edges of the door as seen in Figure 3.4 to prevent ^{222}Rn leakage. There were no gaps on door edges, seen even after a month of applying the silicon and foam sealant strip. Therefore, the airtightness of the chamber was increased, to make the chamber suitable for radon detector calibration test.

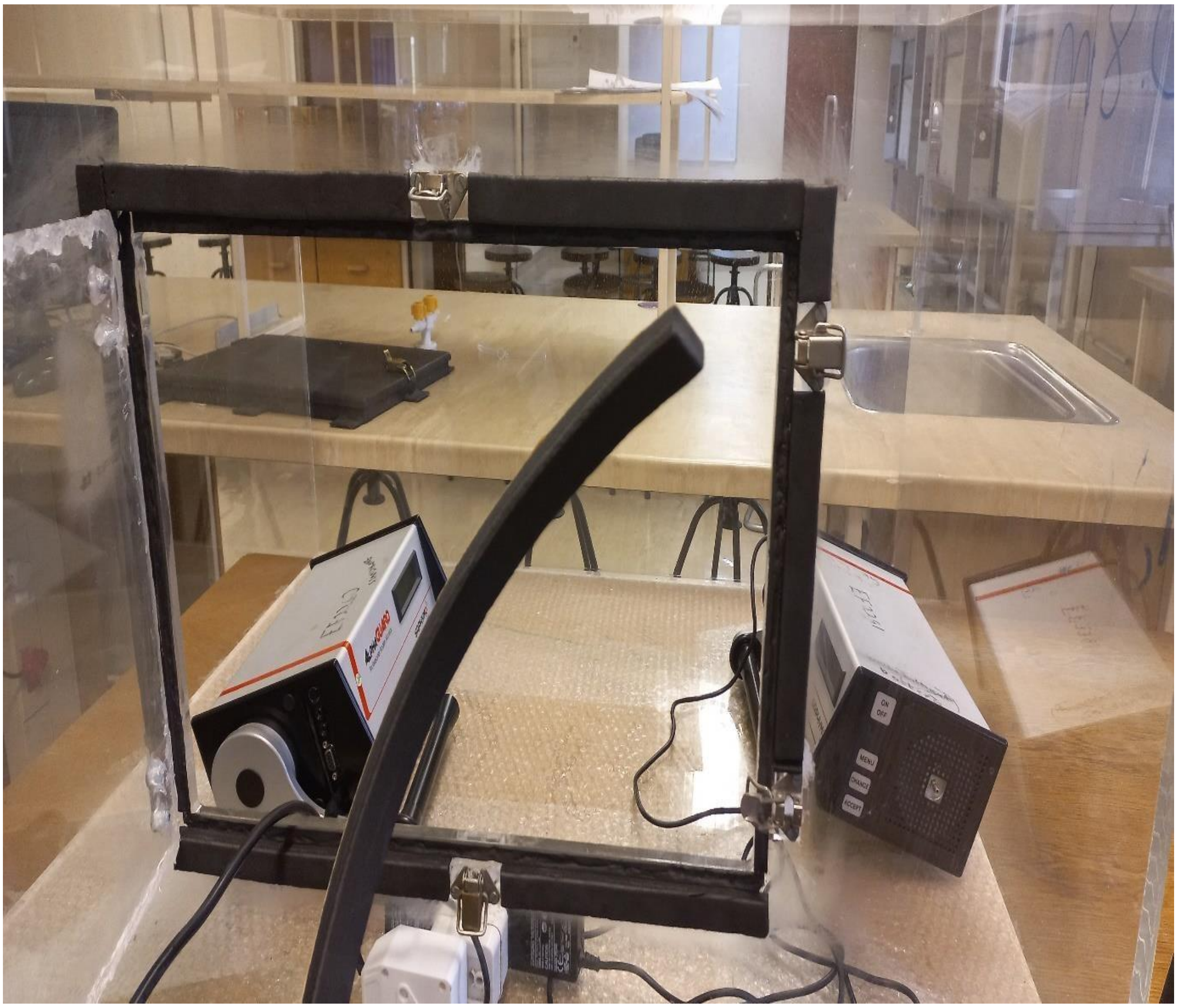

Figure 3.4: Chamber tightness enhancement using foam sealing strip.

The foam sealing strip enhanced the tightness of the chamber, even the sound of the internal noise by the equipment undergoing test lessened.

3.3 Radon chamber set-up

The radon generator system consisted of a glass bottle, centrifugal tube, ^{222}Rn source and inlet tube as seen in Figure 3.5. The glass bottle was filled with 250 ml of distilled water, the lid of the glass bottle has two holes for insertion of the centrifugal tube and inlet tube. A glass beaker was used to precisely measure the amount of water to be used. The two holes on the metallic lid of the glass were drilled with an 18 V Ryobi lithium-ion battery cordless driver driller. The circular holes are good for fitting the inlet tube and centrifugal tube.

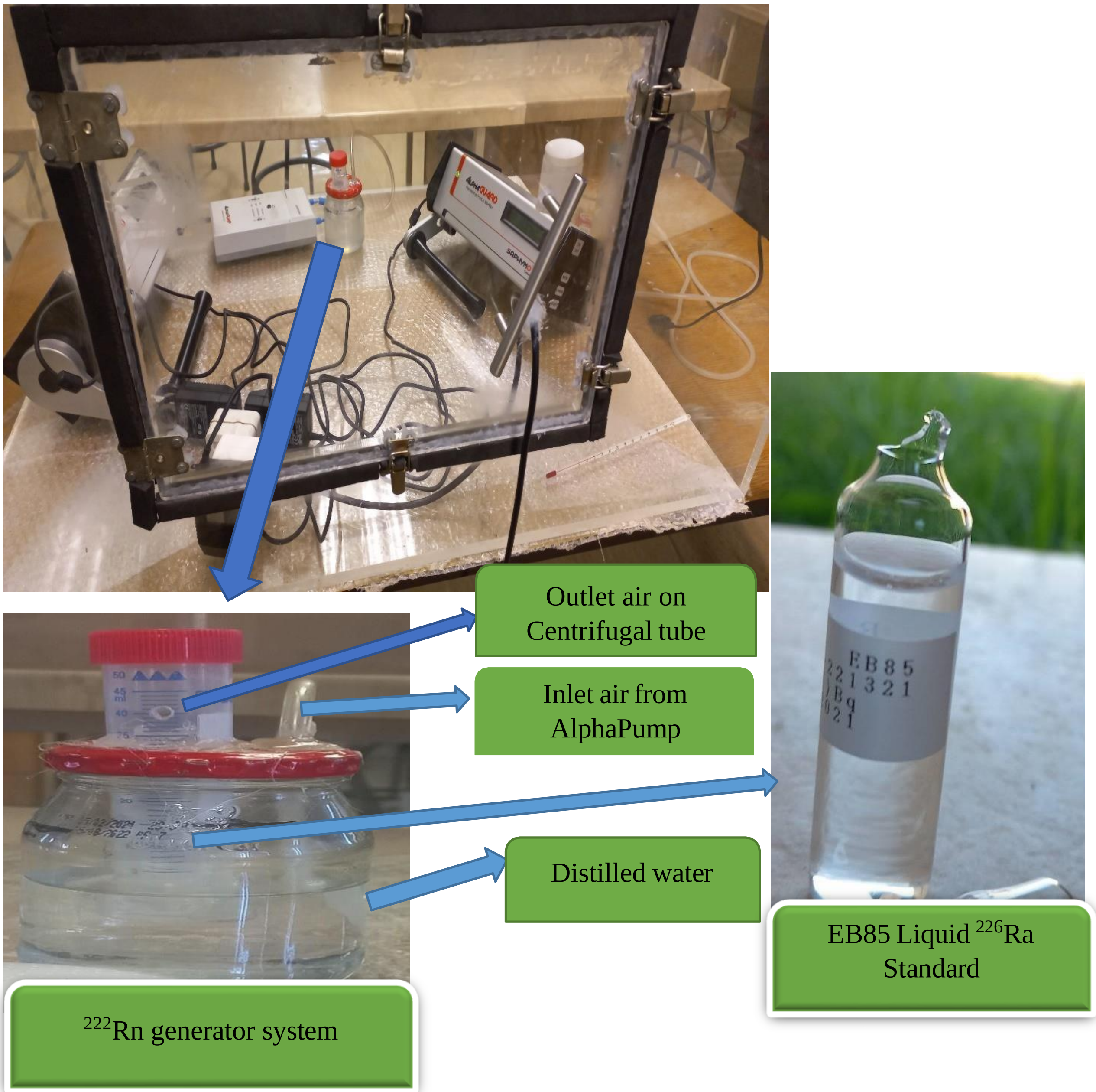

Figure 3.5: Radon chamber setup

The glass bottle volume was 0.00225 m^3 and airtight as no gas escaped from the lid but only on the centrifugal tube outlet hole. A 50 ml centrifugal tube made of polypropylene material, with a skirted conical base shape was used as a ^{222}Rn standard source holder. The centrifugal tube was also drilled to have three holes:

- two holes at the bottom to serve as inlet of pressurized air to bubble ^{222}Rn from the liquid ^{226}Ra source.
- the other hole position was near the top of the centrifugal tube cap. It acted as an outlet, to disperse bubbled ^{222}Rn gas into the chamber, as indicated in Figure 3.5.

Groundwater and surface water contain minerals, pesticides and bacteria. The distillation process of water removes about 99.9% of minerals and other contaminants such as calcium, magnesium, fluoride, lead and chloramine (Bruce Djovak, 2013). Distilled water is good for laboratory use as it is free from most impurities.

Cold glue gun was used to seal the gaps on the outer edges of the circular centrifugal tube and the inlet tube to avoid ^{222}Rn escape. The purpose of spraying glue was to bond the lid and the tubes, such that openings that might lead to leakage were closed.

For uninterrupted measurements during load shedding, a Mecer 2400 VA inverter with two 12 V batteries was used as seen in Figure 3.6 for providing power to the radon monitors and the Alphapump. The room environmental conditions were checked to ensure that Mecer 2400 VA operational conditions of 0 to 90 % humidity and operational temperature of 0 to 40 °C were met. Moreover, the batteries were rated to last 150 – 200 cycles, for occasional stage 1 – 2 of load shedding, the life span of the batteries was two years, for constant stage 2 to 6 the lifespan was a few months (Geewiz, 2018). Therefore, the Mecer 2400 VA inverter was suitable for the experiment as there was also the university power-supply by generators, that took less than 15 min to kick-start during load-shedding.

Figure 3.6: Mecer 2400va inverter for uninterrupted experimental measurements during load shedding.

3.4 Radon monitor

The Alphaguard is a portable measuring instrument for radon activity concentration and is battery operated. The battery is inbuilt and operates for 10 to 15 days of radon monitoring. In addition, it measures the relative humidity, air pressure and temperature using inbuilt sensors. The results are stored in a ring memory, and the last data set is retrievable though the RS-232 interface connected to the PC for data analysis. The Alphaguard has a high detection efficiency, quick response to concentration gradients, long-term maintenance free operation and it utilises 3D alpha spectroscopy. It is insensitive to vibrations and shocks, such that in high humidity areas it provides accurate results. It contains an ionization chamber with a 0.56 litre active cylindrical volume, and when powered, it has an operating voltage of +750 V DC, as illustrated in Figure 3.7. The anode and cathode electrodes make up the ionization chamber.

When the input signal is received via diffusion, a glass filter permits the ^{222}Rn signal to pass through and be processed by the preamplifier unit, which then transfers the signals to the electronic network for digital processing, according to (Saphymo, 2012). It is mostly used in laboratories as a reference device (Bloomberg, 2018, Janik, 2017).

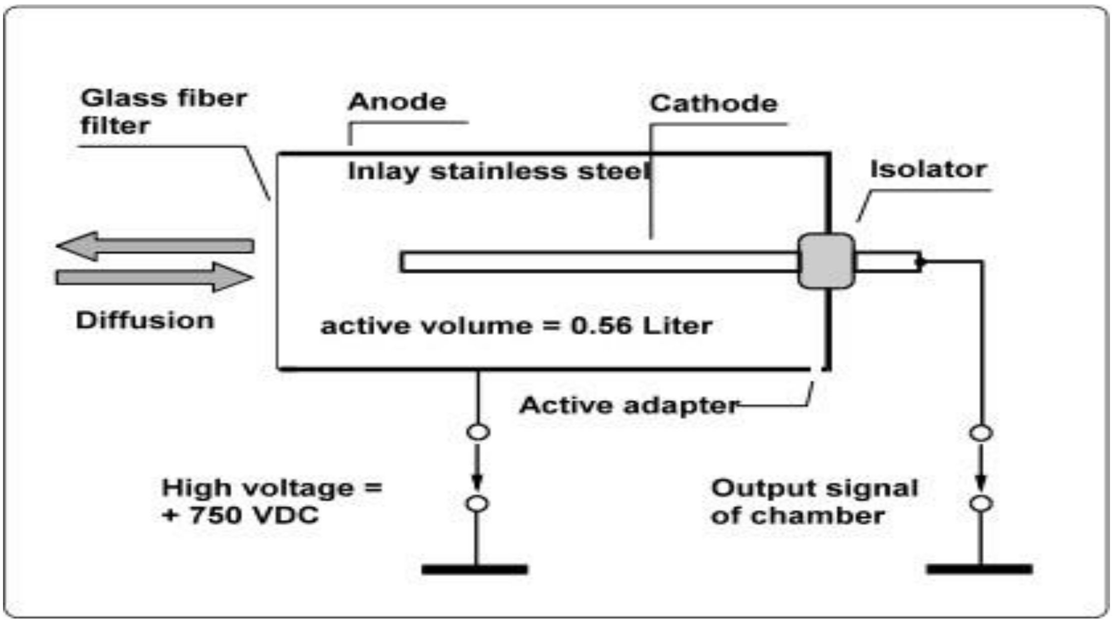

Figure 3.7: The Alphaguard's ionization chamber in a schematic diagram (Saphymo, 2012).

3.4.1 Alphaguard housing

The Alphaguard is made up of aluminum which houses all the electronic parts for measurement operations. The dimensions of the Alphaguard housing are as follows: length: 230 mm; width: 340 mm and height: 120 mm. In Figure 3.8, the Alphaguard is shown to have a multifunctional display which shows the measurement of radon activity concentration with its statistical error bar and climatic parameters are displayed. The operational indicator lamp shows time in terms of hours and days while the measurement is in progress. For hours, if there is a flashing green light, the Alphaguard operational time is more than 75 hours, otherwise there will be a red-light flashing indicating that there is less than 75 hours of operation. If an external battery is connected as a power supply, a green light indicates that there is more than 9 days of operation, if not, a red light will indicate that there is less than 9 days of operation (Saphymo, 2012).

.

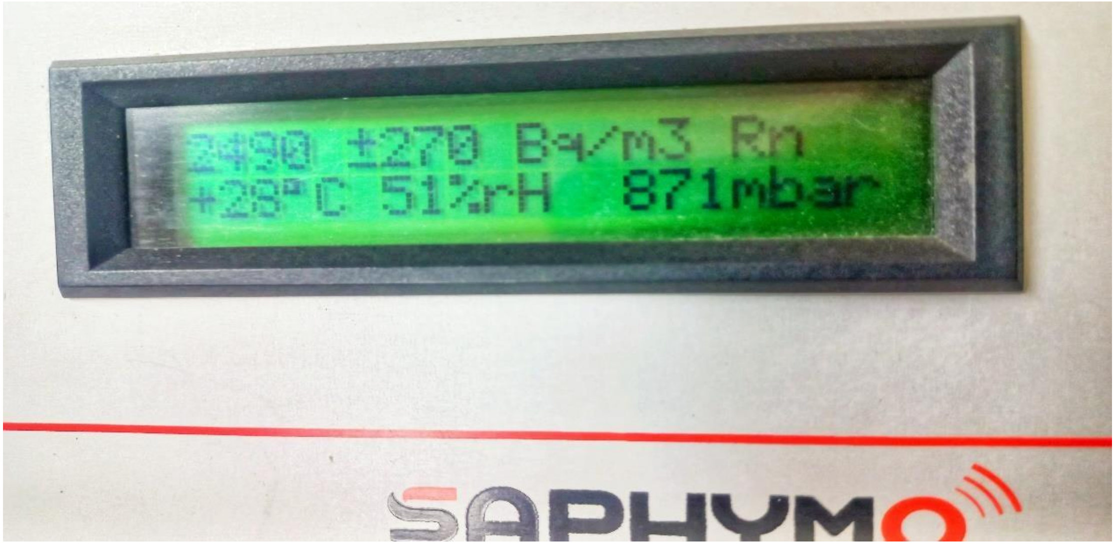

Figure 3.8: Alphaguard dimensions (Saphymo, 2012).

3.4.2 Alphapump

The Alphapump was used to convey the radon gas from the radon standard to the chamber. It is a battery-operated device that is used to pump gases and continuous cycling operations are performed with it.

3.4.3 Airthings Wave Plus monitor

The Airthings Wave Plus monitor (Model 2910, Airthings), was used to measure radon. It gave a detailed report of six air quality parameters, namely:

- humidity
- temperature
- carbon dioxide
- air pressure
- volatile organic compounds
- radon

The Airthings Wave Plus monitor in Figure 3.9 is circular in shape and similar to a smoke detector. It differs from the active radon monitors in a sense that it does not have indicator lights that are on and On mode always. It is portable in such a way that it can be mounted on a wall and placed on shelves.

Figure 3.9: Airthings Wave Plus monitor for radon measurement and other climatic conditions.

On the back of the Airthings Wave Plus monitor there is a removable magnetic plate that could be screwed on a wall, then it easy for the main unit of the monitor to be attached to the wall.

To check the air quality of the location under measurement, a hand was waved in front of the Aithings Wave Plus monitor. After waving as in Figure 3.10, three colors indicated the quality of the air as follows:

- Red indicated a poor air quality
- Yellow indicated a fair quality and,
- Green indicated a good air quality

.

Figure 3.10: Depiction of a good air quality indicating that radon gas levels were below acceptable level.

3.5 Radon source

The radon source (see Appendix A) that was used was EB85 from CMI in Czech Republic, which is a measurement standard in a form of a radioactive solution of ^{226}Ra that emanates a known quantity of ^{222}Radon-gas.

The radioactive solution of ^{226}Ra was stored in the emanation bulb, a glass vessel which allows undisturbed radon accumulation within a 100 % humidity atmosphere. Then the accumulated radon gas is transferred to the container via the gas valves using the gas tight Alphapump. Finally, the measured radon concentration was compared to the activity released by the standard material so that the deviations could be calculated.

3.6 Experimental procedure for calibration

A gas tight electronic Alphapump was used to transfer accumulated radon gas from the radium standard solution (EB85) in the glass bulb, into the radon chamber. The reference radon atmosphere from the radium standard into the radon chamber was from a known activity concentration value of 1860 Bq. The two Alphaguard radon monitors undergoing a calibration test were exposed to the reference radon atmosphere. Comparison between reference radon standard values and the two values of the Alphaguard radon monitor were observed and necessary adjustments to align the radon monitors to the reference standard were made. The Alphaguard was turned off and the Airthings Wave Plus monitor was also exposed to the reference radon atmosphere, to study the behaviour of radon and environmental conditions after reaching stabilisation for a period of 40 days as depicted in Figure 3.11.

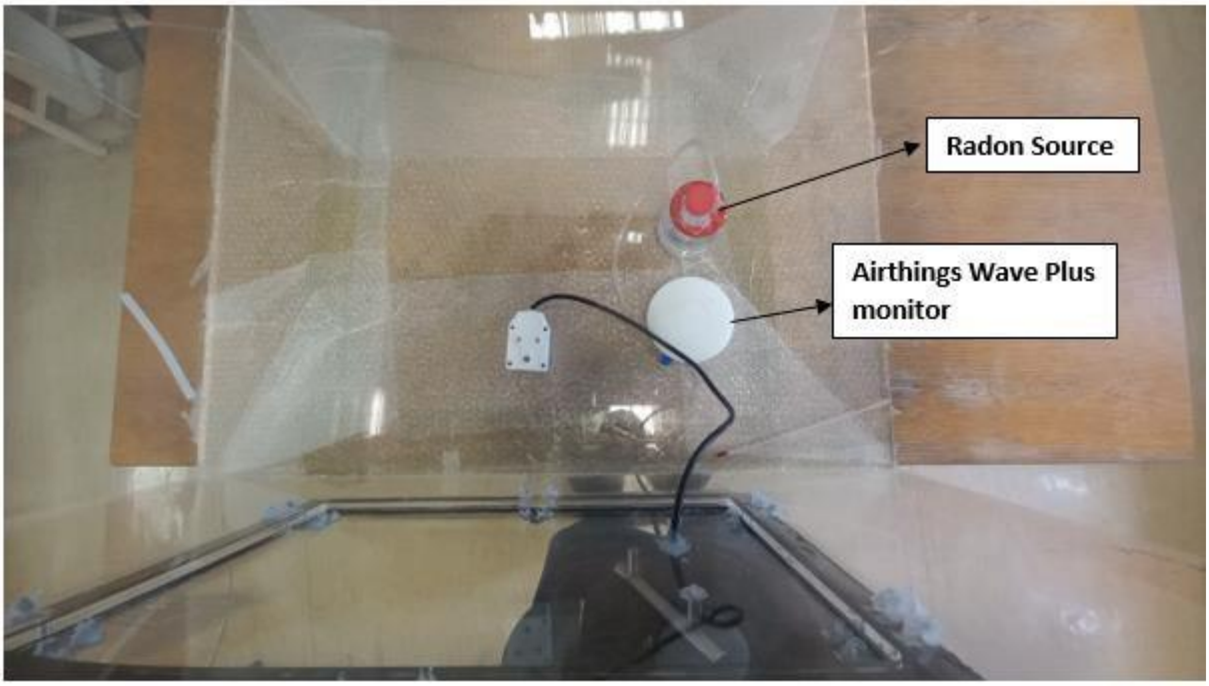

Figure 3.11: ^{222}Rn activity measurement after a period of 40 days.

3.7 Data analysis

The DataEXPECT software and Airthings App were used to collect raw data of ^{222}Rn activity concentration, relative humidity, temperature and pressure, from the two Alphaguard and Airthings Wave Plus monitor (Saphymo, 2012; Airthings, 2023). Microsoft Excel spreadsheet was used to analyse the data and to plot graphs of the behaviour of environmental conditions and ^{222}Rn activity concentration radon.

3.7.1 Theoretical and experimental curve for calibration

The Bateman equation was used to obtain the ^{222}Rn activity concentration from the parent nuclide, ^{226}Ra (liquid ^{226}Ra EB85 standard solution). The computed curve of the radon ingrowth obtained for a period of forty days was tabulated and used as a calibration curve. The experimental curves of the two Alphaguard were compared against the calibration curve. The calibration factor was obtained, which consists of the average activities of the two Alphaguard and the average activity of the reference radon standard, expressed as:

$$K = \frac{C_{ref}}{C_{lab-}C_0} \tag{3.1}$$

where K is the calibration factor, C_{ref} is the standard reference average ^{222}Rn activity, C_{lab} is the average measured from the Alphaguard and C_0 is the background radon activity of the chamber.

For determining tightness of the chamber, the average air pressure from the Airthings Wave Plus monitor was compared with the average air pressure from the two Alphaguard.

Percentage deviation was also computed to determine the deviation from the standard source as:

$$PD[\%] = \frac{(C_{avg} - C_{avgref})}{C_{avgref}} x100\% \tag{3.2}$$

where, C_{avg} is the average ^{222}Rn activity measured by the Alphaguard, and C_{avgref} is the average ^{222}Rn activity by the radon standard source.

3.7.2 Homogeneity of radon in the chamber

From Section 2.8, uniformity of radon is achieved through measurement of radon in different locations in the chamber. Due to the design of the chamber, two Alphaguards used could be in ground positions in the chamber. Therefore, the period taken for radon activity to stabilise was evaluated, as assurance to uniform radon activity in an accumulation type of radon chamber.

3.8 Radon leakage rate

The EB85 radon standard was placed in the chamber for less than 6 hours, and it was removed. The radon activity concentration was measured continuously with time, and it was this data which was used to obtain the initial radon concentration, which was used to determine the initial slope for the ideal decay curve with no leakage (M_I), initial slope for decay curve with leakage (M_L), and leakage rate (λ_v)from section 2.8.2, equation 21 to 24. The background radon concentration of the laboratory was measured.

CHAPTER 4: RESULTS AND DISCUSSIONS

This chapter outlines the procedural results obtained in the radon chamber calibration process. Theoretical and experimental values were compared to calibrate and evaluate the performance of the radon chamber. Results of calibration tests with Alphapump operating and turned off were observed and necessary derivations of the nature of the radon chamber and performance of radon detectors were interpreted.

4.1 Theoretical estimate of radon standard values

From Section 3.7.1, a radium liquid solution with an activity of 1.86 kBq traceable to CMI measurement system of ^{226}Ra was used to estimate ^{222}Rn activity for a period of 40 days. The estimated ^{222}Rn activity concentration values were used as theoretical radon standard values for comparison with experimental values in Table 4.1. The Bateman equation (Chapter 2, Section 2.1.2.1) was used to determine the ^{222}Rn ingrowth, shown in Figure 4.1.

Table 4.1: Results for the theoretical ^{222}Rn curve for calibration.

Period (Days)	**Time (Days)**	**Theoretical ^{222}Rn activity curve (kBq)**
1	86400	0.64
2	172800	1.18
3	259200	1.62
4	345600	2.00
5	432000	2.31
6	518400	2.57
7	604800	2.78
8	691200	2.96
9	777600	3.11
10	864000	3.24
11	950400	3.35
12	1036800	3.43
13	1123200	3.51
14	1209600	3.57
15	1296000	3.62
16	1382400	3.66
17	1468800	3.70
18	1555200	3.73
19	1641600	3.75
20	1728000	3.77
21	1814400	3.79
22	1900800	3.80
23	1987200	3.81
24	2073600	3.82
25	2160000	3.83
26	2246400	3.84
27	2332800	3.85
28	2419200	3.85
29	2505600	3.85
30	2592000	3.86
31	2678400	3.86
32	2764800	3.86
33	2851200	3.87
34	2937600	3.87
35	3024000	3.87
36	3110400	3.87
37	3196800	3.87
38	3283200	3.87
39	3369600	3.87
40	3456000	3.87

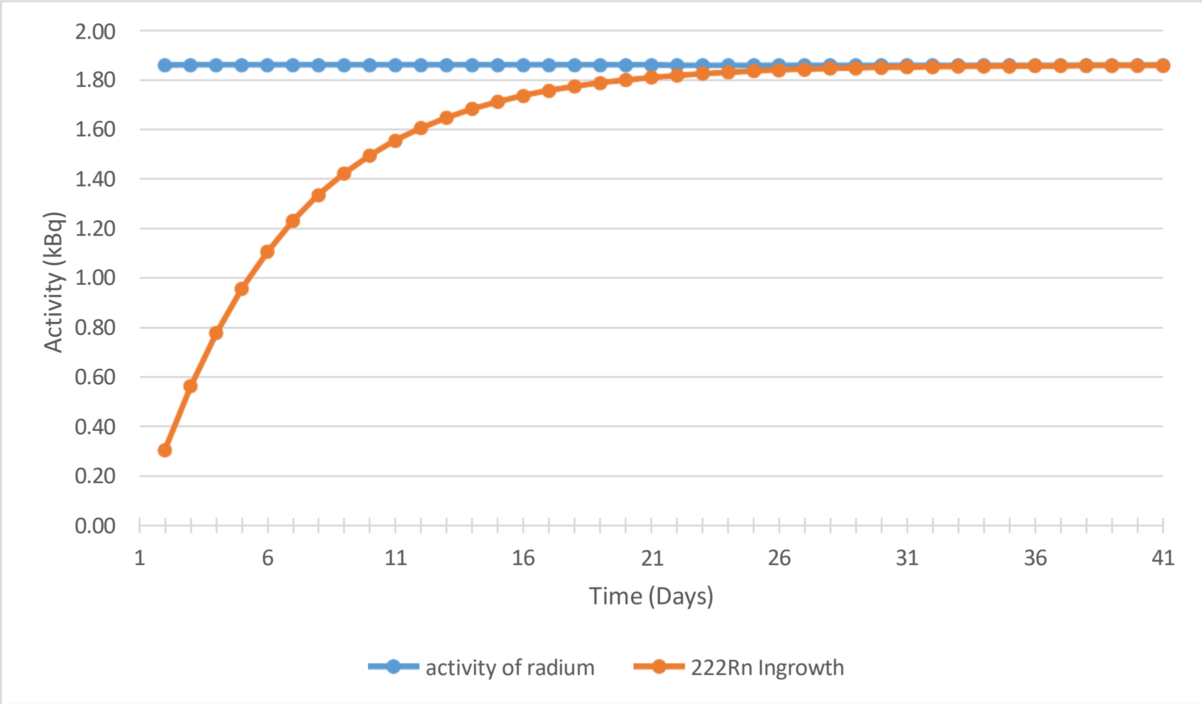

Figure 4.1: Secular equilibrium of nuclides 1.86 kBq liquid ^{226}Ra source and ^{222}Rn.

In secular equilibrium (Section 2.2.1), ^{222}Rn activity grows to equal the activity of the parent ^{226}Ra, as shown in Figure 4.1, from day 28 and onward. However, the figure does not truly estimate the activity of ^{222}Rn that would have been accumulated in a chamber of volume 0.5 m^3 over a period of 40 days. Hence, the activity of ^{222}Rn was divided by 0.5 m^3 to estimate the concentration of ^{222}Rn in the chamber over a period of 40 days, as seen in the Figure 4.2.

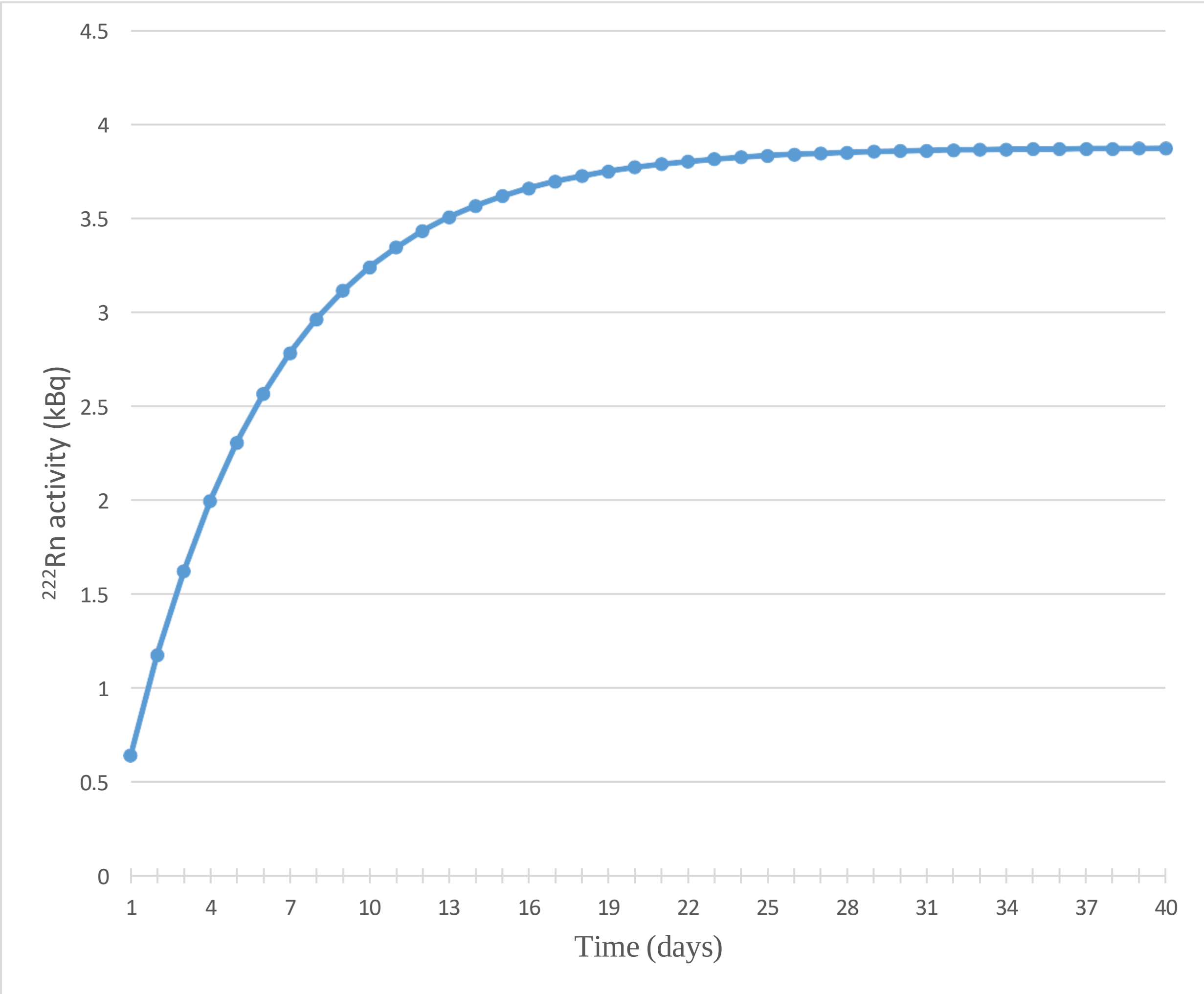

Figure 4.2: ^{222}Rn ingrowth obtained from Bateman equation used as the theoretical radon calibration curve.

The expected behavior of the radon monitors under test is theoretically depicted in Figure 4.2. The curve was used as a standard radon calibration curve to calibrate and determine deviation of radon monitors under test from the standard ^{222}Rn source values.

4.2 Calibration of radon monitors

Two Alphaguards with calibration error of ± 3% (see Appendix B) were exposed to a ^{222}Rn atmosphere for a period of 40 days, to determine their proximity to the ^{222}Rn standard source calibration curve values. According to Figure 4.3, the two Alphaguards under test were not fluctuating a lot and behaved similarly to the calibration curve of the ^{222}Rn standard. As seen from Table 4.2 (grey color) and Figure 4.3, as the days go by, a huge difference is seen between the calibration curve and monitors under test from day 10. For Alphaguard AG2260 an average activity difference of 1.20 kBq/m^3 exist, while for AG2261 an average activity of 1.01 kBq/m^3 exist in comparison to the calibration curve as seen in Table 4.2 (orange color). Therefore, there was a need for Alphaguards to be adjusted to get accurate results, if they were to be taken for environmental monitoring of radon and its progenies. Starting from day 12, it was seen that ^{222}Rn began the process of stabilization.

Table 4.2: Response of radon monitors to the calibration curve.

Period (Days)	Experimental values of AG2260 (kBq/m^3)	Radon standard source values (kBq/m^3)	Experimental values of AG2261 (kBq/m^3)
1	0.22	0.64	0.30
2	0.76	1.18	0.95
3	1.16	1.62	1.37
4	1.43	2.00	1.65
5	1.65	2.31	1.84
6	1.81	2.57	2.02
7	1.98	2.78	2.18
8	2.03	2.96	2.22
9	2.09	3.11	2.30
10	2.20	3.24	2.40
11	2.27	3.35	2.46
12	2.30	3.43	2.50
13	2.35	3.51	2.55
14	2.38	3.57	2.58
15	2.28	3.62	2.45
16	2.37	3.66	2.56
17	2.42	3.70	2.61
18	2.47	3.73	2.64
19	2.45	3.75	2.65
20	2.45	3.77	2.64
21	2.46	3.79	2.66
22	2.47	3.80	2.69
23	2.52	3.81	2.72
24	2.52	3.82	2.72
25	2.52	3.83	2.70
26	2.51	3.84	2.70
27	2.50	3.85	2.70
28	2.49	3.85	2.71
29	2.45	3.85	2.61
30	2.40	3.86	2.61
31	2.36	3.86	2.55
32	2.38	3.86	2.59
33	2.32	3.87	2.52
34	2.35	3.87	2.53
35	2.31	3.87	2.51
36	2.33	3.87	2.51
37	2.31	3.87	2.51
38	2.34	3.87	2.50
39	2.39	3.87	2.56
40	2.36	3.87	2.55
Average difference	1.20		1.01

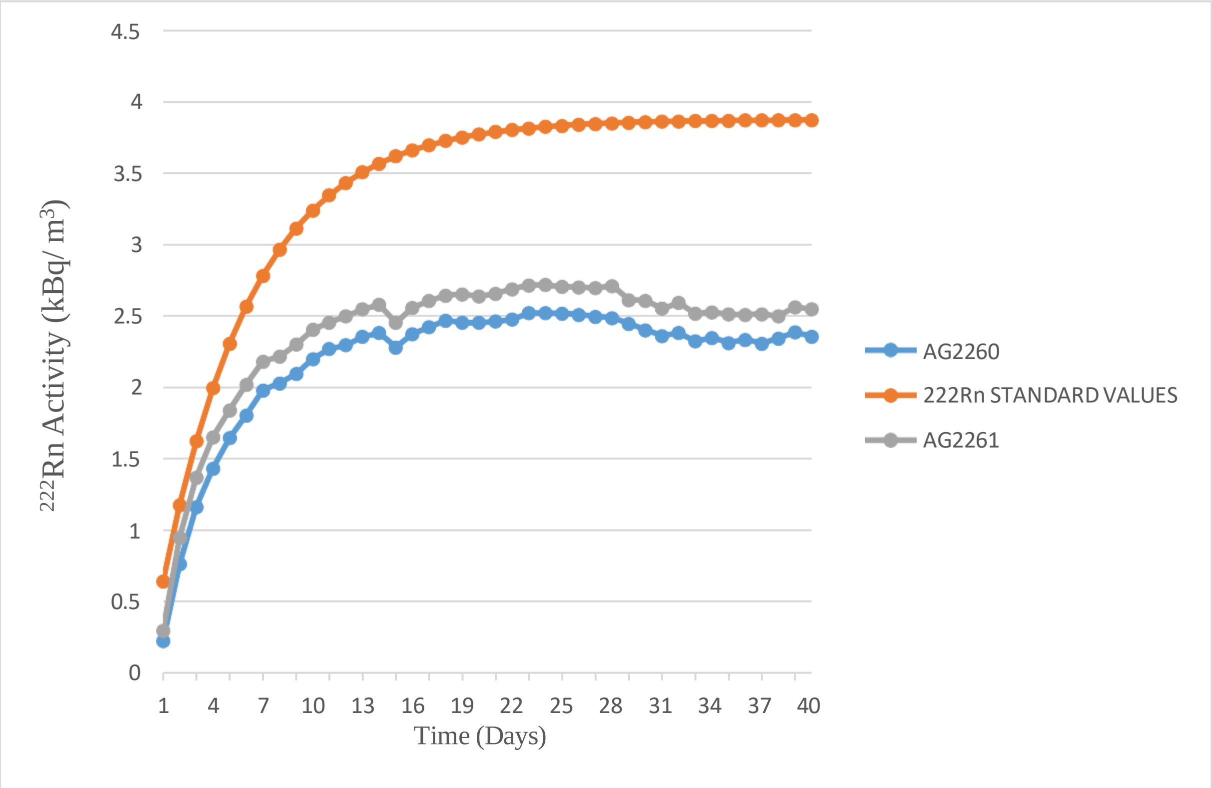

Figure 4.3: Calibration curve and radon monitors.

Table 4.3: Determination of calibrated values from experimental and radon standard values (Chapter 3, Section 3.7, Equation 3.1).

Time (Days)	Experimental values AG2260 (kBq/m^3)	Experimental values AG2261 (kBq/m^3)	Radon standard values	Calibrated AG2260 values (kBq/m^3)	Calibrated AG2261 values (kBq/m^3)
1	0.22	0.3	0.64	0.35	0.42
2	0.76	0.95	1.18	1.18	1.35
3	1.16	1.37	1.62	1.8	1.94
4	1.43	1.65	2	2.21	2.34
5	1.65	1.84	2.31	2.54	2.61
6	1.81	2.02	2.57	2.79	2.87
7	1.98	2.18	2.78	3.06	3.1
8	2.03	2.22	2.96	3.14	3.15
9	2.09	2.3	3.11	3.24	3.27
10	2.2	2.4	3.24	3.4	3.41
11	2.27	2.46	3.35	3.51	3.49
12	2.3	2.5	3.43	3.55	3.54
13	2.35	2.55	3.51	3.64	3.62
14	2.38	2.58	3.57	3.68	3.66
15	2.28	2.45	3.62	3.52	3.48
16	2.37	2.56	3.66	3.67	3.63
17	2.42	2.61	3.7	3.74	3.7
18	2.47	2.64	3.73	3.81	3.75
19	2.45	2.65	3.75	3.79	3.77
20	2.45	2.64	3.77	3.79	3.74
21	2.46	2.66	3.79	3.81	3.77
22	2.47	2.69	3.8	3.82	3.82
23	2.52	2.72	3.81	3.9	3.86
24	2.52	2.72	3.82	3.89	3.86

25	2.52	2.7	3.83	3.89	3.84
26	2.51	2.7	3.84	3.88	3.84
27	2.5	2.7	3.85	3.86	3.83
28	2.49	2.71	3.85	3.84	3.85
29	2.45	2.61	3.85	3.78	3.71
30	2.4	2.61	3.86	3.71	3.7
31	2.36	2.55	3.86	3.65	3.62
32	2.38	2.59	3.86	3.68	3.68
33	2.32	2.52	3.87	3.59	3.57
34	2.35	2.53	3.87	3.63	3.59
35	2.31	2.51	3.87	3.57	3.57
36	2.33	2.51	3.87	3.61	3.56
37	2.31	2.51	3.87	3.57	3.57
38	2.34	2.5	3.87	3.62	3.54
39	2.39	2.56	3.87	3.69	3.64
40	2.36	2.55	3.87	3.64	3.61
Calibration factor values				1.55	1.42
Average	2.184	2.3755	3.387	3.376	3.371
Standard deviation	0.489	0.499	0.788	0.755	0.709

To be able to relate measurements results from both Alphaguards, to become traceable or in alignment to the calibration curve, a calibration factor was supposed to be determined. Equation 3.1 from Chapter 3, Section 3.7, was used and a calibration factor was obtained for AG2260 and AG2261 as 1.55 and 1.42, respectively. Figure 4.4 and Figure 4.5 show the proximity of AG2260 and AG2261 to the calibration curve after the application of the calibration factor. Therefore, this means that all measurement done with both the Alphaguards were to be multiplied by the calibration factors obtained to be accurate according to the traceable radon standard source used. Measuring instruments have errors that can be due to faultiness in their data handling, environmental factors such as noise, strong winds and vibrations. A dip seen in Figure 4.4 and 4.5, day 15 is due to increase in the air pressure, that decreases the radon measurement, indicating possible radon leakage.

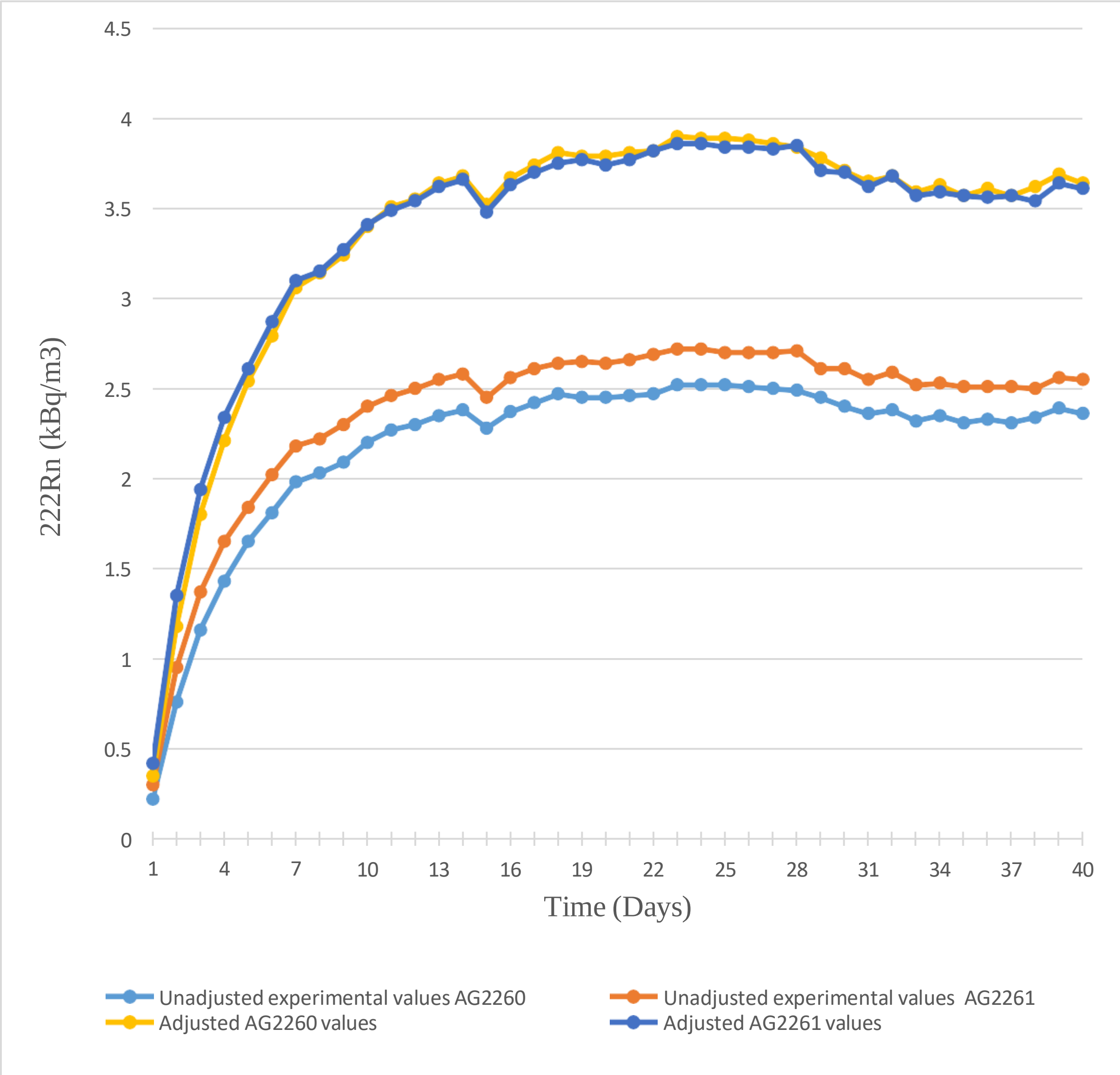

Figure 4.4: Results for calibration factor application.

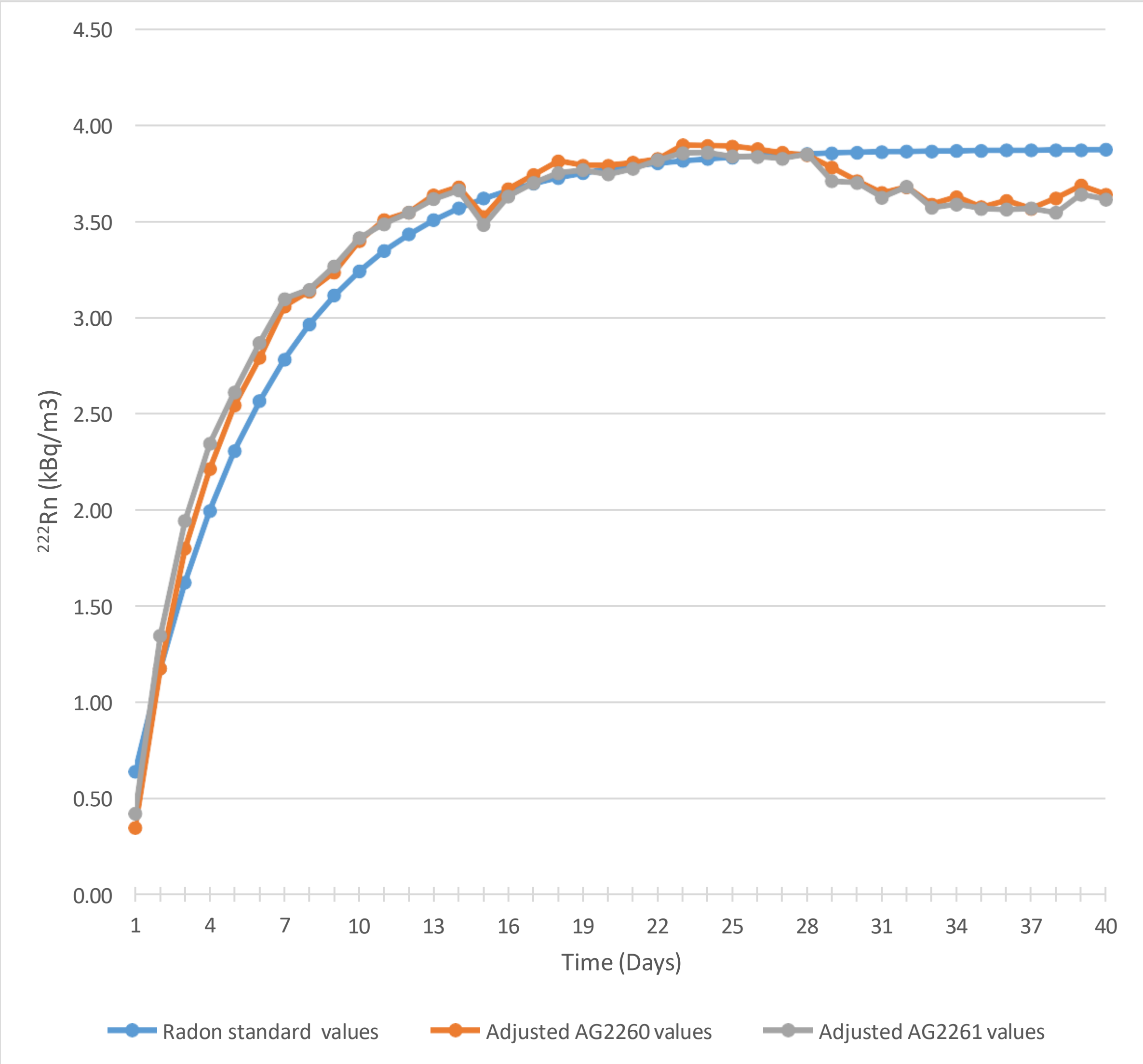

Figure 4.5: Proximity of adjusted Alphaguards values to the calibration curve.

Starting from day 28, after the activity of ^{222}Rn had stabilized, there seemed to be a loss of ^{222}Rn activity. A stable ^{222}Rn activity concentration for a period of 14 days, beginning from day 17 to day 28 was observed. The designed chamber was able to reach the stability of ^{222}Rn activity concentration in 17 days at an Alphaguard airflow speed of 0.3 l/min. From day 3 to day 14 the activity of ^{222}Rn was above the calibration curve before being in alignment or near to the calibration curve. Uncertainties or high values of deviations in this chamber are due to a non-uniform radon atmosphere within the chamber. Therefore, a fan at a constant speed is needed in the chamber, to keep the radon atmosphere constant. Without the fan, radon atmosphere is constant for few days in the chamber.

4.3 Behavior of environmental conditions of the radon chamber

The environmental parameters of the designed chamber are essential in calibration of radon monitors, as some radon monitors are affected and not operational in harsh environmental conditions. For instance, the Alphaguard operates at a temperature range of -10°C to 50°C, relative humidity of 0% to 95% and air pressure of 700 mbar to 1100 mbar. The environmental parameters as seen in Table 4.4 slightly changed by a difference not less than the value of 5.

Table 4.4: The behaviour of environmental parameters in the radon chamber for a period of 40 days.

Time (Days)	**Temperature (°C)**	**Relative air pressure (mbar)**	**Relative humidity (%)**	**Radon activity (Bq/m^3)**
1	21.92	882.08	49.63	298.9
2	21.7	881.17	61.8	948.17
3	21.63	882.67	67.12	1368.67
4	21.98	880.92	69.77	1651.67
5	23.08	878.09	71.42	1840.33
6	22.3	873.28	74.44	2021
7	21.29	874.03	76.17	2182
8	26	877.86	74.4	2215.33
9	27.36	877.26	76.27	2301.33
10	26.3	876.06	79.27	2404
11	25.31	874.89	79.96	2455.33
12	26.14	877.48	79.48	2496.67
13	24.25	879.58	82.02	2546.67
14	22.91	877.08	82.42	2578
15	27.68	877.19	79	2452
16	23.63	877.62	83.98	2557.33
17	21.65	880.43	84.19	2605.33
18	19.8	885.1	84.23	2642.67
19	20.07	887.63	83.65	2652.67
20	21.65	888.14	82.6	2637.33
21	22.38	886.07	82.81	2658
22	22.44	883.83	82.98	2689.33
23	21.62	882.84	83.77	2715.33
24	21.51	881.49	83.67	2716.67
25	21.42	880.75	83.65	2703.33
26	22.34	881.04	82.92	2701.33
27	24.35	880.34	82.31	2695.33
28	23.5	878.87	83.33	2710.67
29	26.03	880.85	81.65	2612
30	26.56	882.41	82.19	2606.67
31	27.44	881.35	81.98	2552
32	25	877.16	84.1	2592
33	27.3	878.29	81.48	2515.33
34	26.32	881.15	83.13	2527.33
35	27.3	881.81	82.08	2511.33
36	26.8	880.12	82.6	2508.67
37	26.7	880.82	83.04	2513.33
38	26.8	883.77	82.69	2496.67
39	23.42	883.71	84.75	2563.33
40	24.26	882.41	82.79	2546
Minimum	19.8	873.28	49.63	298.9
Maximum	27.68	888.14	84.75	2716.67
Average	24.00	880.44	79.49	2374.75
Standard Deviation	2.33	3.34	6.97	499.28

In Figure 4.6, it is seen that there is a relationship between humidity and ^{222}Rn, that as humidity increased ^{222}Rn also increased until day 15. The environmental conditions throughout the period of 40 days were constant, the increase and decrease of radon was not affected by environmental parameters.

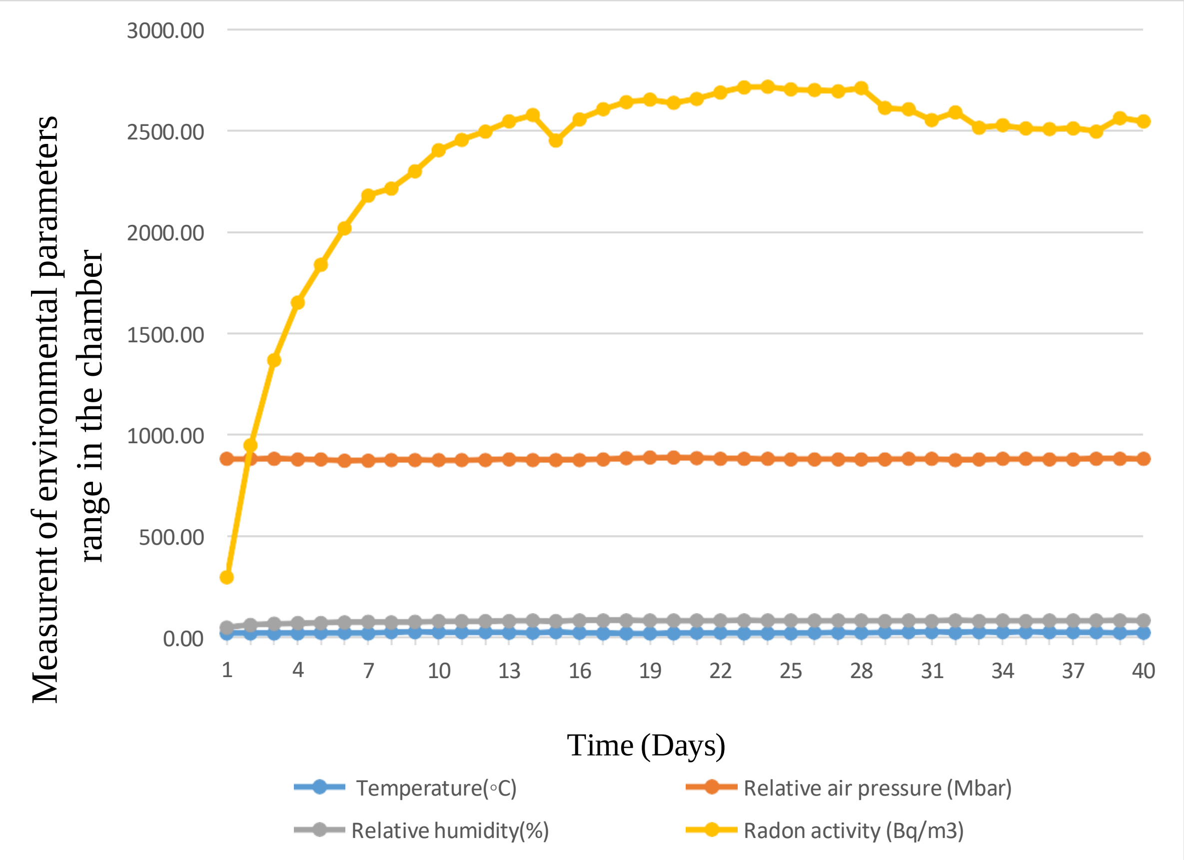

Figure 4.6: Behaviour of environmental parameters at airflow rate of 0.3 L/min in the radon chamber.

4.4 Radon chamber operation without Alphapump

The Alphapump was turned off to evaluate the behavior of radon and environmental parameters at steady conditions by a radon monitor, as shown in Table 4.5 and Figure 4.7.

Table 4.5: Environmental parameters after 40 days.

Time (Days)	**Radon activity (Bq/m^3)**	**Temperature(°C)**	**Relative humidity (%)**	**Relative air pressure (mbar)**
1	502.96	19.45	64.81	880.38
2	838.04	19.37	65.71	880.33
3	1328.96	19.31	66.4	880.29
4	1551.17	19.25	66.94	880.21
5	1811.96	19.21	67.4	880.17
6	2306.79	19.18	67.77	880.13
7	2734.33	19.17	68.1	880.08
8	2689.83	19.16	68.38	880.04
9	2903.63	19.17	68.63	880.04
10	2833.33	19.18	68.83	880.04
11	3000.17	19.21	69.02	880
12	3124.83	19.24	69.19	879.96
13	3379.83	19.27	69.35	879.92
14	3316.67	19.31	69.5	879.88
15	3497.04	19.34	69.63	879.88
16	3446.92	19.38	69.75	879.83
17	3083.92	19.41	69.88	879.83
18	3214.29	19.43	69.98	879.83
19	3023.29	19.44	70.1	879.79
20	2886.58	19.46	70.23	879.79
21	3389.25	19.49	70.31	879.75
22	3256.29	19.52	70.38	879.71
23	3519.58	19.55	70.46	879.71
24	3637.38	19.57	70.54	879.71
25	3336.08	19.58	70.63	879.71
26	3280.79	19.59	70.71	879.71
27	3770.54	19.6	70.79	879.75
28	3514.13	19.61	70.88	879.79
29	3327.08	19.61	70.96	879.83
30	2907.08	19.61	71.04	879.88
31	2923.58	19.61	71.13	879.92
32	3441.33	19.61	71.21	879.96
33	3220.04	19.61	71.29	879.96
34	3195.54	19.6	71.38	879.96
35	3590.92	19.59	71.44	880
36	3569.71	19.59	71.52	880.04
37	4022.46	19.58	71.58	880.08
38	3820.46	19.56	71.65	880.13
39	3075.83	19.55	71.73	880.17
40	3264	22.13	63.63	880.21
Min	502.96	19.16	63.63	879.71
Max	4022.46	22.13	71.73	880.38
Average	2988.42	19.50	69.57	879.96
Standard deviation	766.13	0.45	1.93	0.18

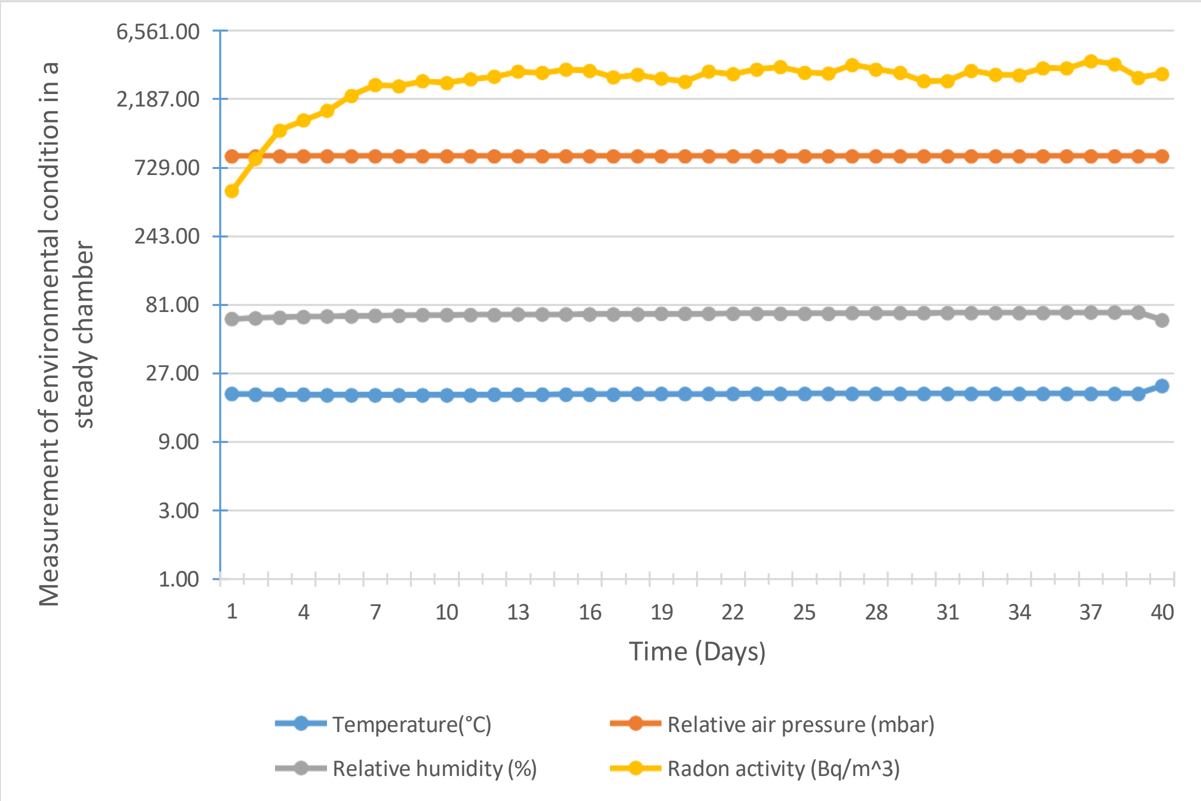

Figure 4.7: Environmental conditions in a steady chamber.

The environmental conditions in a chamber with Alphapump switched off are constant. As seen in Table 4.5 the difference or standard deviation of the measured values in a period of 40 days was less than 2 for environmental conditions. ^{222}Rn activity was not dependent on environmental conditions.

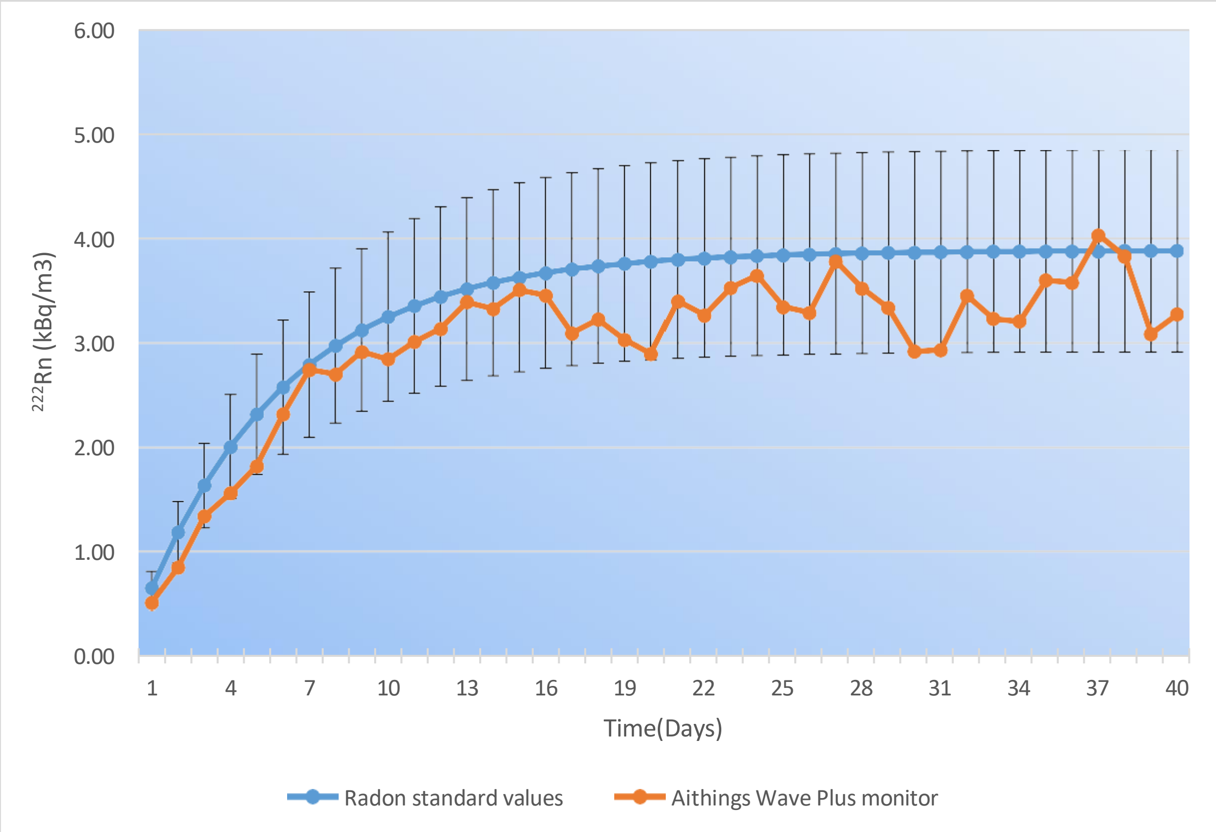

Figure 4.8: ^{222}Rn behaviour without Alphapump.

The ^{222}Rn measured by the Airthings Wave Plus showed that the ^{222}Rn activity from day 15 and onwards was fluctuating as it stabilises in ranges between 2.89 kBq/m^3 to 4.02 kBq/m^3. This indicated that ^{222}Rn activity in the chamber was not uniform and would stabilise at a later stage. Error bars are seen in Figure 4.8 obtained by adding and subtracting 25 % of each value of radon standard over a period of days, to estimate the percentagerange that the Airthing Wave Plus monitor fell in as compared to the reference radon standard. The percentage range of ±25 %, is seen to be a good estimate, that showed that the monitor is performing well.

4.5 Chamber validation

4.5.1 Operation

For validation of the chamber, the guideline from National Radon Safety Board was followed which states that the temperature of the chamber must be in ranges of 18 °C to 27 °C, and humidity must range from 20 % to 75 %, as stated in Appendix C. The results obtained as seen on Table 4.5 show that the minimum and maximum temperature ranged from 19.16 °C to 22.13 °C and humidity ranged from 63.63 % to 71.73 %. Therefore, the chamber is within the ranges stated by NRSB (2022) in terms of temperature and humidity. When the Alphapump was turned on to bubble and circulate ^{222}Rn atmosphere in the chamber, the obtained ranges for temperature were 19.8°C to 27.68 °C, for humidity they were 49.63% to 84.75%. Therefore, the chamber is off the range by a minimal difference of 0.68 °C for temperature and 9.75% for humidity when compared to NRSB (2022). The percentage deviation obtained from the ^{222}Rn standard source, for Airthings Wave Plus monitor, AG2260 and AG2261 Alphaguard monitor were ±11.78 %, ±35.52 % and ±29.88 %, respectively. This indicates that the chamber operates better when the Alphapump is switched off rather than when it was on as there is probable leakage.

4.5.2 Leakage test

The leakage test was done by observing the air pressure when the Alphapump was on and when it was off. The average air pressure when the Alphapump was on is 880.64 mbar and 879.96 mbar when it was off as determined in Table 4.4 and Table 4.5. The difference between when the Alphapump was on and off is 0.48 mbar in a period of 40 days. This proved that the leakage was small throughout the experiment, and the chamber needed few adjustments to be completely airtight, such that there is no leakage. In Section 3.8 chamber leakage rate was determined, whereby the initial radon concentration activity was 400 Bq/m^3. The background radon activity in the laboratory was measured to be 20 Bq/m^3. Using Equation 2.20, 2. 21, 2.22 and 2.23 in Section 2.8.2, the initial slope for ideal decay curve with no leakage (M_I) and with leakage (M_L), resulted -3.02 Bq/m^3 and -6.022 Bq/m^3, respectively. The leakage rate λ_v , was calculated to be 0.0079 Bq/m^3·hr^{-1} (Abo-Elmagd, 2014). A graphical depiction of the determination of radon leakage rate from the chamber using decay curves is presented in Figure 4.9 and data for plotting the graph in Appendix D.

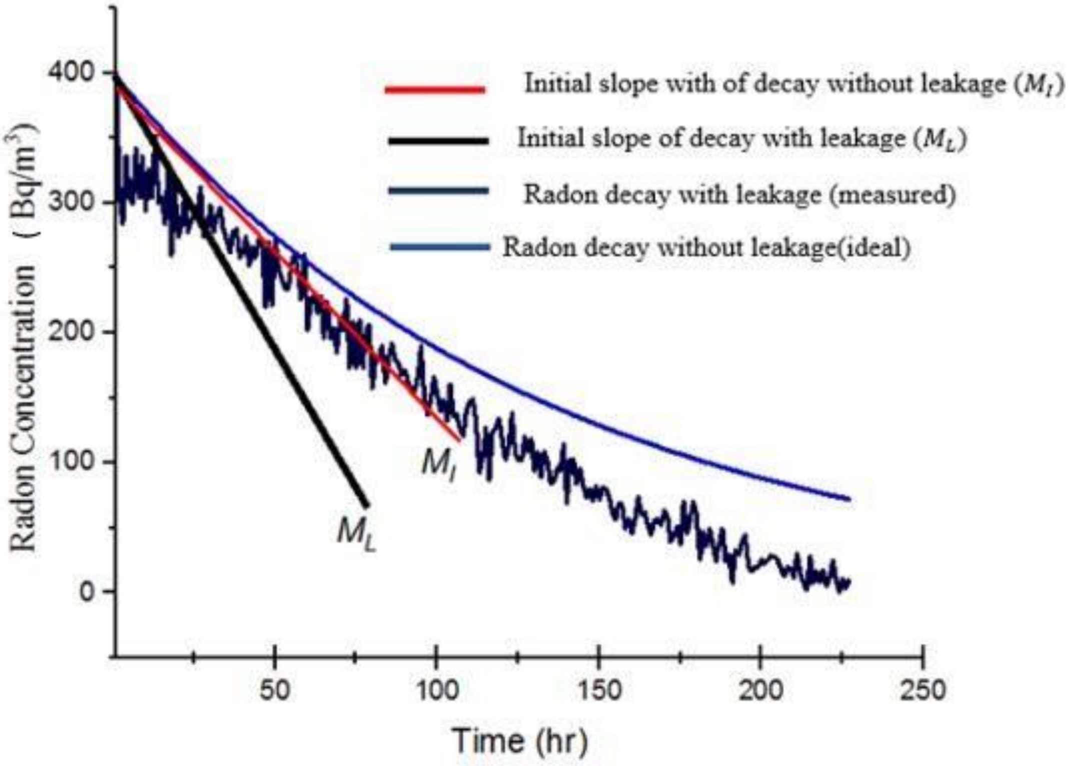

Figure 4.9: Radon decay curves for ideal chamber (no leakage) and real chamber (with leakage - measured).

4.6 Mitigation strategy to reduce radon build-up in the room due to chamber leakage

In the course of the study, it was observed that there was a leakage from the radon chamber to the room. The windows and door of the laboratory were opened to allow cross ventilation and circulation of air between the laboratory and its surroundings, thereby reducing the 222Rn concentration in the laboratory. Table 4.6 shows the reduction of radon activity concentration when one of the mitigation strategies of ^{222}Rn reduction has been applied. From day one to day ten, there was a significant decrease of radon activity, the difference as seen in row 1 column 3 is 0.93367 kBq/m^3. The average ^{222}Rn activity concentration was 0.2779 kBq/m^3 and the deviation from the average was 0.4742 kBq/m^3. From the first to the second day, it is seen on Table 4.6 and Figure 4.10 that 1.5820 kBq/m^3 reduced to 0.6483 kBq/m^3. This means that the ventilation strategy for radon reduction method applied was successful, as radon level in the workplace must be below 1000 Bq/m^3 for occupational radiation protection.

Table 4.6: Reduction of radon in a room.

Time (Days)	^{222}Rn (kBq/m^3)	Change in ^{222}Rn concentration (kBq/m^3)
1	1.582	0.93367
2	0.6483	0.37063
3	0.2777	0.1541
4	0.1236	0.06183
5	0.0618	0.03049
6	0.0313	0.01087
7	0.0204	0.007
8	0.0134	0.00291
9	0.0105	0.00044
10	0.0101	0.0005
Average	0.2779	0.1572
Standard deviation	0.4742	0.2812

Figure 4.10 shows ^{222}Rn activity concentration has been minimised to the lowest activity concentration as possible in the laboratory during the removal of Alphaguard monitors for data collection after forty days. From day six to day ten, there was stability of the ^{222}Rn activity in the laboratory and a gradual, slight decrease of the activity was also observed. From day one to day four there was an exponential decrease of the ^{222}Rn activity concentration.

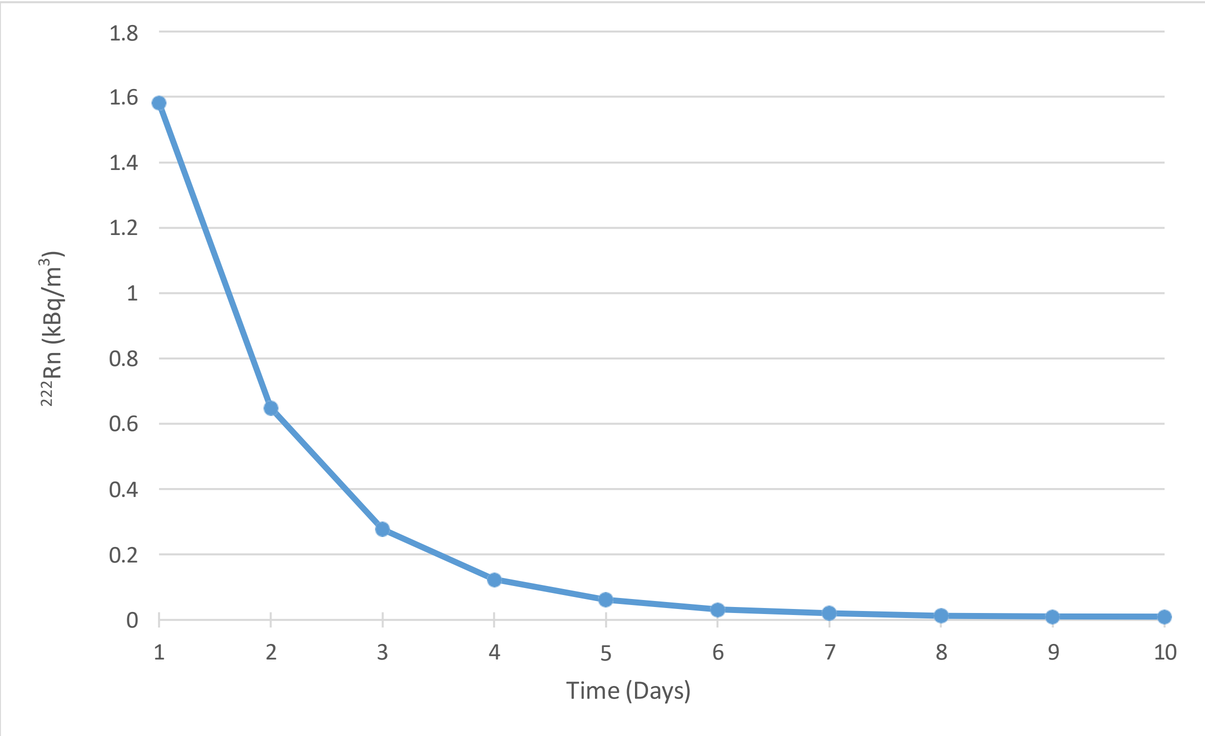

Figure 4.10: Reduction of ^{222}Rn concentration in the laboratory within in 10 days.

CHAPTER 5: CONCLUSIONS AND RECOMMENDATIONS

5.1 Conclusions

The radon chamber is important in housing the reference radon atmosphere for calibration of devices under test. The radon chamber wall was made of $6x10^{-3}$m thick sheets of perspex materials. Six perspex sheets were joined together to form a rectangular box of volume 0.5 m^3 with dimensions of 0.8 m (length) x 1 m (breadth) x 0.6 m (height). The radon chamber included tools such as the Alphapump, two Alphaguard, Airthing Wave Plus monitor, EB85 liquid radium standard solution and electrical wires.

The objectives of the study were achieved:

- radon monitors were calibrated by exposing them to a radon atmosphere,
- environmental parameters were measured,
- a method to measure radon leakage was devised,
- a radon mitigation strategy to reduce radon in a laboratory was applied.

A radon atmosphere was created by a radon generation system, which bubbled out radon gas from the EB85 liquid radium standard solution of activity 1.86 kBq/m^3. To determine its accumulation over a period of 40 days in the chamber, it was divided by the volume of the chamber, to estimate its concentration.

The Alphaguard AG2260 and AG2261 were first exposed to the radon atmosphere, for a period of 40 days and recorded radon activities ranging from 0.225 kBq/m^3 to 2.521 kBq/m^3 for Alphaguard AG2260, and 0.299 kBq/m^3 to 2.717 kBq/m^3 for AG2261. The theoretical radon atmosphere ranged from 0.641 kBq/m^3 to 3.872 kBq/m^3. A theoretical calibration curve was obtained through modelling the radon activity over a period of 40 days in Chapter 4 Section 4.1. Bateman's equation was used to calibrate radon monitors and to determine the percentage of deviation.

For Alphaguard AG2260, an average difference of 1.20 kBq/m^3 was determined, while for AG2261 an average of 1.01 kBq/m^3 was determined in comparison to the calibration curve. To align to the calibration curve, calibration factors were obtained for AG2260 and AG2261 as 1.55 kBq/m^3 and 1.42 kBq/m^3, respectively. According to the results, calibration factors obtained must be applied if there is environmental monitoring, so that the results can be traceable to the standard used.

The temperature observed during the experiment ranged from 19.8 °C to 27.68 °C and relative humidity ranged from 49.63 % to 84.75 %. An observation of the performance of the chamber for validation in terms of environmental conditions of the chamber by comparison to United States National Radon Safety Board (NRSB) to compare the environmental parameters, the temperature must range from 18 °C to 27 °C and humidity from 20 % to 75 % (NRSB, 2012). The designed chamber is in minimal difference to the United States national radon safety board criteria. When the Alphapump was not operational in the chamber, the designed chamber is in the ranges set by the NRSB (2022).

5.2 Recommendations

In a future study, a recently calibrated Alphaguard radon monitor should be used as a reference standard, together with a solid ^{226}Ra standard. This would enhance the accuracy or precision of the instruments to be calibrated. Furthermore, the chamber should be equiped with fans to make the ^{222}Rn activity homogenous in the chamber, stanless steel sheet will be considered as encasing material. Figure 5.1 illustrates the desired future plans for the project on a smaller scale.

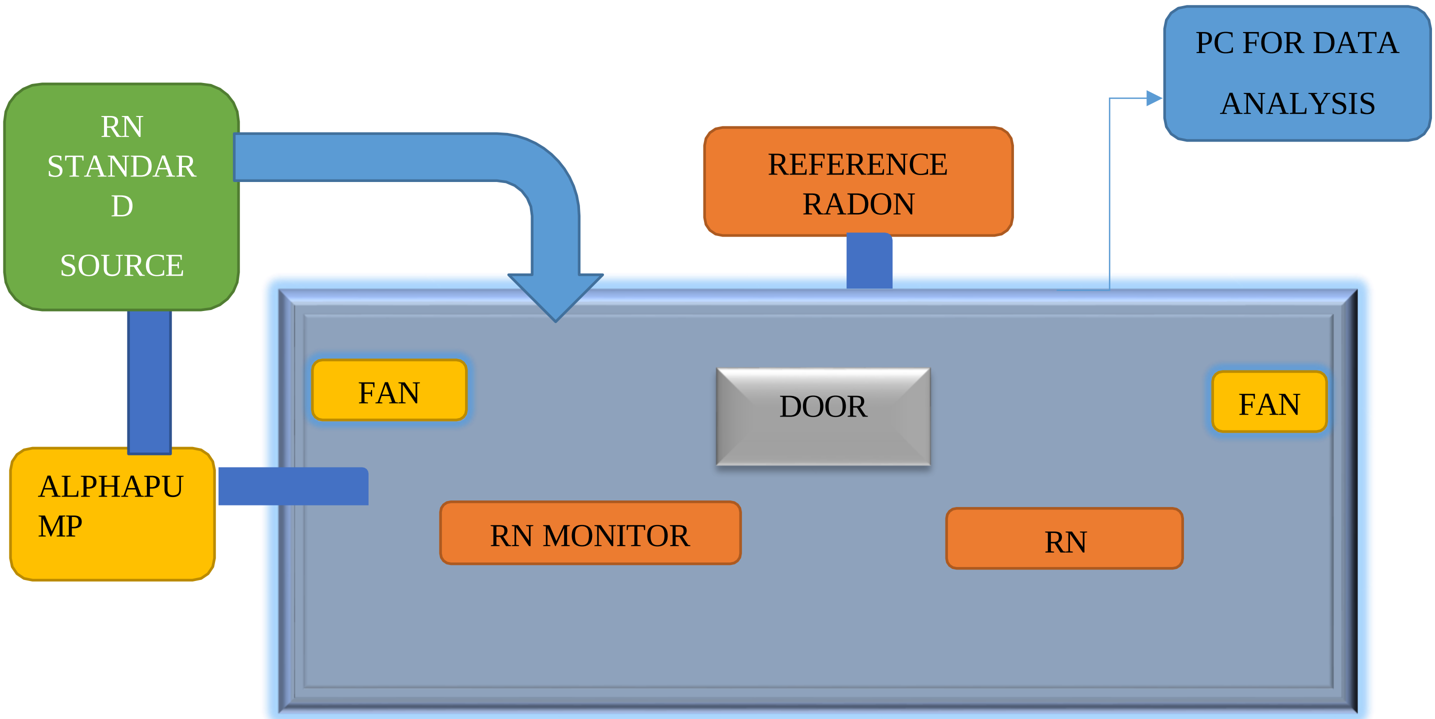

Figure 5.1: Prototype 2D schematic design of the radon calibration system.

REFERENCES

AARST. 2015. *National radon proficiency program (NRPP)* [Online]. Available: http://aarst-nrpp.com/wp/wp-content/uploads/2015/02/AARST_NRPP-Policy-Manual_April_21_2015.pdf [Accessed 28 August 2016].

ABDALLA, A., ALI, A., AL-JARALLAH, M., OKADA, G., KAWAGUCHI, N. & YANAGIDA, T. 2019. Radon detection using alpha scintillation KACST cell. *Nuclear Instruments and Methods in Physics Research Section A: Accelerators, Spectrometers, Detectors and Associated Equipment*, 922**,** 84-90.

ABO-ELMAGD, M. 2014. Radon exhalation rates corrected for leakage and back diffusion – Evaluation of radon chambers and radon sources with application to ceramic tile. *Journal of Radiation Research and Applied Sciences,* 7**,** 390-398.

ACME, K. 2022. *Plexiglass vs. Glass: Which is Better for Custom Framing?* [Online]. Acme Plastic. Available: https://www.acmeplastics.com/content/plexiglass-vs-glass-which-is-better-for-custom-framing/ [Accessed 26 July 2023 2023].

AIRTHINGS (2023). *Airthings Wave Plus Indoor Air Quality Monitor + Radon*. [online] www.airthings.com. Available at: https://www.airthings.com/en/wave-plus [Accessed 4 Feb. 2023].

AKBARI, K., MAHMOUDI, J. & GHANBARI, M. 2013. Influence of indoor air conditions on radon concentration in a detached house. *Journal of Environmental Radioactivity,* 116**,** 166-173.

AL-AZMI, D. 2009. The use of soil gas as radon source in radon chambers. *Radiation Measurements,* 44**,** 306-310.

ALTUGLAS, I. 2006. Plexiglass general information and properties. *In:* GROUP, A. (ed.). Philadelphia, USA: Arkerma Inc.

ARNOLD, D., MERTES, F., RÖTTGER, S. & MARINGER, F. 2020. *16ENV10 MetroRADON Deliverable D1 Method for the traceable calibration of radon (222Rn) measurement instruments at low activity concentrations (100 Bq/m3 to 300 Bq/m3) with relative uncertainties ≤ 5 % (k = 1).*

AWHIDA, A. A. S. 2017. *Novel method of measurement of radon exhalation from building material.* Doctoral Dissertation, University of Belgrade.

AYMAN, A., AHMED, I. & TAYSEER, A.-N. 2017. Radon Calibration System. *In:* FERIZ, A. (ed.) *Radon.* Rijeka: IntechOpen.

AZIMI-GARAKANI, D. 1992. A comparison of different radon chambers. *Nuclear Instruments and Methods in Physics Research Section B: Beam Interactions with Materials and Atoms,* 71**,** 99-102.

BASKARAN, M. 2016. *Radon: A Tracer for Geological, Geophysical and Geochemical Studies*, Switzerland, Springer Geochemistry.

BATEMAN, H. 1910. The transformation of the electrodynamical equations. *Proceedings of the London Mathematical Society,* 2**,** 223-264.

BLAHUŠIAK, P., KRIVOŠÍK, M., SLUČIAK, J., JAVORNÍK, A., ZÁLEŠÁKOVÁ, M., CHYTIL, M., MÜLLEROVÁ, M. & HOLÝ, K. 2020. Development of 222Rn in air secondary standard in the Slovak Republic. *Radiation Protection Dosimetry,* 191**,** 160-165.

BLOOMBERG. 2018. *Bertin Launches the Latest AlphaGUARD Radon Gas Measurement Solution* [Online]. Available: https://www.bloomberg.com/research/stocks/private/snapshot.asp?privcapid=129470425 [Accessed 25 September 2018 2018].

BREDHOFF, N. 2014. *Device calibration* [Online]. Available: https://archive.epa.gov/reg3artd/archive/web/pdf/nrsb_nancy_bredhof_042014.pdf [Accessed 26 August 2016].

BRUCE DJOVAK, I., SHARON SKIPTON, O. 2013. Drinking Water Treatment: Distilation. *In:* NEBRASKA-LINCOLN, U. O. (ed.) *UNL Extension publications.* Lincoln: Nebguides.

CARDELLINI, F., CHIABERTO, E., GARLATI, L., GIUFFRIDA, D., LEONARDI, F., MAGNONI, M., MINCHILLO, G., PRANDSTATTER, A., SERENA, E., TREVISI, R., TRIPODI, R. & VESCHETTI, M. 2016. Metrological aspects of international intercomparison of passive radon detectors under field conditions in Marie Curie's tunnel in Lurisia. *Nukleonika,* 61**,** 257-261.

CENTOMANI, G., DI CARLO, C., LEPORE, L. & REMETTI, R. 2019. Design and commissioning of an innovative radon chamber with a single 226Ra source and continuous variation and control of concentration vs. time. *Nuclear Instruments and Methods in Physics Research Section A: Accelerators, Spectrometers, Detectors and Associated Equipment,* 940**,** 109-115.

CHO, B., HWANG, J., LEE, B., OH, Y. H. & CHOO, C. 2020. Radon Concentrations in Raw Water and Treated Water Used for Bottled Water in South Korea. *Sustainability,* 12**,** 5313.

CHO, Z. H. 2003. Tomography. *In:* MEYERS, R. A. (ed.) *Encyclopedia of Physical Science and Technology (Third Edition).* New York: Academic Press.

COLLUM, B. 2017. 2 - Radiation. *In:* COLLUM, B. (ed.) *Nuclear Facilities.* Woodhead Publishing.

DANFORTH, J. M., PEARSON, D. D. & GOODARZI, A. A. 2023. Ionizing radiation toxicology. *Reference Module in Biomedical Sciences.* Elsevier.

DIVISION, P. E.-I. M. 2018. *Radon Chamber – Radon Sources | Pylon Electronics-Radon* [Online]. Available: https://pylonelectronics-radon.com/2017/07/20/radon-chamber-concentration-changes-using-a-single-flow-through-radon-source/ [Accessed 12 Jun. 2018]. [Accessed 11 JUNE 2018].

EL-TAHER, A. 2018. An Overview of Instrumentation for Measuring Radon in Environmental Studies. *Journal of Radiation and Nuclear Applications,* 3**,** 135.

ELZAIN, A. E. A. 2017. Radon Monitoring in the Environment. *In:* ADROVIC, F. (ed.) *Radon.* IntechOpen.

EZZULDDIN, S. K. & MANSOUR, H. H. 2020. Radon and radium activity concentration measurement in drinking water resources in Kurdistan Region-Iraq. *Journal of Radioanalytical and Nuclear Chemistry,* 324**,** 963-976.

FARJANA, S. H., HUDA, N. & MAHMUD, M. P. Life-Cycle environmental impact assessment of mineral industries. IOP Conference Series: Materials Science and Engineering, 2018. IOP Publishing, 012016.

FONTES, J. 2005. CHAPTER 12 - Humidity Sensors. *In:* WILSON, J. S. (ed.) *Sensor Technology Handbook.* Burlington: Newnes.

FUENTE, M., RABAGO, D., HERRERA, S., QUINDOS, L., FUENTE, I., FOLEY, M. & SAINZ, C. 2018. Performance of radon monitors in a purpose-built radon chamber. *Journal of Radiological Protection,* 38**,** 1111.

GEEWIZ 2018. 2400VA Mecer Inverter + 2x 100AH Batteries Trolley (8 HOUR BATTERY LIFE) KIT - 1440W (150-200 cycles) - 12 Month Warranty.

GEORGE, A. C. 2021. *Tertiary Radon Chamber Accreditation* [Online]. NRSB. Available: https://nrsb.org/radon-chambers/tertiary-radon-chamber-application-info/ [Accessed 05 February 2021].

GUNDERSEN, L., SCHUMANN, R., OTTON, J., DUBIEL, R., OWEN, D. & DICKINSON, K. 1992. Geology of radon in the United States.

HARARAH, S. M. A. I. 2007. *Investigation of radon pollution in groundwater in the southern part of*

Gaza strip - Palestine. Master of Science in Water Resources Management, The Islamic University Gaza.

HEIDARY, S., SETAYESHI, S., GHANNADI-MARAGHEH, M. & NEGARESTANI, A. 2011. Monitoring and measurement of radon activity in a new design of radon calibration chamber. *Radiation Measurements,* 46**,** 694-700.

HNIZDO, E., MURRAY, J. & KLEMPMAN, S. 1997. Lung cancer in relation to exposure to silica dust, silicosis and uranium production in South African gold miners. *Thorax,* 52**,** 271-275.

IOVINE, R. S., PIOCHI, M., AVINO, R., CUOCO, E., MINOPOLI, C., SANTI, A., CALIRO, S., PIERSANTI, A. & GALLI, G. 2022. Radon (222Rn) levels in thermal waters of the geothermally active Campi Flegrei volcanic caldera (Southern Italy): A framework study using a RAD7 radon detector. *Journal of Volcanology and Geothermal Research,* 431**,** 107641.

IRLINGER, J. 2015. *Development of an electronic monitor for the determination of individual radon and thoron exposure.* Doctorate, LMU München.

JACOBI, W. & ANDRE, K. 1963. The vertical distribution of radon 222, radon 220 and their decay products in the atmosphere. *Journal of Geophysical Research,* 68**,** 3799-3814.

JAI-WON CHUNG, T.-I. H., & GYU-SIK KIM 2020. Effect of Temperature and Humidity on Indoor Radon Concentration. *International Journal of Trend in Scientific Research and Development,* 4**,** 688–693.

JANIK, M. 2017. *Intercomparisons Exercises of Radon and Thoron Monitors Provided by Four Laboratories: A Review*. *Japanese Journal of Health Physics*, 52, 114-121.

JANIK, M., TOKONAMI, S., KOVÁCS, T., KÁVÁSI, N., KRANROD, C., SORIMACHI, A., TAKAHASHI, H., MIYAHARA, N. & ISHIKAWA, T. 2009. International intercomparisons of integrating radon detectors in the NIRS radon chamber. *Applied Radiation and Isotopes,* 67**,** 1691-1696.

JENKINS, D. 2020. *Radiation Detection for Nuclear Physics Methods and industrial applications,* Bristol UK.

KAMUNDA, C., MATHUTHU, M. & MADHUKU, M. 2017. Determination of Radon in mine dwellings of gauteng province of South Africa using AlphaGUARD radon professional monitor. *J Environ Toxicol Stud,* 1**,** 1-4.

KANIVETS, V., LAPTEV, G., KONOPLEV, A., LISOVYI, H., DERKACH, G. & VOITSEKHOVYCH, O. 2020. Distribution and dynamics of radionuclides in the Chernobyl cooling pond. *Behavior of Radionuclides in the Environment II.* Springer.

KEITH, D. J., HARPER C 2012. *CHEMICAL, PHYSICAL, AND RADIOLOGICAL INFORMATION,* Atlanta Agency for Toxic Substances and Disease Registry (US).

KHALID, N., AB MAJID, A., YAHAYA, R., YASIR, M. S. & MOHAMED, F. 2014. Construction of Radon Chamber for Determination of Radon Emanation Using Continuous Radon Monitor. *Malaysian Journal of Analytical Sciences,* 18**,** 618-628.

KHAN, M. A., KHATTAK, N. U., HANIF, M. & QADIR, A. 2022. Assessment of soil-gas radon concentration over lithologies: a case study from district Karak, Khyber Pakhtunkhwa, Pakistan. *Environmental Monitoring and Assessment,* 195**,** 117.

KIM, M.-J., KIM, S.-H., KIM, D.-H., JEON, H.-J. & CHO, S.-Y. 2013. New-type of Multi-purpose Standard Radon Chamber in South Korea.

KÓNYA, J. & NAGY, N. M. 2018. Chapter 4 - Radioactive Decay. *In:* KÓNYA, J. & NAGY, N. M. (eds.) *Nuclear and Radiochemistry (Second Edition).* Elsevier.

KOTRAPPA, P. 2015. Electret ion chambers for characterizing indoor, outdoor, geologic and other sources of radon. *Radon. Hauppauge, NY: Nova Science Publishers, Inc*, 2-36.

KOTRAPPA, P. & STIEFF, F. 2007. One cubic metre NIST traceable radon test chamber. *Radiation Protection Dosimetry,* 128, 500-502.

KOTRAPPA, P. & STIEFF, F. 2012. Characterization and use of an accumulating type of radon test chamber. *in proceedings of AARST*.

L'ANNUNZIATA, M. F. 2016. Chapter 4 - Alpha Radiation. *In:* L'ANNUNZIATA, M. F. (ed.) *Radioactivity (Second Edition).* Boston: Elsevier.

L'ANNUNZIATA, M. F. 2020. *Handbook of Radioactivity Analysis*, Elsevier.

LEHTO, J., FOURNIER, C. & OMTVEDT, J. 2017. Basics of Nuclear Physics and of Radiation Detection and Measurement. *Norway: University of Oslo*.

LEUNG, J. K., JIA, D. & TSO, M. A radon exposure chamber in Hong Kong. Proceedings of the Eighth International Congress of the International Radiation Protection Association, Montreal, May, 1992. 22.

LOPES, I., VESTERBACKA, P. & KELLEHER, K. 2017. Comparison of radon (Rn-222) concentration in Portugal and Finland underground waters. *Journal of Radioanalytical and Nuclear Chemistry,* 311, 1867-1873.

LUCAS, H. F. & MARKUN, F. J. J. O. E. R. 1992. The determination of 226Ra and 228Ra in water and solids by the least squares gamma spectrometric method. 15, 1-18.

MACRAE, R. M. & KEMP, T. J. 2018. Oganesson: A Most Unusual 'Inert Gas'. *Science Progress,* 101, 101-120.

MAGILL, J. & GALY, J. 2005. *Radioactivity Radionuclides Radiation,* Germany, Springer.

MALLEY, M. C. 2011. *Radioactivity: a history of a mysterious science*, OUP USA.

MAMONT-CIEŚLA, STAWARZ, O., KARPIŃSKA, M., KAPAŁA, J., KOZAK, K., GRZĄDZIEL, D., CHALUPNIK, S., CHMIELEWSKA, I., OLSZEWSKI, J., PRZYLIBSKI, T. & A, Ż. 2010. Intercomparison of radon CR-39 detector systems conducted in CLOR's calibration chamber. *Nukleonika -Original Edition-*, 55, 589-593.

MATERESE, R. 2018. *Kelvin: Introduction* [Online]. Available: https://www.nist.gov/si-redefinition/kelvin-introduction [Accessed 18 July 2021].

MILLER, C., HOWARTH,CB. 2020. Results of the 2018 PHE intercomparison of passiveradon detectors.

MOORE, J. A. & KEARFOTT, K. J. 2005. A simple radon chamber for educational use. *Health physics,* 89, S78-S84.

NASTRO, V., CARNÌ, D., VITALE, A., LAMONACA, F. & VASILE, M. 2018. Passive and active methods for Radon pollution measurements in historical heritage buildings. *Measurement,* 114, 526-533.

NOVIKOV, D. A., DULTSEV, F. F., KAMENOVA-TOTZEVA, R. & KORNEEVA, T. V. 2021. Hydrogeological conditions and hydrogeochemistry of radon waters in the Zaeltsovsky–Mochishche zone of Novosibirsk, Russia. *Environmental Earth Sciences,* 80, 216.

NRSB. 2012. *Radon Chamber Accreditation Policy* [Online]. Available: http://www.nrsb.org/images/file/RCA%20Policy%20V1201.pdf [Accessed 28 August 2016].

NRSB. 2022. *NRSB Accreditted Chambers* [Online]. New York. Available: https://nrsb.org/radon-chambers/nrsb-accredited-chambers/ [Accessed 05 May 2022 2022].

NWAILA, G. T., GHORBANI, Y., ZHANG, S. E., FRIMMEL, H. E., TOLMAY, L. C. K., ROSE, D. H., NWAILA, P. C. & BOURDEAU, J. E. 2021. Valorisation of mine waste - Part I: Characteristics of, and sampling methodology for, consolidated mineralised tailings by using Witwatersrand gold mines (South Africa) as an example. *Journal of Environmental Management,* 295**,** 113013.

OJOVAN, M. I. & LEE, W. E. 2014. 2 - Nuclear Decay. *In:* OJOVAN, M. I. & LEE, W. E. (eds.) *An Introduction to Nuclear Waste Immobilisation (Second Edition).* Oxford: Elsevier.

OTHMAN, N., RASHID, A. S. A., HASHIM, S., SANUSI, M. S. M. & BERY, A. 2021. Radon gas migration through soil–A review. *Journal of Mines, Metals and Fuels,* 69**,** 3-8.

PANDA, S. K., CHOUDHURY, S., SARAF, A. K. & DAS, J. D. 2007. MODIS land surface temperature data detects thermal anomaly preceding 8 October 2005 Kashmir earthquake. *International Journal of Remote Sensing,* 28**,** 4587-4596.

PECI, A., WINTER, A.-L., LI, Y., GNANESHAN, S., LIU, J., MUBAREKA, S. & GUBBAY, J. B. 2019. Effects of absolute humidity, relative humidity, temperature, and wind speed on influenza activity in Toronto, Ontario, Canada. *Applied and environmental microbiology,* 85**,** e02426-18.

PELCZAR, K., ZUZEL, G., WÓJCIK, M., POCAR, A. & IANNI, A. 2021. An online radon monitor for low-background detector assembly facilities. *The European Physical Journal C,* 81**,** 86.

PIERRE, S., CASSETTE, P., SABOT, B., FRECHOU, C., ANTOHE, A., BARNA, C., BLAHUŠIAK, P., CARDELLINI, F., DERSCH, R., HONIG, A., JUGET, F., KRIVOŠÍK, M., LUCA, A., MARINGER, F., MERTES, F., RÖTTGER, S., SAHAGIA, M., SLUČIAK, J., STIETKA, M. & TEODORESCU, C. 2021. International comparison of activity measurements of radon 222 - EURAMET Project n°1475 - EURAMET.RI(II)-S8.Rn-222. *Metrologia,* 58**,** 06015.

PLASTIC, C. 2023. *Acrylic vs Polycarbonate* [Online]. Cambian Plastics. Available: https://cambrianplastics.co.nz/product/acrylic-vs-polycarbonate/ [Accessed 25 August 2023 2023].

RABAGO, D., FUENTE, I., CELAYA, S., FERNANDEZ, A., FERNANDEZ, E., QUINDOS, J., POL, R., CINELLI, G., QUINDOS, L. & SAINZ, C. 2020. Intercomparison of Indoor Radon Measurements Under Field Conditions In the Framework of MetroRADON European Project. *International Journal of Environmental Research and Public Health,* 17**,** 1780.

RADEBE, M. 2019. *The design of a radon chamber for the calibration of radon monitors at the Centre for Applied Radiation Science and Technology, Mafikeng, South Africa.* Masters Degree, North-West University.

REINDERS, L. 2021. Introduction and Basic Science. *The Fairy Tale of Nuclear Fusion.* Springer.

RGM, P. 2008 *PARC RGM* [Online]. Available: http://www.parcrgm.co.za/products.htm [Accessed 05 December 2016].

RIGGIO, A. & SANTULIN, M. 2015. Earthquake forecasting: a review of radon as seismic precursor. *Bollettino di Geofisica Teorica ed Applicata,* 56.

RÖTTGER, A., RÖTTGER, S., GROSSI, C., VARGAS, A., CURCOLL, R., OTAHAL, P., HERNÁNDEZ CEBALLOS, M. Á., CINELLI, G., CHAMBERS, S., BARBOSA, S., IOAN, M.-R., RADULESCU, I., KIKAJ, D., CHUNG, E., ARNOLD, T., YVER, C., FUENTE, M., MERTES, F. & MOROSH, V. 2021. New metrology for radon at the environmental level. *Measurement Science and Technology,* 32.

SAHU, P., PANIGRAHI, D. C. & MISHRA, D. P. 2016. A comprehensive review on sources of radon and factors affecting radon concentration in underground uranium mines. *Environmental Earth Sciences,* 75**,** 617.

SANJON, E. P., MAIER, A., HINRICHS, A., KRAFT, G., DROSSEL, B. & FOURNIER, C. 2019. A combined experimental and theoretical study of radon solubility in fat and water. *Scientific Reports,* 9**,** 10768.

SAPHYMO, G. 2012. AlphaGUARD Portable Radon Monitor User Manual. 56.

SHAOXIAN, B. & SHIZHU, W. 2019. Chapter 1 - Properties of gases. *In:* SHAOXIAN, B. & SHIZHU, W. (eds.) *Gas Thermohydrodynamic Lubrication and Seals.* Academic Press.

SHWEIKANI, R., BADR, I., MAGED, A., ANDAM, A. & DURRANI, S. 1995. A new calibrated chamber for parametric studies of radon and thoron gases. *Radiation measurements,* 25**,** 613-614.

SHWEIKANI, R. & RAJA, G. 2005. Design, construct and test of a calibration radon chamber. *Radiation measurements,* 40**,** 316-319.

SINGH, P., SINGH, P., SINGH, S., SAHOO, B. K., SAPRA, B. K. & BAJWA, B. S. 2015. A study of indoor radon, thoron and their progeny measurement in Tosham region Haryana, India. *Journal of Radiation Research and Applied Sciences,* 8**,** 226-233.

SÓTI, Z., MAGILL, J. & DREHER, R. 2019. Karlsruhe Nuclide Chart–New 10th edition 2018. *EPJ Nuclear Sciences & Technologies,* 5**,** 6.

SUKANYA, S., NOBLE, J. & JOSEPH, S. 2022. Application of radon (222Rn) as an environmental tracer in hydrogeological and geological investigations: An overview. *Chemosphere,* 303**,** 135141.

SYAM, N. S., LIM, S., LEE, H. Y. & LEE, S. H. 2020. Determination of radon leakage from sample container for gamma spectrometry measurement of 226Ra. *Journal of Environmental Radioactivity,* 220-221**,** 106275.

TAHERI, M., HOSSEINI POOYA, S. M. 2013. A calibration setting with uncertainty measurements for passive/active radon monitors using flow-through source type. *Applied Radiation and Isotopes,* 73**,** 49-51.

TAMAKUMA, Y., KRANROD, C., HOSODA, M. & TOKONAMI, S. 2023. Status of Radon Traceability and Calibration Techniques for Radon Gas. *Radiation Environment and Medicine,* 12**,** 12-24.

TIEFENBACHER, K. F. 2019. Chapter Ten - Glossary of Terms in Wafers, Waffles and Adjuncts. *In:* TIEFENBACHER, K. F. (ed.) *The Technology of Wafers and Waffles II.* Academic Press.

TIN, A. 2014. *Radon measurement devices and protocols* [Online]. Available: https://idph.iowa.gov/Portals/1/Files/Radon/Radon%20Measurement.pdf [Accessed 23 August 2016].

WELCH, L. E., PAUL, B. E. & JONES, M. D. Use of electret ionization chambers to measure radon in Caves. Proceedings of the 2016 International Radon Symposium, 2016. 1-18.

YAHIA, E. M. 2019. Chapter 1 - Introduction. *In:* YAHIA, E. M. (ed.) *Postharvest Technology of Perishable Horticultural Commodities.* Woodhead Publishing.

ZEEB, H., SHANNOUN, F. & WORLD HEALTH, O. 2009. WHO handbook on indoor radon: a public health perspective. World Health Organization.

APPENDICES

Appendix A: Reference standard

Czech Metrology Institute
Okružní 31, 638 00 Brno, Czech Republic
phone +420 545 555 111
www.cmi.cz

Workplace: Regional Inspectorate Prague, Radiová 1136/3, 102 00 Praha 10
Department of Radionuclide Standards Production, Radiová 1288/1a
phone +420 266 020 460

CERTIFICATE
of the measurement standard of activity

Certificate No.: 1035-SE-40645-21 Type: EB 85 Serial No.: 160921-221321

Radionuclide: Ra-226 Half life: 1600 (7) years

Specific activity of Ra-226: 369,0 (22) Bq / g Mass of the solution: 5,040 (1) g

Activity of Ra-226: 1860 (11) Bq

Radionuclide impurities: -

Reference date: 20.10.2021

Description:
The measurement standard is in the form of a radioactive solution in a 5 ml glass ampoule.
The activity of the measurement standard is calculated from the mass and specific activity of the standardized solution.

Metrological traceability:
The declared Ra-226 activity is traceable to CMI Measurement Standards of Ra-226 activity.

Chemical composition:
Carrier solution consists of 1 g $BaCl_2$/l + 10 g HCl/l in distilled water.

Note:
1 g Ra-226 = 3,658E10 Bq
Ra-226 activity was determined by ionization chamber.

Date of the certificate issue: 4.10.2021 Certificate validity period: 3 years

Customer:
CARST
Private Bag X2046
2745 Mmabatho
South Africa

Český metrologický institut -10/2-

Dominika Sosnová
Head of Department
Radionuclide Standards Production
RI Prague

Vladimír Sochor
Deputy Director of RI Prague

R. Obraz
Checked by: Renata Obrazová

Appendix B: Alphaguard manual

12. Technical DATA

12.1. Basic functions PQ2000

Type of radon detector	Ionization chamber, HV ≈ 750 VDC
Mode of operation	3D-alpha spectroscopy a n d current mode
Total detector volume	0,62 liter (38 cubic inches)
Active detector volume	0,56 liter (34 cubic inches)
Type of Rn-FP filter (detector entry window)	Glass fiber filter (retention coefficient >99,9 %)
Detector filling mechanism	Design-optimized for fast passive diffusion
Transient response function (time delay) (TRENDMODE OFF)	Signal > 30 % after 10 min Signal > 70 % after 20 min Signal > 90 % after 30 min
Detector signal acquisition	fast digital signal sampling network, using three separate ADC-channels
Spectral signal extraction	DSP (Digital Signal Processing), on-line-cross correlation algorithms
Detector efficiency	1 CPM at 20 Bq/m³ (or at 0,55 pCi/l)
Background signal due to internal detector contamination	< 1 Bq/m³ (0.03 pCi/l)
Range of radon concentrations (Rn-222) - Lower limit - Upper limit	 2 Bq/m³ (<0.05 pCi/l) 2.000.000 Bq/m³ (54 000 pCi/l)
Resolution on LCD display	1 Bq/m³ (0.01 pCi/l)
Fold back protection	> 10.000.000 Bq/m³ (> 300 000 pCi/l) verified
System linearity error	< 3% within total range
Instrument calibration error (Rn-222)	± 3 % (plus uncertainty of the primary standard)
Measurement modes and cycles	Diffusion mode: 10 min or 60 min (user selectable)
Data capacity (non-volatile)	~ 3.400 measurement points ~ 21 days at 10 min measuring cycle ~ 4 months at 60 min measuring cycle
Operation from internal battery	10 days
Power Consumption - Charging mode (LED: red) - Trickle charging mode (LED: green) - Battery operation (LED: flashing red/green)	 640 mA (7,7 W) 160 mA (1,92 W) 12 mA (0,072 W)
Weight (incl. Internal Pb-accumulator)	4,5 kg (10 lbs)
System operating range - Temperature - Atmospheric pressure - Humidity (non-condensing)	 - 10°C ... + 50°C (+14 ...+122 ° F) 700 mbar ... 1100 mbar 0 % rH ... 95 % rH

Saphymo GmbH 08/2012 43

Appendix C: Radon chamber accreditation policy

National Radon Safety Board
NRSB
Certified Radon Professionals

Document: Chamber Accreditation
Date first issued: 5/1/1999
Version#: 010120
Page 5 of 17

Radon Chamber Accreditation Policy

3.3.4 The chamber design must show how exposure of personnel to radon leakage from the chamber in the immediate vicinity of the chamber or from the exhaust air is avoided.

3.3.5 The chamber design must show how the exhaust air from the radon chamber is diluted. Exhaust vented outdoors should avoid radon reentry to the indoors.

3.4 Chamber Environmental Conditions

3.4.1 The chamber must demonstrate consistent, homogeneous, and well defined concentrations of radon inside for a period of time sufficient for the type of test being conducted.

3.4.2 A secondary chamber must have control of environmental conditions to test the effects of temperature and humidity that may affect the performance of instruments and devices.

3.4.3 The chamber must demonstrate the capability of maintaining a stable temperature between 18 - 27 ° C (64 – 80°F) and relative humidity values between 20 – 75 % for the duration of an exposure period.

Appendix D: Data plot for radon leakage

Time(hr)	**Radon Concentration with leakage (Bq/m^3)**	**Radon concentration without leakage (Ideal) (Bq/m3)**
1	400	396.991371862815
2	302	394.005373333799
3	284	391.041834202763
4	336	388.100585539766
5	304	385.181459685484
6	300	382.284290241654
7	342	379.408912061592
8	304	376.555161240773
9	336	373.722875107495
10	294	370.9118922136
11	326	368.122052325273
12	304	365.353196413913
13	352	362.605166647059
14	300	359.877806379401
15	304	357.170960143848
16	284	354.484473642662
17	330	351.81819373867
18	260	349.171968446531
19	318	346.545646924069
20	274	343.939079463682
21	282	341.352117483802
22	304	338.784613520428
23	278	336.236421218721
24	286	333.707395324658
25	292	331.197391676757
26	294	328.706267197854
27	312	326.233879886952
28	274	323.780088811125
29	280	321.344754097481
30	298	318.927736925195
31	278	316.52889951759
32	290	314.148105134288
33	296	311.785218063412
34	280	309.440103613852
35	272	307.112628107586
36	262	304.802658872063
37	278	302.510064232634
38	280	300.234713505054

39	258	297.976476988026
40	262	295.735225955813
41	274	293.510832650894
42	252	291.303170276689
43	266	289.112112990324
44	258	286.937535895465
45	272	284.779315035191
46	266	282.637327384933
47	220	280.51145084546
48	270	278.401564235919
49	222	276.307547286928
50	272	274.229280633717
51	250	272.166645809331
52	242	270.119525237867
53	234	268.087802227783
54	234	266.071360965236
55	252	264.070086507488
56	262	262.08386477635
57	250	260.112582551679
58	226	258.156127464927
59	260	256.214387992732
60	202	254.287253450566
61	226	252.374613986418
62	228	250.476360574541
63	216	248.592385009231
64	228	246.722579898659
65	196	244.866838658754
66	224	243.025055507123
67	196	241.197125457023
68	204	239.382944311378
69	185	237.582408656834
70	212	235.795415857871
71	202	234.021864050948
72	226	232.261652138697
73	173	230.514679784163
74	208	228.780847405081
75	174	227.060056168201
76	210	225.352207983655
77	173	223.657205499364
78	202	221.97495209549
79	206	220.305351878928
80	158	218.648309677839
81	180	217.003731036227

82	181	215.371522208553
83	190	213.75159015439
84	162	212.143842533124
85	182	210.548187698684
86	192	208.964534694325
87	179	207.392793247437
88	177	205.832873764403
89	168	204.28468732549
90	171	202.748145679781
91	163	201.223161240145
92	154	199.709647078244
93	156	198.207516919577
94	166	196.716685138562
95	190	195.237066753658
96	150	193.768577422516
97	137	192.311133437177
98	150	190.864651719294
99	166	189.429049815402
100	152	188.004245892215
101	140	186.590158731961
102	148	185.186707727754
103	133	183.793812878998
104	160	182.411394786827
105	136	181.03937464958
106	137	179.677674258307
107	126	178.326215992313
108	121	176.984922814733
109	140	175.653718268138
110	147	174.332526470181
111	149	173.021272109269
112	131	171.71988044027
113	93	170.428277280253
114	105	169.14638900426
115	127	167.874142541106
116	87	166.611465369219
117	123	165.3582855125
118	127	164.114531536226
119	134	162.880132542974
120	119	161.655018168581
121	103	160.439118578133
122	113	159.232364461984
123	138	158.034687031807
124	108	156.846018016669

125	102	155.666289659143
126	102	154.495434711444
127	120	153.333386431595
128	109	152.180078579625
129	118	151.035445413791
130	94	149.89942168683
131	108	148.771942642243
132	89	147.6529440106
133	108	146.542362005879
134	101	145.440133321828
135	84	144.346195128358
136	86	143.260485067961
137	96	142.182941252155
138	94	141.113502257957
139	114	140.052107124382
140	69	138.998695348966
141	102	137.953206884319
142	103	136.915582134701
143	84	135.885761952627
144	95	134.863687635493
145	83	133.849300922231
146	74	132.842543989988
147	80	131.84335945083
148	71	130.851690348468
149	82	129.867480155016
150	72	128.890672767767
151	81	127.921212505992
152	80	126.959044107771
153	74	126.004112726839
154	62	125.056363929462
155	56.5	124.115743691331
156	69	123.182198394487
157	68	122.255674824262
158	49.5	121.336120166245
159	56.5	120.423482003273
160	46.5	119.517708312441
161	56.5	118.618747462139
162	74	117.726548209108
163	60	116.841059695519
164	62	115.962231446073
165	51	115.090013365124
166	45	114.224355733826
167	55.5	113.365209207294

168	56.5	112.512524811797
169	52.5	111.666253941961
170	63	110.826348358001
171	60	109.992760182972
172	39.5	109.16544190004
173	43.5	108.344346349768
174	50.5	107.529426727436
175	38	106.720636580367
176	70	105.917929805282
177	46	105.12126064567
178	56	104.330583689183
179	70	103.545853865042
180	60	102.767026441474
181	25.5	101.994057023157
182	47	101.226901548694
183	36	100.465516288095
184	49.5	99.7098578402919
185	36	98.9598831306593
186	24.5	98.2155494085606
187	38	97.4768142449113
188	49	96.7436355297603
189	24	96.0159714698892
190	29.5	95.2937805864305
191	8	94.5770217125028
192	32.5	93.8656539908642
193	29.5	93.1596368715837
194	39.5	92.4589301097292
195	44.5	91.7634937630737
196	21	91.0732881898187
197	16.5	90.388274046334
198	20	89.7084122849155
199	20	89.033664151559
200	25.5	88.3639911837513
201	22.5	87.6993552082777
202	25.5	87.0397183390461
203	28.5	86.3850429749273
204	28	85.7352917976115
205	25	85.0904277694813
206	18.5	84.4504141315003
207	13	83.8152144011179
208	19.5	83.1847923701893
209	18.5	82.5591121029122
210	12	81.9381379337775

211	30	81.3218344655372
212	14.5	80.7101665671859
213	8	80.1030993719585
214	2	79.500598275343
215	28	78.9026289331073
216	8	78.3091572593422
217	16.5	77.7201494245179
218	9	77.1355718535558
219	17.5	76.5553912239146
220	5.5	75.9795744636909
221	11.5	75.4080887497338
222	24.5	74.8409015057743
223	10	74.2779804005678
224	0.5	73.7192933460517
225	11	73.1648084955158
226	3.5	72.6144942417874
227	9.5	72.0683192154291